Study of $D^0/\bar{D}^0 \to K^0_S\pi^0\pi^+\pi^-$ at BESIII and Simulation and Reconstruction of STCF DTOF

Yutong Feng
Supervisor: Haiping Peng

Thesis Mid-term Talk

2026.10.14

Outline

- Works on BESIII
  - Introduction
  - Study of $D^0/\overline{D}^0 \to K_S^0\pi^0\pi^+\pi^-$
  - Measurement of $e^+e^- \to \eta J/\psi$ Cross Section
- Works on STCF
  - Introduction
  - Simulation and Reconstruction of STCF DTOF
- Summary and Prospect

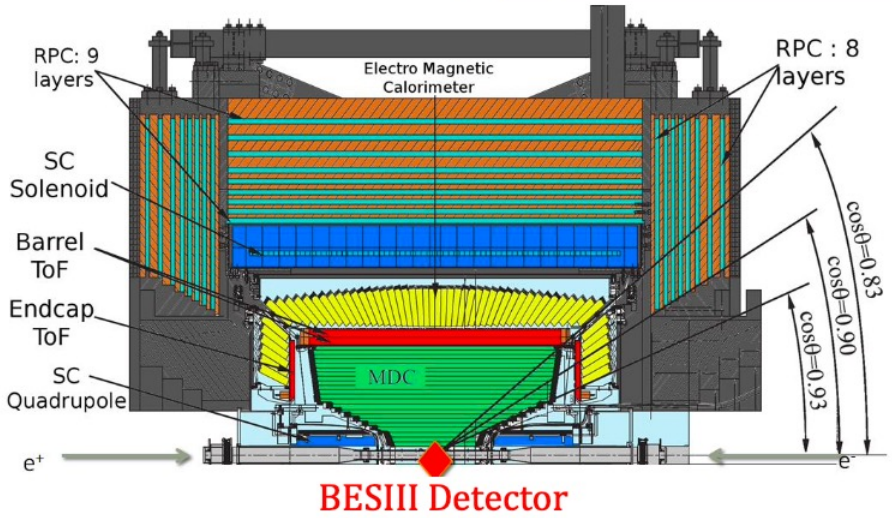
Outline

- Works on BESIII
  - Introduction
  - Study of $D^0/\bar{D}^0 \to K_S^0\pi^0\pi^+\pi^-$
  - Measurement of $e^+e^- \to \eta J/\psi$ Cross Section
- Works on STCF
  - Introduction
  - Simulation and Reconstruction of STCF DTOF
- Summary and Prospect

BEPCII and BESIII

Electromagnetic Calorimeter
CsI(Tl): L = 28 cm
Barrel $\sigma_E = 2.5\%$
Endcap $\sigma_E = 5.0\%$

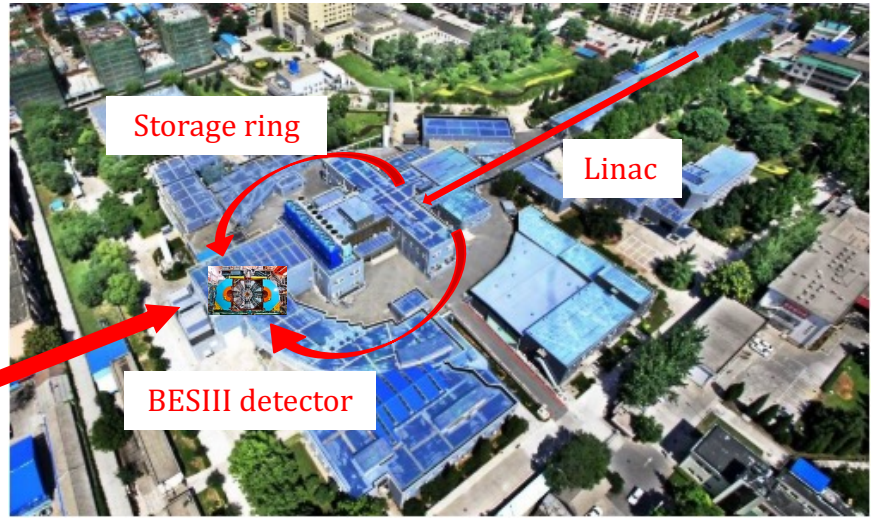
Muon Counter RPC
Barrel: 9 layers
Endcaps: 8 layers
$\sigma_{spatial}$=1.48 cm



BESIII Detector

Main Drift Chamber
Small cell, 43 layer
σ_{xy}=130 μm
$dE/dx \sim 6\%$
$\sigma_p/p = 0.5\%$ at 1GeV

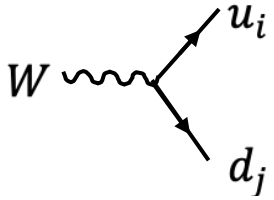
Time Of Flight
Plastic scintillator
σ_T(barrel) = 68 ps
σ_T(endcap) = 110 ps
(update to 60 ps with MRPC)



$E_{cm} = 1.84 - 4.95$ GeV
Peak luminosity @$E_{cm} = 3.773$ GeV:
1.1×10^{33} cm^{-2}s^{-1}
Circumference: 237.53 m
Crossing angle: 2×11 mrad

Motivation

- $\mathcal{L} \propto -\frac{g}{\sqrt{2}}(\bar{u}_L, \bar{c}_L, \bar{t}_L)\gamma^\mu W_\mu^+ V_{CKM} \begin{pmatrix} d_L \\ s_L \\ b_L \end{pmatrix} + h.c.$

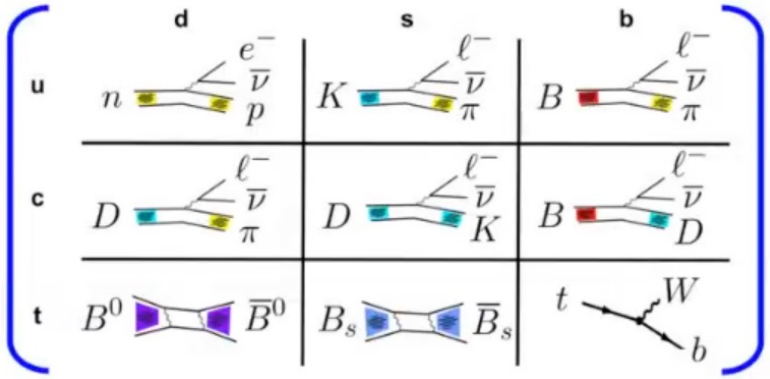


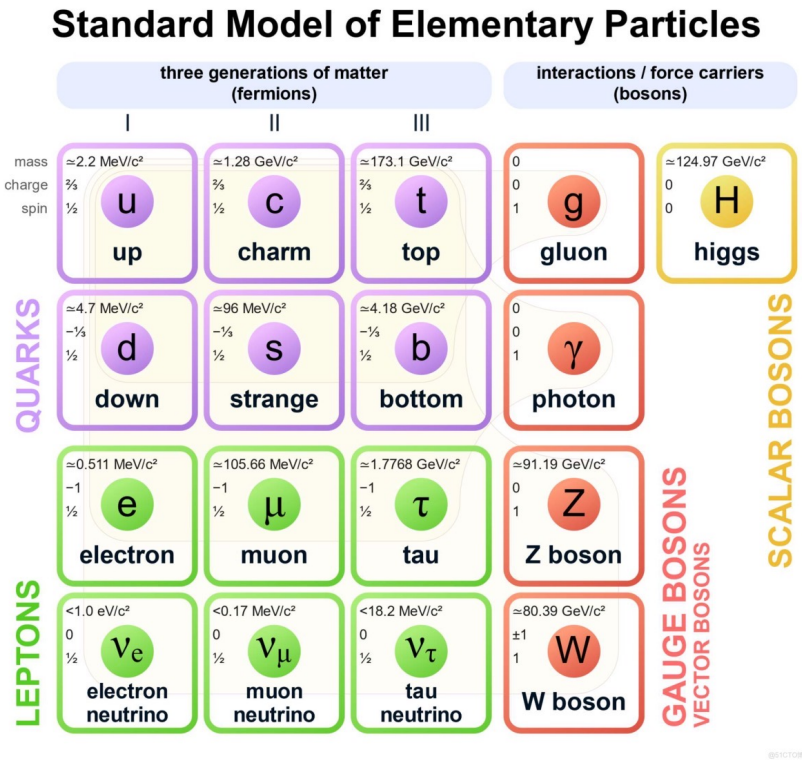
$$V_{CKM} \equiv V_L^u V_L^{d\dagger} = \begin{pmatrix} V_{ud} & V_{us} & V_{ub} \\ V_{cd} & V_{cs} & V_{cb} \\ V_{td} & V_{ts} & V_{tb} \end{pmatrix}$$

3×3 unitary complex matrix

Mass eigenstates are not weak interaction eigenstates.

$V =$





Motivation

- Different parameterization of CKM matrix

$$V_{CKM} = \begin{pmatrix} 1 & 0 & 0 \\ 0 & c_{23} & s_{23} \\ 0 & -s_{23} & c_{23} \end{pmatrix} \begin{pmatrix} c_{13} & 0 & s_{13}e^{-i\delta} \\ 0 & 1 & 0 \\ -s_{13}e^{i\delta} & 0 & c_{13} \end{pmatrix} \begin{pmatrix} c_{12} & s_{12} & 0 \\ -s_{12} & c_{12} & 0 \\ 0 & 0 & 1 \end{pmatrix}$$

$$= \begin{pmatrix} c_{12}c_{13} & s_{12}c_{13} & s_{13}e^{-i\delta} \\ -s_{12}c_{23} - c_{12}s_{23}s_{13}e^{i\delta} & c_{12}c_{23} - s_{12}s_{23}s_{13}e^{i\delta} & s_{23}c_{13} \\ s_{12}s_{23} - c_{12}c_{23}s_{13}e^{i\delta} & -c_{12}s_{23} - s_{12}c_{23}s_{13}e^{i\delta} & c_{23}c_{13} \end{pmatrix}$$

  - ✓ 3 mixing angles: $s_{ij} = \sin\theta_{ij}, c_{ij} = \cos\theta_{ij}$
  - ✓ 1 CPV KM phase: δ is the phase for all CPV phenomena in flavor-changing processes in SM.

- Wolfenstein parameterization

$$V_{CKM} = \begin{pmatrix} 1 - \lambda^2/2 & \lambda & A\lambda^3(\rho - i\eta) \\ -\lambda & 1 - \lambda^2/2 & A\lambda^2 \\ A\lambda^3(1 - \rho - i\eta) & -A\lambda^2 & 1 \end{pmatrix} + \mathcal{O}(\lambda^4)$$

$$s_{12} = \lambda = \frac{|V_{us}|}{\sqrt{|V_{ud}|^2 + |V_{us}|^2}}, \qquad s_{23} = A\lambda^2 = \lambda \left|\frac{V_{cb}}{V_{us}}\right|,$$

$$s_{13}e^{i\delta} = V_{ub}^* = A\lambda^3(\rho + i\eta) = \frac{A\lambda^3(\bar{\rho} + i\bar{\eta})\sqrt{1 - A^2\lambda^4}}{\sqrt{a - \lambda^2}[1 - A^2\lambda^4(\bar{\rho} + i\bar{\eta})]}$$

Motivation

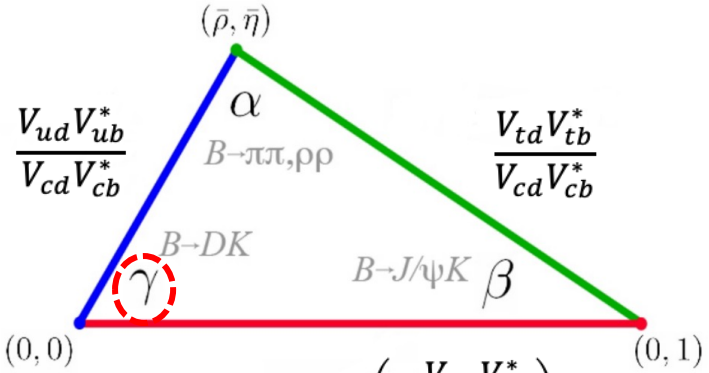
- $V_{CKM}^{\dagger}V_{CKM} = V_{CKM}V_{CKM}^{\dagger} = 1 \Rightarrow \Sigma_i V_{ij}V_{ik}^* = \delta_{jk}, \quad \Sigma_j V_{ij}V_{kj}^* = \delta_{ik}$

$$V_{ud}V_{ub}^* + V_{cd}V_{cb}^* + V_{td}V_{tb}^* = 0 \Rightarrow \frac{V_{ud}V_{ub}^*}{V_{cd}V_{cb}^*} + \frac{V_{td}V_{tb}^*}{V_{cd}V_{cb}^*} + 1 = 0$$

$$\alpha \equiv \phi_2 = \arg\left(-\frac{V_{td}V_{tb}^*}{V_{ud}V_{ub}^*}\right)$$

$$\beta \equiv \phi_1 = \arg\left(-\frac{V_{cd}V_{cb}^*}{V_{td}V_{tb}^*}\right)$$

$$\gamma \equiv \phi_3 = \arg\left(-\frac{V_{ud}V_{ub}^*}{V_{cd}V_{cb}^*}\right)$$



$$\gamma \equiv \varphi_3 \equiv \arg\left(-\frac{V_{ud}V_{ub}^*}{V_{cd}V_{cb}^*}\right)$$

✓ Involving $b \to c$ and $b \to u$:

γ can be measured by $B \to D +$ hardron

Motivation

➢ Measurement of γ/φ_3

$$A(B^- \to (f)_D K^-) = A_B\left(A_f + r_B e^{i(\delta_B-\gamma)}\bar{A}_f\right)$$
$$= A_B\left(a_f e^{i\delta_D} + r_B e^{i(\phi_B-\gamma)}\bar{a}_f e^{i\bar{\delta}_D}\right)$$

r_B: ratio of two amplitude,

δ_B: strong phase difference.

$$\frac{A(B^-\to\bar{D}^0K^-)}{A(B^-\to D^0K^-)} = r_B e^{i(\delta_B-\gamma)}$$

- Decay rate:

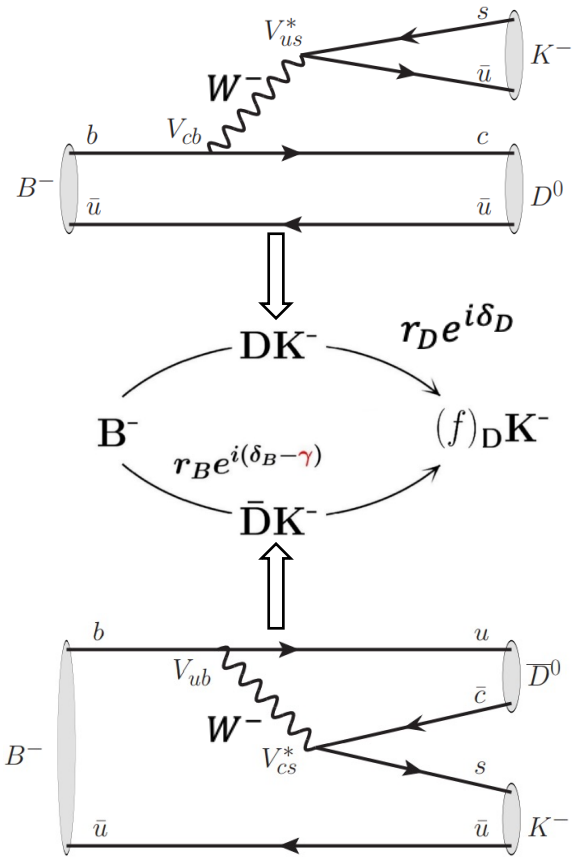
$$\Gamma(B^- \to [f]_D K^-) = |A_B|^2\left[1 + r_B^2 r_D^2 + 2R_f r_D r_B \cos(\delta_B - \gamma - \Delta\delta_D)\right]$$

Inputs from $D^0 \to f$ and $\bar{D}^0 \to f$ decays are needed

$$\left(r_D^f\right)^2 = \frac{\int |\bar{A}_f|^2 d\Phi}{\int |A_f|^2 d\Phi} \qquad R_f e^{-i\delta_D^f} = \frac{\int A_f^* \bar{A}_f d\Phi}{\sqrt{\int |A_f|^2 d\Phi \int |\bar{A}_f|^2 d\Phi}} \qquad c_i(s_i) = \frac{\int |A_f||\bar{A}_f| \cos\Delta\delta_D^f \ (\sin\Delta\delta_D^f) d\Phi_i}{\sqrt{\int |A_f|^2 d\Phi_i \int |\bar{A}_f|^2 d\Phi_i}}$$

- Different D decay models:
  - ✓ ADS: CF and DCS decays (e.g. $K\pi, K\pi\pi^0$) ← R_f, δ_D^f
  - ✓ GLW: (Quasi-)CP eigenstates (e.g. $KK, \pi^+\pi^-\pi^0$) ← F_+
  - ✓ GGSZ: Multi-body Self-conjugate decay (e.g. $K_S^0\pi^+\pi^-\pi^0$) ← c_i, s_i

$V_{cb}V_{us}^* \sim A\lambda^3$



$V_{ub}V_{cs}^* \sim A\lambda^3(\rho - i\eta)$

$D^0\bar{D}^0$ Data Sample

➢ Quantum correlated (QC) $D^0\bar{D}^0$ decay at $\psi(3770)$

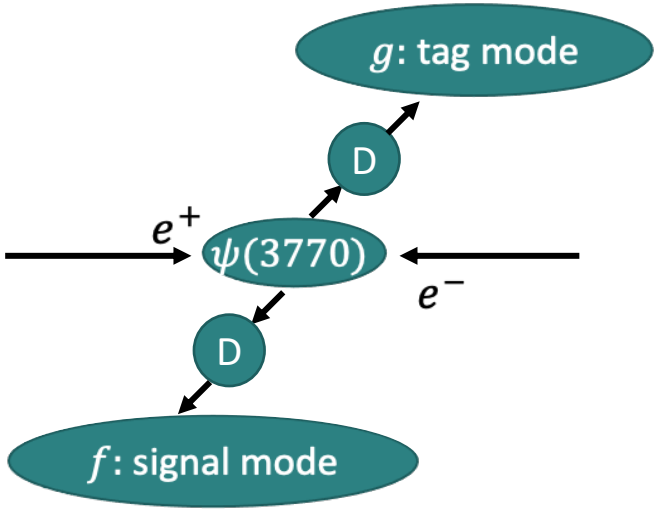
$$e^+e^- \to \psi(3770) \to D^0\bar{D}^0 \to fg \xrightarrow{C_{\psi(3770)}=-1} |\psi(3770)\rangle \to \frac{1}{\sqrt{2}}(|D^0\rangle|\bar{D}^0\rangle - |\bar{D}^0\rangle|D^0\rangle)$$

No CPV

$$\Gamma(f|g) \propto \left(1+\frac{y^2-x^2}{2}\right)\left[(r_D^f)^2+(r_D^g)^2-2r_D^f r_D^g R_f R_g \cos(\Delta\delta_D^f-\Delta\delta_D^g)\right]+\frac{y^2+x^2}{2}\left[1+(r_D^f r_D^g)^2-2r_D^f r_D^g R_f R_g \cos(\Delta\delta_D^f+\Delta\delta_D^g)\right]$$

$\propto$ Number of events coherence factor strong phase difference

- QC $D^0\bar{D}^0$ produced at BESIII
  - ✓ 20.3 fb^{-1} @ $\sqrt{s}$ = 3.773 GeV ~73.4 M $D^0\bar{D}^0$ pairs
- Double Tag Method
  - ✓ Single Tag (ST): reconstruct one $D/\bar{D}$
  - ✓ Double Tag(DT): reconstruct both $D\bar{D}$



Outline

- Works on BESIII
  - Introduction
  - Study of $D^0/\bar{D}^0 \to K_S^0\pi^0\pi^+\pi^-$
  - Measurement of $e^+e^- \to \eta J/\psi$ Cross Section
- Works on STCF
  - Introduction
  - Simulation and Reconstruction of STCF DTOF
- Summary and Prospect

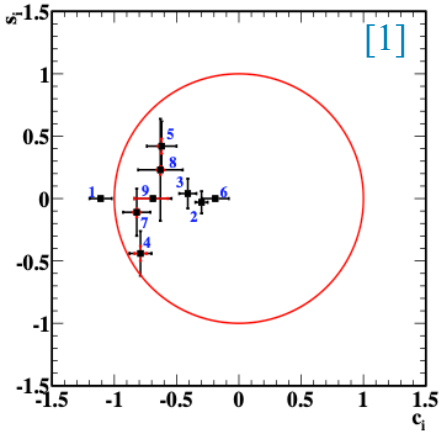
Motivation

- Multi-body self-conjugate D decay with large branching fraction
  - Provide strong phase parameters as input of GGSZ method.
  - Only Rough Results by CLEO[1] (Bin the PHSP with resonance mass region.) ~ 25× CLEO
- Many potential processes $D \to VV, VP$ and AP.
  - Study for the features in the polarization of $D^0 \to K^*(892)\rho(770)$.
  - Lack of accurate experimental measurements.

TABLE VIII. Results for $D^0 \to K^0\pi^+\pi^-\pi^0$.

Amplitude	Fraction (%)	Phase	Branching fraction (%)
Four-body nonresonant	21.0±14.7±15.0	−0.45±0.55	2.2±1.6±1.7
$K^{*-}\rho^+$ longitudinal	19.3±7.4	0	
$K^{*-}\rho^+$ transverse	21.1±12.0	2.0±0.48	
$K^{*-}\rho^+$ total	40.4±12.5±8.4		6.2±2.3±2.0
$\bar{K}^0\omega$	19.5±4.3±1.4		2.3±0.7±0.6
$\bar{K}^{*0}\rho^0$ transverse	4.2±3.7		1.3±1.2
$K_1(1270)^-\pi^+$	4.8±1.5		1.0±0.4
$\bar{K}^{*0}\pi^+\pi^-$	12.7±7.0		3.9±2.3

Reference: D. Coffman *et al.* (Mark III Collaboration), Phys. Rev. D **45**, 2196 (1992)

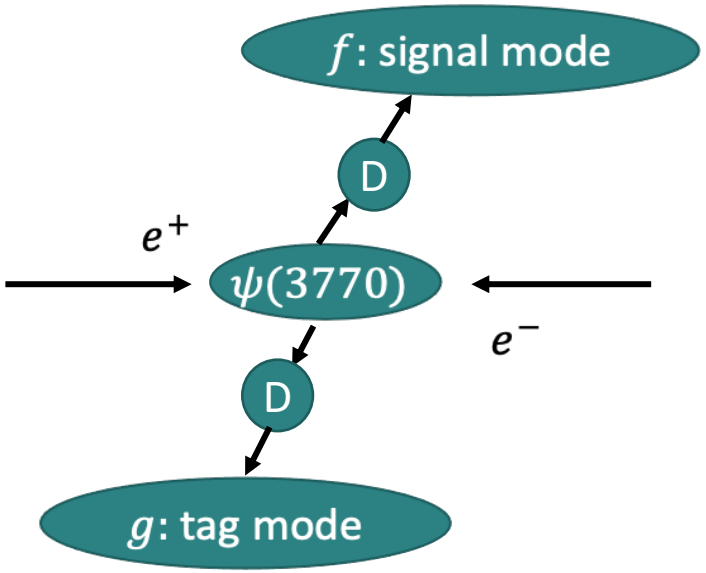


Double Tag Method

➢ Tag Mode

Type	Tag mode
(quasi-)flavor	$K^+\pi^-$, $K^+\pi^-\pi^0$, $K^+\pi^-\pi^+\pi^-$, $K^+e^-\bar{\nu}_e$
CP-even	K^+K^-, $\pi^+\pi^-$, $K^0_S\pi^0\pi^0$, $K^0_L\pi^0$
CP-odd	$K^0_S\pi^0$, $K^0_S\eta_{\gamma\gamma}$, $K^0_S\eta'_{\gamma\pi^+\pi^-}$, $K^0_S\eta'_{\pi^+\pi^-\eta_{\gamma\gamma}}$, $K^0_L\pi^0\pi^0$
CP-mixed	$K^0_{S,L}\pi^+\pi^-$, $K^0_S\pi^+\pi^-\pi^0$, $\pi^+\pi^-\pi^0$

: tag modes used in amplitude analysis



➢ Signal Mode

Signal $D^0 \to K^0_S\pi^0\pi^+\pi^-$

Event Selection

Initial Selection

20.3 fb^{-1} $\psi(3770)$ Data Samples in BOSS version 7.1.2 used for $D^0 \to K_S^0\pi^0\pi^+\pi^-$ with decay mode $K_S^0 \to \pi^+\pi^-, \pi^0 \to \gamma\gamma$.

- Good Charged tracks
  - ✓ |Rz| < 10.0 cm, |Rxy| < 1.0 cm
  - ✓ |cos θ| < 0.93
- Good Showers
  - ✓ $E > 25$ MeV for barrel ($|\cos\theta| < 0.8$)
  - ✓ $E > 50$ MeV for endcap ($0.86 < |\cos\theta| < 0.92$)
  - ✓ $0 \le t_{TDC} \le 14$ (× 50 ns)
  - ✓ $\theta_{\gamma-chrg} > 10°$
- Particle Identification (dE/dx and TOF)

  Use SimplePID
  - ✓ π: $CL_\pi > CL_K$, $CL_\pi > 0$
  - ✓ K: $CL_K > CL_\pi$, $CL_K > 0$
  - ✓ e : $CL_e > CL_K$, $CL_e > CL_\pi$, $CL_K > 0$
- $\pi^0 \to \gamma\gamma$ candidate
  - ✓ Reject γ both in endcap
  - ✓ $[0.115, 0.150]$ GeV/c^2, $\chi^2_{1C} < 50$
- $\eta \to \gamma\gamma$ candidate
  - ✓ $[0.505, 0.575]$ GeV/c^2, $\chi^2_{1C} < 50$
- $K_S^0 \to \pi^+\pi^-$ candidate
  - ✓ |Rz| < 20.0 cm, |cos θ| < 0.93
  - ✓ $L/\sigma_L > 2$, $\chi^2_{vtx,\,svtx} < 100$
  - ✓ $[0.487, 0.511]$ GeV/c^2
- η' candidate
  - ✓ $\pi^+\pi^-\eta$: $[0.940, 0.976]$ GeV/c^2
  - ✓ $\rho\gamma$: $[0.940, 0.976]$ GeV/c^2,
    $\rho \to \pi^+\pi^-$: $[0.626, 0.924]$ GeV/c^2

Event Selection

Initial Selection

➢ ST Selection

- Cosmic ray rejection for $K^+\pi^-$ tag mode
- K_S^0 rejection
  - ✓ $K^+\pi^-\pi^+\pi^-$: $|M_{\pi^+\pi^-} - 0.4976| > 0.03\ \mathrm{GeV/c^2}$
  - ✓ $\pi^+\pi^-\pi^0$: $M_{\pi^+\pi^-} \in [0.48, 0.52]\ \mathrm{GeV/c^2}$
- Minimum |ΔE| to select the best ST D^0
- Cut of ΔE and M_{BC} are defined as:

$$\Delta E = E_{\bar{D}^0} - E_{beam}$$

$$M_{BC} = \sqrt{E_{beam}^2 - |\vec{p}_{\bar{D}^0}|^2}$$

Decay modes	Data ΔE cut (GeV)	MC ΔE cut (GeV)
$\bar{D}^0 \to K^+\pi^-$	$(-0.027, 0.027)$	$(-0.027, 0.027)$
$\bar{D}^0 \to K^+\pi^-\pi^0$	$(-0.062, 0.049)$	$(-0.062, 0.049)$
$\bar{D}^0 \to K^+\pi^+\pi^-\pi^-$	$(-0.026, 0.024)$	$(-0.026, 0.024)$
$\bar{D}^0 \to K_S^0\pi^+\pi^-$	$(-0.024, 0.024)$	$(-0.024, 0.024)$
$\bar{D}^0 \to K_S^0\pi^+\pi^-\pi^0$	$(-0.050, 0.038)$	$(-0.050, 0.038)$
$\bar{D}^0 \to \pi^+\pi^-\pi^+\pi^-$	$(-0.031, 0.028)$	$(-0.031, 0.028)$
$\bar{D}^0 \to \pi^+\pi^-\pi^0$	$(-0.063, 0.050)$	$(-0.058, 0.045)$
$\bar{D}^0 \to K^+K^-$	$(-0.026, 0.027)$	$(-0.027, 0.027)$
$\bar{D}^0 \to \pi^+\pi^-$	$(-0.037, 0.038)$	$(-0.032, 0.032)$
$\bar{D}^0 \to K_S^0\pi^0\pi^0$	$(-0.084, 0.060)$	$(-0.069, 0.040)$
$\bar{D}^0 \to K_S^0\pi^0$	$(-0.069, 0.053)$	$(-0.066, 0.049)$
$\bar{D}^0 \to K_S^0\eta_{\gamma\gamma}$	$(-0.045, 0.045)$	$(-0.044, 0.043)$
$\bar{D}^0 \to K_S^0\eta'_{\pi^+\pi^-\eta_{\gamma\gamma}}$	$(-0.030, 0.030)$	$(-0.030, 0.029)$
$\bar{D}^0 \to K_S^0\eta'_{\gamma\pi^+\pi^-}$	$(-0.033, 0.027)$	$(-0.034, 0.029)$

Event Selection

For Amplitude Analysis Modes

$$\bar{D}^0 \to K^+\pi^-, K^+\pi^-\pi^0, K^+\pi^-\pi^+\pi^-$$

➢ DT Selection

- 3C Kinematic fit

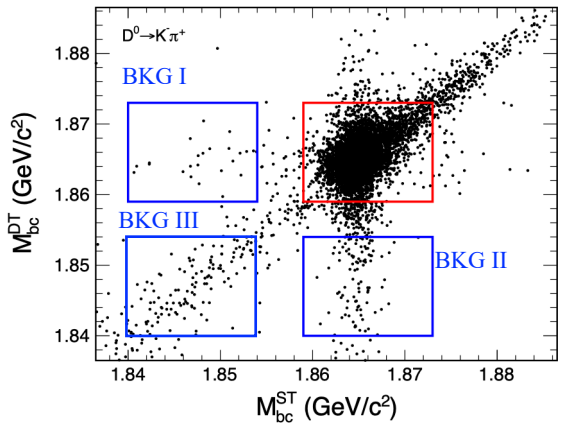
  Constrain: π^0, K_S^0, D^0 mass

- ΔE requirement for DT tag $D^0 \to K_S^0\pi^+\pi^-\pi^0$

  $(\mu - 3.5\sigma, \mu + 3.5\sigma)$: $(-0.050, 0.038)$ [GeV]

In M_{BC} spectrum:

- Signal region $(\bar{\mu} \pm 3.5\bar{\sigma}) \in (1.859, 1.873)$
- Sideband region $6\sigma \in (1.840, 1.854)$

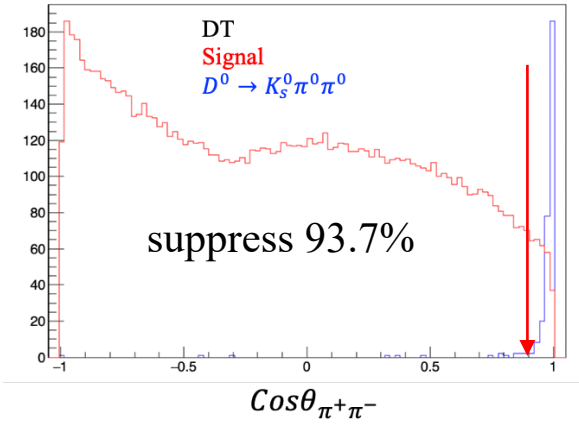


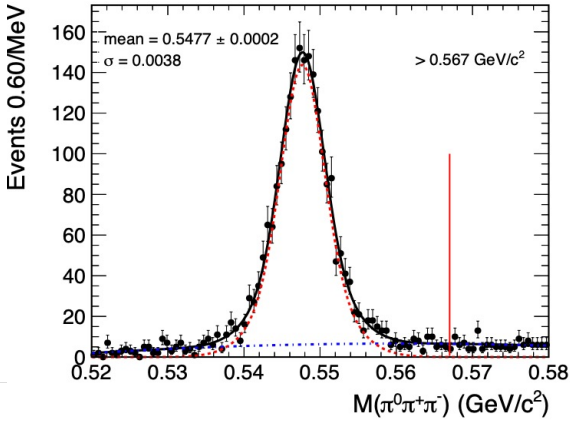
- Veto $D^0 \to \pi^0\pi^0K_S^0$ Peaking BKG

  $\cos\theta_{\pi^+\pi^-} < 0.9$

- Veto η:

  $M(\pi^0\pi^+\pi^-) > 0.567\ \mathrm{GeV/c^2}$





Amplitude Analysis

Likelihood Fit

➢ PDF Function:

$$P(p) = \epsilon(p)\left[\omega \frac{f_s(p)}{\int f_s(p)\epsilon(p)\mathrm{d}\Phi} + (1-\omega)\frac{f_b(p)/\epsilon(p)}{\int f_b(p)/\epsilon(p) \times \epsilon(p)\mathrm{d}\Phi}\right]$$

efficiency (PHSP MC)

Purity (M_{bc} 2D fit)

Signal PDF (QC amplitude)

background PDF (efficiency correction)

MC integral

➢ Log-likelihood in Amplitude Fit:

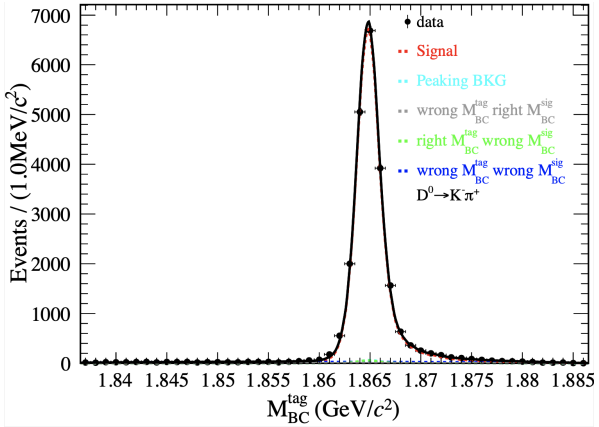
$$\ln L = \sum_i^{N_{data}} \ln\left[f\frac{f_s(p_i)}{\int f_s(p)\epsilon(p)\mathrm{d}\Phi} + (1-f)\frac{f_b(p_i)/\epsilon(p_i)}{\int f_b(p)/\epsilon(p) \times \epsilon(p)\mathrm{d}\Phi}\right] + \sum_i^{N_{data}} \ln \epsilon(p_i)$$

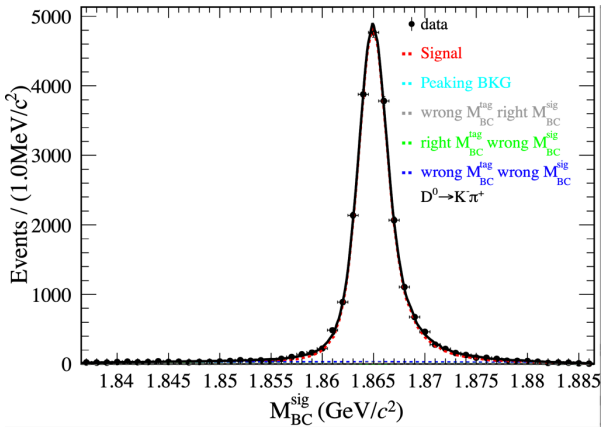
Amplitude Analysis

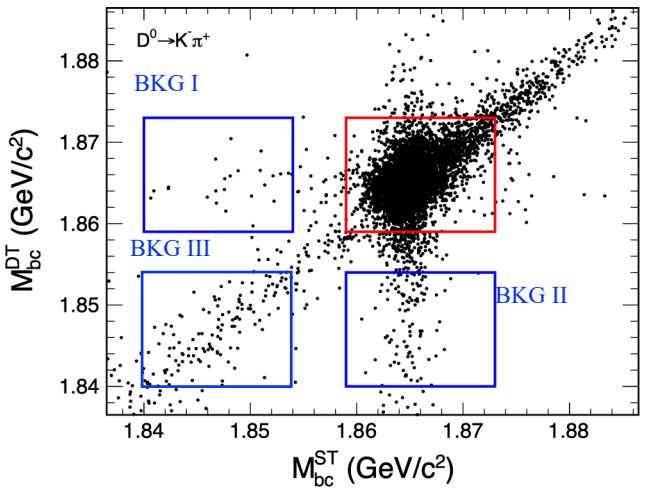
Signal Yields & Purity

➢ Fit Method

- Sig: MC Shape $s(x,y)\otimes\mathrm{Gauss}(x,y)$
- BKG I: $\mathrm{Argus}(x)\times$MC Shape $s(y)$
- BKG II: $\mathrm{Argus}(y)\times$MC Shape $s(x)$
- BKG III: $\mathrm{T}(x-y;\mu,\sigma(x+y),n)\times\mathrm{Argus}(x)\times\mathrm{Argus}(y)$
- Peaking BKG: Estimated and modeled by Inc MC







$$T(y;\mu,\sigma,n) = \frac{\Gamma(n/2+0.5)}{\sigma\sqrt{n\pi}\Gamma(n/2)}\left[1+\frac{1}{2}\left(\frac{y-\mu}{\sigma}\right)^2\right]^{-\frac{n+1}{2}}$$

Signal region $(\bar{\mu}-3.5\bar{\sigma},\bar{\mu}+3.5\bar{\sigma})\in(1.859,1.873)$

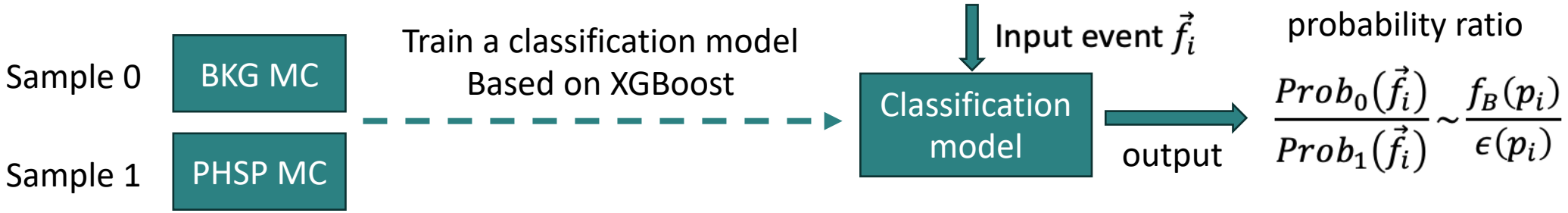
ST mode	Signal Yield	Signal Purity
$\bar{D}^0\to K^+\pi^-$	25222.2 ± 25.9	$(97.5\pm0.1)\%$
$\bar{D}^0\to K^+\pi^-\pi^0$	43992.5 ± 46.9	$(93.9\pm0.1)\%$
$D^0\to K^+\pi^-\pi^-\pi^+$	24045.0 ± 52.1	$(92.3\pm0.2)\%$

~93259.7

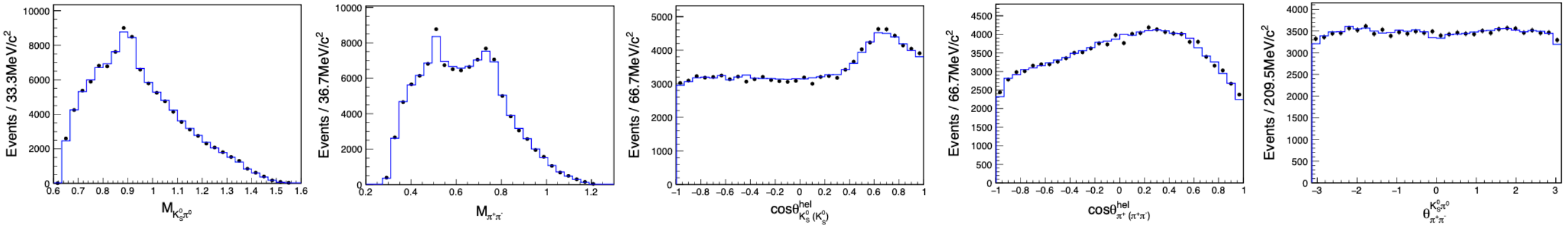
Amplitude Analysis

Background PDF

- BKG PDF $f_b(p)$ is described by Inclusive MC, using ML



Features: $\vec{f} = \{M_{K_S^0\pi^0}, M_{\pi^+\pi^-}, \cos\theta_{K_S^0}^{K_S^0\pi^0}, \cos\theta_{\pi^+}^{\pi^+\pi^-}, \phi_{\pi^+\pi^-}^{K_S^0\pi^0}\}$



Data Point: Evts of BKG; Blue Hist: PHSP Signal MC sampled by weight obtained from ML

$\chi = -0.5$

Amplitude Analysis

Signal PDF

- QC signal amplitude

$$\frac{d\Gamma(D^0 \to f)}{d\Phi_f} \propto |A_f|^2 + r_{\bar{g}}^2 |\bar{A}_f|^2 - r_{\bar{g}} R_{\bar{g}} e^{i\delta_{\bar{g}}} A_f \bar{A}_f^* - r_{\bar{g}} R_{\bar{g}} e^{-i\delta_{\bar{g}}} A_f^* \bar{A}_f$$

$$= |A_f - r_{\bar{g}} R_{\bar{g}} e^{-i\delta_{\bar{g}}} \bar{A}_f|^2 + r_{\bar{g}}^2 (1 - R_{\bar{g}}^2) |\bar{A}_f|^2 \ .$$

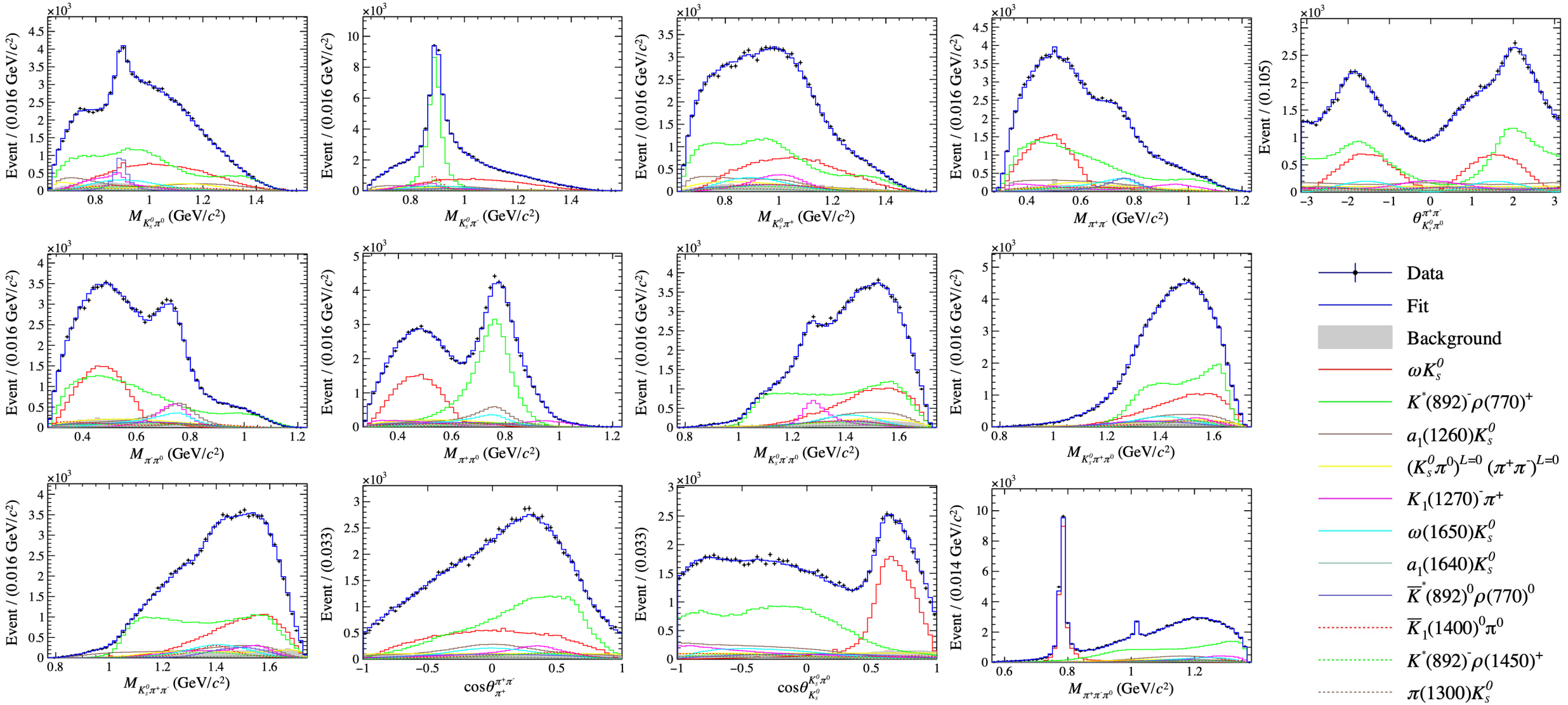
Neglect DDbar mixing

- D^0 amplitude: $A_f(p) = \sum_i \Lambda_i U_i(p)$, Λ_i: complex coupling factor
- Partial wave amplitude: $U_i(p) = S_i(p) B_{L_D}(p) P_{R_1}(p) B_{L_{R_1}}(p) P_{R_2}(p) B_{L_{R_2}}(p)$
- B_L : Blatt-Weisskopf barrier factor; P_R: Propagator
- S_i : spin factor constructed in covariant Zemach tensor;
- $\bar{D}^0$ amplitude: $\bar{A}_f(p) = \sum_i \Lambda_i \bar{U}_i(p) = \sum_i \Lambda_i U_i(\bar{p})$, suppose CP conservation

  $\bar{p}$: CP –conjugate of phase space point *p*;
- Amplitude Consider the Isospin symmetry in strong decay (CG coefficients)

Amplitude Analysis

Fit Result



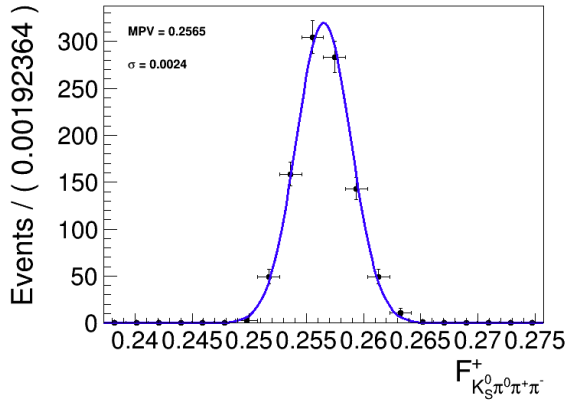
Amplitude Analysis

CP-even Fraction & Longitudinal Polarization Fraction

➢ CP-even Fraction

$$F_+ = \frac{\int |A_+(p)|^2 \, d\Phi}{\int |A_+(p)|^2 + |A_-(p)|^2 \, d\Phi} \quad , \qquad A_\pm(p) = \frac{1}{\sqrt{2}}[A_{D^0}(p) \pm A_{\bar{D}^0}(p)]$$

$$F_+ = 0.257 \pm 0.002 \pm 0.006 \ (\mathbf{non-\eta})$$



➢ Longitudinal Polarization Fraction

$$f_L = \frac{|H_{00}|^2}{|H_{11} + H_{-1-1} + H_{00}|^2}$$

Process	$D^0 \to K^{*-}(892)\,\rho(770)^+$	$D^0 \to \bar{K}^{*0}(892)\,\rho(770)^0$
$D \to V_1V_2 \to (P_1P_2)(P_3P_4)$	$0.509 \pm 0.005 \pm 0.012$	$0.108 \pm 0.008 \pm 0.013$
$D \to V_1V_2$	$0.468 \pm 0.005 \pm 0.011$	$0.077 \pm 0.007 \pm 0.010$

Amplitude Analysis

Systematic Uncertainty

I. Background Estimation
II. Detection Efficiency
III. Resonance line shape
IV. Radius of the Centrifugal Barrier
V. Quantum Correlation Correction
VI. Extra Partial Waves
VII. Fit Bias

(in units of stat. error)

Parameters	I	II	III	IV	V	VI	VII	Total
$M_{K^*(892)^-}$	0.07	0.13	0.31	1.55	0.41	0.19	0.00	1.65
$\Gamma_{K^*(892)^-}$	0.27	0.43	0.73	1.01	0.05	0.19	0.00	1.36
$M_{\bar{K}^*(892)^0}$	0.03	0.13	0.77	1.18	0.03	0.37	0.00	1.46
$\Gamma_{\bar{K}^*(892)^0}$	0.28	0.02	1.03	0.95	0.21	0.13	0.00	1.45
$M_{a_1(1260)}$	0.27	0.19	0.62	0.60	0.11	0.03	0.00	0.93
$\Gamma_{a_1(1260)}$	0.76	0.80	2.07	1.24	0.68	0.63	0.00	2.80
$M_{K_1(1270)}$	0.36	0.13	0.96	0.64	0.45	0.45	0.00	1.37
$\Gamma_{K_1(1270)}$	0.05	0.07	0.16	0.13	0.02	0.08	0.00	0.24
$M_{\pi(1300)}$	1.75	1.83	2.65	2.30	1.34	1.78	0.00	4.87
$\Gamma_{\pi(1300)}$	0.58	0.49	1.03	1.03	0.52	0.05	0.00	1.72
LASS a	0.14	0.24	0.91	0.66	0.17	1.07	0.00	1.59
LASS r	0.13	0.26	0.56	0.67	0.40	0.53	0.00	1.14
$\pi\pi_S\, s_0^{prod}$	0.00	0.10	0.23	0.55	0.40	0.15	0.00	0.74
$F_+^{K_S^0\pi^0\pi^+\pi^-}$	0.50	0.51	2.59	0.65	0.12	0.22	0.03	2.78
$f_L\,(D \to VV)$								
$D^0 \to K^*(892)^-\rho(770)^+$	0.00	0.30	1.00	1.88	0.16	0.50	0.01	2.22
$D^0 \to \bar{K}^*(892)^0\rho(770)^0$	0.17	0.06	0.12	1.32	0.04	0.45	0.16	1.43
$f_L\,(D \to VV \to PPPP)$								
$D^0 \to K^*(892)^-\rho(770)^+$	0.00	0.30	1.01	2.03	0.16	0.50	0.02	2.35
$D^0 \to \bar{K}^*(892)^0\rho(770)^0$	0.18	0.07	0.07	1.59	0.06	0.46	0.00	1.67

Fit Fraction	I	II	III	IV	V	VI	VII	Total
$D^0 \to \omega K_S^0$	0.53	0.46	0.50	3.00	0.21	0.12	0.03	3.13
$D^0 \to \omega(1420)K_S^0$	0.27	0.03	3.93	5.00	0.79	0.63	0.23	6.45
$D^0 \to \omega(1650)K_S^0$	0.01	0.46	5.14	4.68	0.18	0.67	0.14	7.00
$D^0 \to a_1(1260)K_S^0$	0.04	0.02	2.11	1.81	0.01	0.06	0.15	2.78
$D^0 \to a_2(1320)K_S^0$	0.11	0.02	0.17	0.30	0.14	1.14	0.07	1.21
$D^0 \to a_1(1640)K_S^0$	0.26	0.14	2.01	2.10	0.04	0.08	0.16	2.93
$D^0 \to \phi K_S^0$	0.12	0.06	0.11	0.29	0.08	0.01	0.06	0.35
$D^0 \to h_1(1170)K_S^0$	0.34	0.08	1.39	0.73	0.10	0.09	0.09	1.62
$D^0 \to \pi(1300)K_S^0$	0.18	0.01	0.72	2.22	0.22	0.12	0.28	2.37
$D^0 \to K(1410)^-\pi^+$	0.06	0.08	0.70	1.07	0.09	1.74	0.02	2.17
$D^0 \to K^*(892)^-\rho(770)^+$	0.40	0.23	0.36	4.05	0.12	0.11	0.15	4.10
$D^0 \to K^*(892)^-\rho(770)^+[S]$	0.44	0.19	0.13	1.52	0.00	0.15	0.04	1.61
$D^0 \to K^*(892)^-\rho(770)^+[P]$	0.20	0.06	0.08	1.90	0.16	0.30	0.13	1.95
$D^0 \to K^*(892)^-\rho(770)^+[D]$	0.05	0.22	0.50	3.20	0.01	0.01	0.02	3.24
$D^0 \to \bar{K}^*(892)^0\rho(770)^0$	0.17	0.22	0.23	1.59	0.06	0.38	0.35	1.71
$D^0 \to \bar{K}^*(892)^0\rho(770)^0[S]$	0.18	0.02	0.41	0.28	0.08	0.03	0.27	0.60
$D^0 \to \bar{K}^*(892)^0\rho(770)^0[P]$	0.05	0.11	0.16	1.33	0.05	0.60	0.03	1.47
$D^0 \to \bar{K}^*(892)^0\rho(770)^0[D]$	0.21	0.25	0.18	1.77	0.01	0.03	0.25	1.83
$D^0 \to K^*(892)^-\rho(1450)^+$	0.33	0.05	0.79	0.74	0.06	0.31	0.19	1.19
$D^0 \to K^*(892)^-\rho(1450)^+[S]$	0.36	0.07	0.77	1.30	0.04	0.04	0.11	1.56
$D^0 \to K^*(892)^-\rho(1450)^+[P]$	0.07	0.12	0.01	0.12	0.05	0.56	0.05	0.59
$D^0 \to K^*(892)^-\rho(1450)^+[D]$	0.03	0.43	0.65	2.70	0.00	0.01	0.05	2.81
$D^0 \to \bar{K}^*(892)^0\rho(1450)^0$	0.00	0.39	0.55	0.46	0.05	0.04	0.06	0.82
$D^0 \to \bar{K}^*(892)^0\rho(1450)^0[D]$	0.00	0.39	0.55	0.46	0.05	0.04	0.06	0.82
$D^0 \to K^*(1680)^-\rho(770)^+$	0.29	0.12	2.15	2.26	0.07	0.20	0.02	3.15
$D^0 \to K^*(1680)^-\rho(770)^+[S]$	0.29	0.12	2.15	2.26	0.07	0.20	0.02	3.15
$D^0 \to K^*(892)^-f_2(1270)$	0.25	0.16	0.88	0.63	0.05	0.46	0.14	1.22
$D^0 \to (K_S^0\pi^-)^{L=0}\rho(770)^+$	0.49	0.15	1.12	1.05	0.00	0.12	0.13	1.63
$D^0 \to (\bar{K}_S^0\pi^0)^{L=0}\rho(770)^0$	0.73	0.10	0.27	1.93	0.01	0.03	0.05	2.08
$D^0 \to \bar{K}^*(892)^0(\pi^+\pi^-)^{L=0}$	0.14	0.44	1.49	1.51	0.26	0.03	0.15	2.19
$D^0 \to (K_S^0\pi^0)^{L=0}(\pi^+\pi^-)^{L=0}$	0.08	0.28	2.38	2.50	0.19	0.10	0.15	3.48
$D^0 \to \bar{K}^*(1680)^0(\pi^+\pi^-)^{L=0}$	0.10	0.10	0.45	1.24	0.07	0.07	0.06	1.33
$D^0 \to (K_S^0\pi^0)^{L=1}\rho(1450)^0$	0.36	0.16	0.52	0.32	0.09	1.15	0.06	1.36
$D^0 \to K_1(1270)^-\pi^+$	0.31	0.18	1.06	0.83	0.05	0.04	0.14	1.40
$D^0 \to K_1(1270)^0\pi^0$	0.04	0.24	0.16	0.40	0.02	0.02	0.19	0.53
$K_1(1270) \to \rho(770)K_S^0[S]$	0.32	0.30	1.45	1.21	0.05	0.12	0.00	1.95
$K_1(1270) \to \rho(1450)K_S^0[D]$	0.12	0.09	0.48	1.04	0.02	0.02	0.11	1.16
$K_1(1270) \to K^*(892)\pi[S]$	0.07	0.01	0.48	0.84	0.00	0.04	0.05	0.98
$K_1(1270) \to K^*(892)\pi[D]$	0.02	0.23	0.79	0.79	0.02	0.07	0.07	1.14
$K_1(1270) \to (K_S^0\pi)^{L=0}\pi[P]$	0.16	0.11	0.73	0.42	0.05	0.12	0.24	0.91
$D^0 \to K_1(1400)^0\pi^0$	0.24	0.21	0.30	0.71	0.02	0.10	0.03	0.84
$D^0 \to K_1(1400)^-\pi^+$	0.25	0.03	0.81	0.57	0.03	0.09	0.02	1.03
$K_1(1400) \to K^*(892)\pi[S]$	0.13	0.09	0.19	1.49	0.15	0.15	0.10	1.53
$K_1(1400) \to \rho(770)K_S^0[D]$	0.16	0.22	1.95	1.01	0.01	0.01	0.12	2.22
$D^0 \to K_2(1430)^-\pi^+$	0.05	0.02	0.13	0.15	0.01	0.35	0.17	0.44
$D^0 \to K_2(1430)^0\pi^0$	0.11	0.14	0.08	0.66	0.01	0.13	0.09	0.71
$K_2(1430) \to K^*(892)\pi[S]$	0.11	0.18	0.13	1.18	0.03	0.17	0.19	1.23
$K_2(1430) \to \rho(770)K_S^0$	0.12	0.11	0.33	1.12	0.01	0.09	0.26	1.21
$D^0 \to K(1460)^-\pi^+$	0.13	0.03	1.11	1.38	0.02	0.08	0.12	1.78
$D^0 \to K(1460)^0\pi^0$	0.43	0.54	1.73	1.14	0.16	0.12	0.01	2.20
$K(1460) \to K^*(892)\pi[S]$	0.41	0.30	2.05	1.68	0.18	0.09	0.08	2.71
$K(1460) \to (K_S^0\pi)^{L=0}\pi$	0.41	0.30	2.03	1.67	0.18	0.09	0.08	2.69
$D^0 \to K_1(1650)^0\pi^0$	0.86	0.17	0.54	0.74	0.10	0.00	0.27	1.30
$D^0 \to K_1(1650)^-\pi^+$	0.18	0.10	0.42	0.86	0.11	0.00	0.14	0.99
$K_1(1650) \to \rho(770)K_S^0[S]$	0.22	0.06	0.54	0.51	0.01	0.04	0.05	0.78
$K_1(1650) \to K^*(892)\pi[S]$	0.02	0.05	0.96	0.87	0.09	0.06	0.06	1.30
$K_1(1650) \to (K_S^0\pi)^{L=0}\pi$	0.25	0.14	0.89	1.30	0.04	0.06	0.06	1.60
$D^0 \to K^*(1680)^0\pi^0$	0.23	0.05	0.17	1.54	0.21	0.14	0.08	1.59
$D^0 \to K^*(1680)^-\pi^+$	0.04	0.06	0.07	1.79	0.23	0.43	0.18	1.86
$D^0 \to K^*(1680)^+\pi^-$	0.08	0.09	0.66	1.43	0.01	0.10	0.24	1.61
$K^*(1680) \to \rho(770)K_S^0[P]$	0.22	0.31	0.67	1.06	0.73	0.18	0.29	1.54
$K^*(1680) \to K^*(892)\pi[P]$	0.22	0.32	0.71	1.12	0.73	0.22	0.18	1.59

Phase (ϕ)	I	II	III	IV	V	VI	VII	Total
$D^0 \to \phi K_S^0$	0.03	0.09	0.48	0.46	0.24	0.31	0.05	0.78
$D^0 \to \pi(1300)K_S^0$	0.23	0.13	1.15	1.58	0.08	0.19	0.07	1.98
$D^0 \to \omega(1420)K_S^0$	0.17	0.91	2.69	2.51	2.80	0.20	0.10	4.72
$D^0 \to \omega(1650)K_S^0$	0.47	0.90	1.64	1.48	3.78	0.27	0.17	4.51
$D^0 \to h_1(1170)K_S^0$	0.46	0.27	0.24	1.80	0.72	0.11	0.00	2.03
$D^0 \to a_1(1260)K_S^0$	0.15	0.24	1.03	2.09	0.33	0.56	0.13	2.44
$D^0 \to a_1(1640)K_S^0$	0.07	0.06	8.06	1.16	0.11	0.46	0.15	8.16
$D^0 \to a_2(1320)K_S^0$	0.09	0.01	0.42	0.31	0.31	0.04	0.02	0.61
$D^0 \to K^*(892)^-\rho(770)^+[S]$	0.24	0.12	0.86	2.50	1.20	0.70	0.09	2.99
$D^0 \to K^*(892)^-\rho(770)^+[P]$	0.06	0.12	2.34	1.58	1.67	0.47	0.11	3.31
$D^0 \to K^*(892)^-\rho(770)^+[D]$	0.29	0.32	0.68	5.01	1.13	0.71	0.08	5.24
$D^0 \to \bar{K}^*(892)^0\rho(770)^0[S]$	0.30	0.05	0.90	1.49	1.02	0.10	0.20	2.05
$D^0 \to \bar{K}^*(892)^0\rho(770)^0[P]$	0.05	0.05	0.40	1.86	0.25	0.25	0.25	1.96
$D^0 \to \bar{K}^*(892)^0\rho(770)^0[D]$	0.02	0.15	0.34	2.84	1.01	0.25	0.06	3.05
$D^0 \to K^*(892)^-\rho(1450)^+[S]$	0.15	0.07	1.21	2.17	0.65	0.02	0.11	2.58
$D^0 \to K^*(892)^-\rho(1450)^+[P]$	0.10	0.21	0.66	0.46	0.22	1.14	0.11	1.44
$D^0 \to K^*(892)^-\rho(1450)^+[D]$	0.07	0.01	2.78	3.62	0.28	0.11	0.05	4.57
$D^0 \to \bar{K}^*(892)^0\rho(1450)^0[D]$	0.06	0.02	2.39	2.57	0.21	0.06	0.01	3.52
$D^0 \to K^*(892)^-f_2(1270)[P]$	0.23	0.10	0.55	0.23	0.24	0.04	0.14	0.70
$D^0 \to K^*(892)^-f_2(1270)[P]$	0.13	0.02	0.19	0.69	0.43	1.44	0.25	1.69
$D^0 \to K_1(1270)^-\pi^+(K_1(1270) \to \rho(770)K_S^0[S])$	0.28	0.07	3.89	1.70	0.97	0.29	0.01	4.37
$D^0 \to K_1(1270)^0\pi^0(K_1(1270) \to \rho(770)K_S^0[S])$	0.36	0.04	1.00	1.68	1.04	0.35	0.21	2.28
$K_1(1270) \to \rho(1450)K_S^0[D]$	0.50	0.57	1.79	1.07	0.56	0.53	0.18	2.36
$K_1(1270) \to K^*(892)\pi[S]$	0.20	0.02	1.58	1.18	0.16	0.08	0.07	1.99
$K_1(1270) \to K^*(892)\pi[D]$	0.11	0.13	3.55	0.73	0.11	0.11	0.09	3.64
$K_1(1270) \to (K_S^0\pi)^{L=0}\pi[P]$	0.02	0.02	0.11	0.07	0.04	0.02	0.01	0.14
$D^0 \to K_1(1400)^-\pi^+(K_1(1400) \to K^*(892)\pi[S])$	0.30	0.30	2.98	0.98	0.97	0.37	0.07	3.33
$D^0 \to K_1(1400)^0\pi^0(K_1(1400) \to K^*(892)\pi[S])$	0.31	0.15	3.02	0.66	0.18	0.16	0.02	3.12
$K_1(1400) \to \rho(770)K_S^0[D]$	0.04	0.07	0.40	0.19	0.10	0.11	0.10	0.48
$D^0 \to K(1460)^0\pi^0(K(1460) \to K^*(892)\pi[S])$	0.27	0.12	3.98	0.73	0.54	0.11	0.03	4.09
$D^0 \to K(1460)^-\pi^+(K(1460) \to K^*(892)\pi[S])$	0.15	0.43	1.58	1.33	0.73	0.19	0.07	2.25
$K(1460) \to (K_S^0\pi)^{L=0}\pi$	0.01	0.06	1.22	1.38	0.05	0.02	0.10	1.85
$D^0 \to K_1(1650)^0\pi^0(K_1(1650) \to \rho(770)K_S^0[S])$	0.05	0.11	2.56	0.08	0.47	0.27	0.22	2.63
$D^0 \to K_1(1650)^-\pi^+(K_1(1650) \to \rho(770)K_S^0[S])$	0.14	0.17	1.19	0.45	0.14	0.16	0.01	1.30
$K_1(1650) \to K^*(892)\pi[S]$	0.18	0.34	4.21	0.88	0.06	0.04	0.20	4.32
$D^0 \to K^*(1680)^0\pi^0(K^*(1680) \to \rho(770)K_S^0[P])$	0.69	0.24	5.46	1.80	0.58	2.01	0.28	6.17
$D^0 \to K^*(1680)^+\pi^-(K^*(1680) \to \rho(770)K_S^0[P])$	0.56	0.11	6.79	0.43	0.14	0.01	0.18	6.83
$D^0 \to K^*(1680)^-\pi^+(K^*(1680) \to \rho(770)K_S^0[P])$	0.28	0.08	5.72	1.70	0.25	3.14	0.27	6.76
$K^*(1680) \to K^*(892)\pi[P]$	0.39	0.04	7.41	1.79	0.08	1.79	0.33	7.85
$D^0 \to K_2(1430)^-\pi^+(K_2(1430) \to K^*(892)\pi[S])$	0.03	0.05	1.21	0.94	0.30	0.37	0.08	1.61
$D^0 \to K_2(1430)^0\pi^0(K_2(1430) \to K^*(892)\pi[S])$	0.10	0.10	0.66	0.64	0.37	0.56	0.14	1.16
$K_2(1430) \to \rho(770)K_S^0$	0.16	0.15	2.14	0.53	0.04	0.64	0.07	2.30
$D^0 \to K^*(1680)^-\rho(770)^+[S]$	0.16	0.04	3.59	0.79	0.23	0.24	0.15	3.70
$D^0 \to K(1410)^-\pi^+$	0.05	0.02	2.61	0.56	0.99	2.62	0.13	3.88
$D^0 \to (K_S^0\pi^0)^{L=1}\rho(1450)^0$	0.06	0.24	0.54	0.48	0.69	0.26	0.01	1.06
$D^0 \to (K_S^0\pi^-)^{L=0}\rho(770)^+$	0.00	0.01	0.13	0.05	0.02	0.00	0.14	0.20
$D^0 \to (K_S^0\pi^0)^{L=0}\rho(770)^0$	0.01	0.01	0.45	0.02	0.02	0.00	0.01	0.45
$D^0 \to \bar{K}^*(892)^0(\pi^+\pi^-)^{L=0}$								
β_3	0.33	0.07	0.22	0.87	0.33	0.02	0.04	1.01
$f_{\pi\pi}$	0.02	0.04	0.15	0.40	0.29	0.10	0.01	0.53
$K_1(1650) \to (K_S^0\pi)^{L=0}\pi$								
β_1	0.14	0.96	0.81	1.76	0.95	0.21	0.05	2.37
β_2	0.29	0.65	1.36	1.95	0.12	0.25	0.13	2.51
$f_{\eta\eta}$	0.16	0.32	0.01	0.47	0.17	0.16	0.07	0.64
$D^0 \to \bar{K}^*(1680)^0(\pi^+\pi^-)^{L=0}$								
β_1	0.51	1.01	0.34	2.20	0.97	0.24	0.00	2.69
β_3	0.34	1.67	0.74	2.34	1.35	0.47	0.40	3.33
$f_{\eta\eta}$	0.36	0.11	0.21	2.25	0.22	0.03	0.05	2.30
$D^0 \to (K_S^0\pi^0)^{L=0}(\pi^+\pi^-)^{L=0}$								
β_2	0.00	0.02	0.00	0.07	0.03	0.00	0.18	0.20
β_4	0.00	0.01	0.04	0.02	0.02	0.00	0.16	0.17
β_5	0.00	0.03	0.07	0.07	0.11	0.01	0.01	0.15
f_{KK}	0.01	0.02	0.03	0.03	0.04	0.00	0.12	0.14
$f_{\pi\pi}$	0.03	0.02	1.50	1.21	0.11	0.00	0.02	1.93
$f_{\eta\eta}$	0.00	0.01	0.02	0.02	0.02	0.00	0.10	0.10

Branching Fraction Measurement

- BFs are calculated by $$\mathcal{B}_f = \frac{\Sigma_g N_{fg}^{\mathrm{DT}}}{\Sigma_g N_g^{\mathrm{ST}} (\epsilon_{fg}^{\mathrm{DT}}/\epsilon_g^{\mathrm{ST}})[1 - \frac{2r_g R_g \cos\delta_g}{1+r_g^2}(2F_+^f - 1)]}.$$

Using $\mathcal{B}(K_S^0 \to \pi^+\pi^-) = (69.20 \pm 0.05)\%$ and $\mathcal{B}(\pi^0 \to \gamma\gamma) = (98.823 \pm 0.034)\%$ as PDG

	Branching fraction
This work	$(5.545 \pm 0.019_{\mathrm{stat.}} \pm 0.029_{\mathrm{sys.}})\%$
PDG	$(5.083 \pm 0.6)\%$

- Branching Fraction of the component (FFs > 1%) in $\bar{D}^0 \to K_S^0\pi^0\pi^+\pi^-$

Component	Branching fraction (%)
ωK_S^0	$1.170 \pm 0.009 \pm 0.027$
ϕK_S^0	$0.058 \pm 0.002 \pm 0.001$
$K^*(892)^-\rho(770)^+$	$2.134 \pm 0.023 \pm 0.089$
$\bar{K}^*(892)^0\rho(770)^0$	$0.227 \pm 0.006 \pm 0.010$
$K^*(892)^-\rho(1450)^+$	$0.176 \pm 0.008 \pm 0.009$
$(K_S^0\pi^0)^{L=1}\rho(1450)^0[P]$	$0.069 \pm 0.004 \pm 0.006$
$(K_S^0\pi^-)^{L=0}\rho(770)^+$	$0.082 \pm 0.006 \pm 0.010$
$\bar{K}^*(892)^0(\pi^+\pi^-)^{L=0}$	$0.073 \pm 0.004 \pm 0.009$
$(K_S^0\pi^0)^{L=0}(\pi^+\pi^-)^{L=0}$	$0.381 \pm 0.010 \pm 0.035$

Component	Branching fraction (%)
$K_1(1270)^-\pi^+$	$0.376 \pm 0.008 \pm 0.012$
$\bar{K}_1(1270)^0\pi^0$	$0.082 \pm 0.003 \pm 0.002$
$\bar{K}_1(1400)^0\pi^0$	$0.224 \pm 0.007 \pm 0.006$
$\bar{K}(1460)^0\pi^0$	$0.113 \pm 0.009 \pm 0.020$
$K(1460)^-\pi^+$	$0.089 \pm 0.005 \pm 0.009$
$a_1(1260)K_S^0$	$0.582 \pm 0.017 \pm 0.046$
$\pi(1300)K_S^0$	$0.113 \pm 0.006 \pm 0.014$
$a_1(1640)K_S^0$	$0.086 \pm 0.008 \pm 0.024$
$\omega(1420)K_S^0$	$0.157 \pm 0.011 \pm 0.068$
$\omega(1650)K_S^0$	$0.373 \pm 0.019 \pm 0.136$

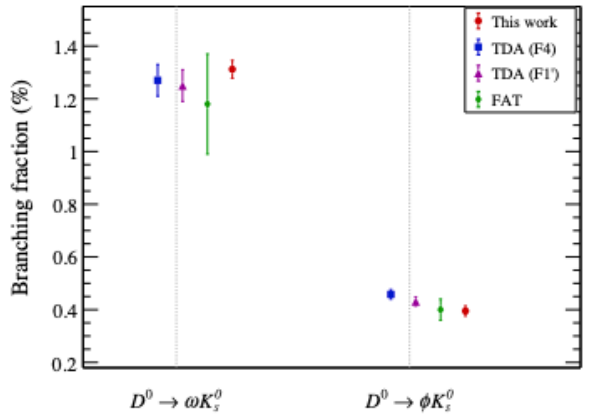


FIG. 4. Comparison of the derived $D^0 \to \omega K_S^0$ and $D^0 \to \phi K_S^0$ branching fractions with theoretical predictions.

Branching Fraction Measurement

Systematic Uncertainty

- Summation of all sources of systematic uncertainty.

Source	Uncertainty (%)
Tracking	0.2
PID	0.1
π^0 reconstruction	0.2
K_S^0 reconstruction	0.2
ST $\bar{D}^0$ yield	0.3
ΔE requirement of the signal side	0.2
DT fit	0.2
Amplitude model	0.1
Quantum correlation correction	0.2
MC statistics	0.1
Total	0.5

Event Selection

For Strong Phase Measurement

- **Partial Reconstruction**

  Tag Modes with missing track K_L^0/ν_e.

  $$E_{miss} = E_{\bar{D}^0} - \Sigma_i E_i,$$
  $$\vec{p}_{miss} = \vec{p}_{\bar{D}^0} - \Sigma_i \vec{p}_i.$$

  - $M_{BC}^{sig} \in [1.86,\ 1.87]\ \mathrm{GeV/c^2}$
  - $K_L^0 + X$ $\quad M_{miss}^2 = E_{miss}^2 - |\vec{p}_{miss}|^2$
    - ✓ No additional charged tracks, no matter good charged track or not for $K_S^0{}_{\to\pi^+\pi^-} + X$ BKG.
    - ✓ No additional π^0 or η.
  - $\nu_e + X$ $\quad U_{miss} = E_{miss} - |\vec{p}_{miss}|$
    - ✓ Only 2 good charged tracks (identified as K, e with opposite charge).
    - ✓ $E/p > 0.8$ (to reject misidentified $\mu^\pm/\pi^\pm$).

- **Kinematic Fit**

  - $K_S^0\pi^+\pi^-(\pi^0)$: Constrain final states to D^0 mass, no χ^2 cut.
  - $K_L^0\pi^+\pi^-$: Constrian K_L^0 missing mass $+2D^0$ mass + total 4-momentum.

Strong Phase Measurement

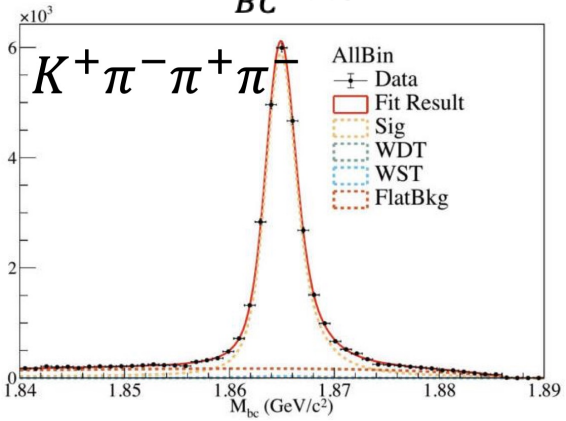
Signal Yields

- **Fully Reconstruction Mode**
  - Signal: MC shape ⊗ Gauss
  - Flat BKG: Argus
  - Peaking BKG: MC shape and fix ratio between Signal by Inc MC
  - Wrong DT and wrong ST BKG: Fix shape and yields by Inc MC
- **Partial Reconstruction Mode**

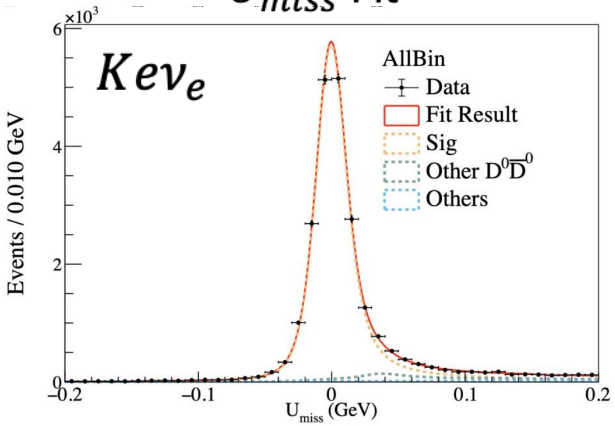
  $Ke\nu_e$
  - Signal: MC shape ⊗ Gauss
  - Other $D^0\bar{D}^0$ BKG: Inc MC shape
  - Flat BKG: 2st Chebychev function

  $K_L^0 + X$
  - Signal: MC shape ⊗ Gauss
  - Peak BKG: Inc MC shape
  - Other $D^0\bar{D}^0(D^+D^-, q\bar{q}, \dots)$ BKG: Inc MC shape
  - Flat BKG: 2st Chebychev function

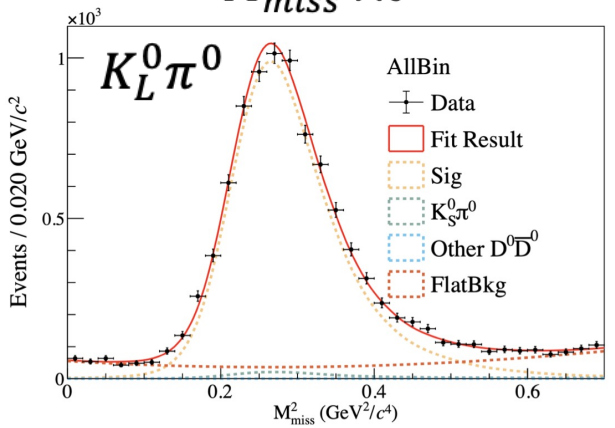
M_{BC}^{sig} Fit



U_{miss} Fit



M_{miss}^2 Fit



Strong Phase Measurement

Binning Scheme

- Uniform Binning:
  according to phase ratio and magnitude ratio

$$-\pi + \frac{2\pi}{N}(i-1) < \Delta\delta_D < -\pi + \frac{2\pi}{N}i, \quad i < 0$$
$$\pi - \frac{2\pi}{N}(-i-1) < \Delta\delta_D < \pi - \frac{2\pi}{N}(-i), \quad i > 0.$$

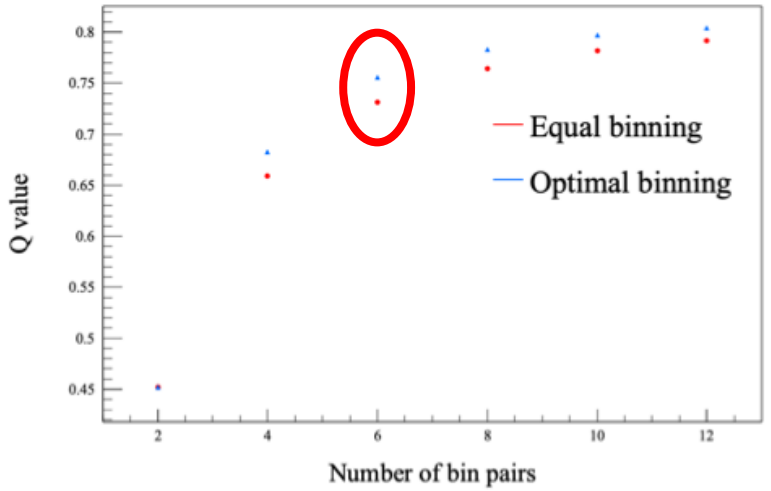
$$r_D e^{-i\delta_D} = \frac{A_{D^0}}{A_{\bar{D}^0}}$$

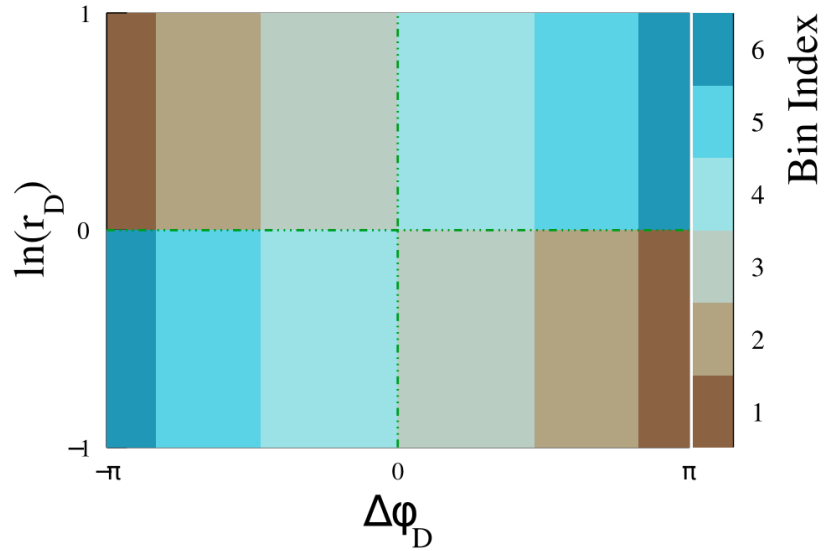
- Optimal Binning:
  optimize with Q value

$$Q_\pm^2 = \frac{\sum_i \left(\frac{1}{\sqrt{N_{B^\pm}^i}}\frac{dN_{B^\pm}^i}{dx_\pm}\right)^2 + \left(\frac{1}{\sqrt{N_{B^\pm}^i}}\frac{dN_{B^\pm}^i}{dy_\pm}\right)^2}{\int_D \left[\left(\frac{1}{\sqrt{\Gamma_{B^\pm}(\mathbf{p})}}\frac{d\Gamma_{B^\pm}(\mathbf{p})}{dx_\pm}\right)^2 + \left(\frac{1}{\sqrt{\Gamma_{B^\pm}(\mathbf{p})}}\frac{d\Gamma_{B^\pm}(\mathbf{p})}{dy_\pm}\right)^2\right] d\mathbf{p}}$$
$$= \frac{\sum_i \left[(2x_\pm K_i + 2\sqrt{K_i\bar{K}_i}c_i)^2 + (2y_\pm K_i + 2\sqrt{K_i\bar{K}_i}s_i)^2\right]/N_{B^\pm}^i}{4\sum_i K_i}$$

$r_B = 0$:

$$x_\pm = r_B\cos(\delta_B \pm \gamma) = 0, y_\pm = r_B\sin(\delta_B \pm \gamma) = 0, x_\pm^2 + y_\pm^2 = r_B = 0$$
$$N_{B^\pm}^i = K_i(x_\pm^2 + y_\pm^2) + \bar{K}_i + 2\sqrt{K_i\bar{K}_i}|(x_\pm c_i + y_\pm s_i) = \bar{K}_i$$





Strong Phase Measurement

Binning Signal Yield

Bin	$K^0_S\pi^0$	$K^0_S\eta_{\gamma\gamma}$	$K^0_S\eta'_{\pi^+\pi^-\eta}$	$K^0_S\eta'_{\pi^+\pi^-\gamma}$	$K^0_S\pi^0\pi^0$	$\pi^+\pi^-$	K^+K^-	$\pi^+\pi^-\pi^0$	$K^0_L\pi^0$	$K^0_L\pi^0\pi^0$
Uniform binning scheme										
1	231.48 ± 16.90	18.70 ± 4.87	$7.48^{+3.46}_{-2.80}$	19.85 ± 4.57	603.70 ± 27.92	595.49 ± 26.55	1624.64 ± 42.22	2577.94 ± 58.41	2913.03 ± 60.08	221.75 ± 40.50
2	217.12 ± 15.84	28.64 ± 6.04	$7.01^{+3.05}_{-2.85}$	20.40 ± 4.52	66.40 ± 10.65	79.14 ± 9.48	220.96 ± 16.01	383.58 ± 24.32	378.21 ± 22.28	176.15 ± 25.22
3	253.01 ± 16.54	36.03 ± 6.47	$8.98^{+3.34}_{-2.68}$	29.50 ± 5.68	35.83 ± 8.46	33.08 ± 6.40	92.74 ± 10.36	165.25 ± 17.49	160.79 ± 15.85	214.66 ± 22.99
4	275.99 ± 17.46	39.27 ± 6.41	9.95 ± 3.16	28.63 ± 5.73	61.73 ± 10.69	42.51 ± 6.96	127.72 ± 10.99	221.23 ± 19.43	199.90 ± 18.07	214.11 ± 24.89
5	409.24 ± 21.10	45.48 ± 6.97	18.96 ± 4.87	50.16 ± 7.15	183.23 ± 16.14	157.46 ± 13.29	481.64 ± 22.87	804.51 ± 33.31	764.62 ± 30.70	386.55 ± 35.86
6	398.10 ± 21.85	47.54 ± 7.73	$12.87^{+4.96}_{-4.30}$	45.22 ± 6.77	763.27 ± 31.57	801.83 ± 29.88	2153.33 ± 48.28	3660.95 ± 68.95	3755.90 ± 67.97	388.46 ± 52.87
Optimal binning scheme										
1	130.95 ± 13.11	10.45 ± 3.46	$6.32^{+3.35}_{-2.70}$	12.47 ± 3.46	506.99 ± 25.02	478.75 ± 23.72	1364.22 ± 38.60	2130.25 ± 52.05	2415.14 ± 54.41	142.59 ± 33.58
2	220.51 ± 15.83	24.58 ± 5.63	$5.51^{+3.13}_{-2.40}$	18.56 ± 4.41	152.08 ± 15.18	181.35 ± 14.56	408.22 ± 21.68	749.69 ± 32.98	782.85 ± 31.60	195.31 ± 28.15
3	350.01 ± 19.64	47.02 ± 7.49	10.95 ± 3.31	38.30 ± 6.36	45.57 ± 9.78	48.94 ± 7.88	164.09 ± 13.78	293.19 ± 22.32	252.06 ± 19.87	288.70 ± 27.73
4	434.25 ± 21.80	51.47 ± 7.35	$10.69^{+4.35}_{-3.72}$	48.62 ± 7.34	107.01 ± 13.40	84.32 ± 9.61	262.23 ± 15.81	443.69 ± 25.98	383.14 ± 23.61	371.07 ± 33.05
5	467.82 ± 23.06	61.27 ± 8.29	24.94 ± 5.41	59.82 ± 7.82	306.74 ± 20.57	311.28 ± 18.70	880.63 ± 31.02	1539.16 ± 45.34	1481.75 ± 42.74	438.12 ± 44.28
6	183.54 ± 14.96	19.53 ± 5.10	$4.80^{+3.69}_{-3.06}$	16.91 ± 4.06	593.83 ± 27.50	605.83 ± 25.89	1614.77 ± 41.86	2772.25 ± 59.46	2868.10 ± 59.24	192.09 ± 38.89

Table 16: Binned signal yields for $K^0_S\pi^+\pi^-\pi^0$ *VS.* $K^0_S\pi^+\pi^-\pi^0$.

Signal Bin \ Tag Bin	1	2	3	4	5	6
Uniform binning scheme						
-6	86.00 ± 12.21	27.51 ± 6.78	39.78 ± 7.78	46.78 ± 9.26	80.61 ± 10.61	167.23 ± 15.83
-5	50.71 ± 8.70	22.85 ± 5.69	$12.67^{+5.00}_{-4.26}$	24.79 ± 5.76	31.58 ± 6.85	115.91 ± 12.67
-4	49.28 ± 8.10	$5.82^{+3.45}_{-2.70}$	$6.02^{+3.31}_{-2.55}$	$9.14^{+4.41}_{-3.61}$	14.30 ± 4.55	62.37 ± 9.42
-3	32.51 ± 6.74	$2.82^{+2.87}_{-2.06}$	$12.04^{+4.53}_{-3.82}$	$10.02^{+4.52}_{-3.76}$	16.98 ± 4.91	37.72 ± 7.25
-2	30.24 ± 7.14	$6.73^{+4.26}_{-3.42}$	$5.76^{+3.55}_{-2.69}$	$4.45^{+3.72}_{-2.91}$	16.36 ± 5.31	57.07 ± 9.40
-1	56.49 ± 10.13	22.24 ± 5.72	27.91 ± 6.43	40.74 ± 7.69	49.70 ± 8.75	96.67 ± 12.71
1	37.95 ± 9.84	16.09 ± 5.20	25.75 ± 6.07	20.74 ± 5.53	50.64 ± 8.70	77.45 ± 11.69
2	18.30 ± 5.93	$4.03^{+5.32}_{-0.00}$	$0.39^{+2.03}_{-0.00}$	$6.37^{+3.97}_{-3.13}$	$4.52^{+4.23}_{-3.26}$	27.50 ± 6.95
3	37.25 ± 6.93	$2.02^{+3.60}_{-0.00}$	$0.00^{+2.59}_{-0.00}$	$6.13^{+3.92}_{-3.13}$	$4.40^{+4.18}_{-3.26}$	39.95 ± 7.48
4	43.38 ± 7.62	$9.87^{+4.45}_{-3.64}$	$2.94^{+3.97}_{-0.00}$	$6.55^{+4.59}_{-3.82}$	$4.27^{+3.43}_{-2.51}$	41.27 ± 7.61
5	45.44 ± 8.57	$4.47^{+3.88}_{-3.11}$	$7.17^{+4.18}_{-3.27}$	$10.56^{+4.98}_{-4.17}$	$9.39^{+6.09}_{-4.94}$	45.91 ± 8.96
6	69.71 ± 11.47	23.85 ± 6.47	34.30 ± 7.36	23.39 ± 6.17	46.57 ± 8.65	76.87 ± 12.58
Optimal binning scheme						
-6	26.34 ± 7.09	34.83 ± 7.22	34.31 ± 7.25	46.62 ± 8.94	75.36 ± 10.35	71.24 ± 10.01
-5	60.55 ± 9.36	32.32 ± 7.27	26.64 ± 6.65	47.28 ± 8.51	86.77 ± 11.31	90.69 ± 11.20
-4	53.85 ± 8.65	18.78 ± 5.62	$13.32^{+5.17}_{-4.41}$	18.63 ± 5.39	46.31 ± 8.61	70.31 ± 9.82
-3	39.24 ± 7.27	$6.16^{+4.94}_{-4.15}$	14.88 ± 4.62	17.88 ± 5.33	32.37 ± 7.15	45.11 ± 7.88
-2	32.72 ± 7.57	$12.00^{+4.88}_{-4.09}$	$14.71^{+5.37}_{-4.60}$	17.77 ± 5.86	29.94 ± 7.19	43.67 ± 8.16
-1	18.98 ± 5.94	31.19 ± 6.92	25.78 ± 6.15	37.67 ± 7.48	70.21 ± 9.94	33.75 ± 8.01
1	$18.63^{+7.52}_{-6.66}$	$13.94^{+5.86}_{-5.04}$	26.20 ± 5.82	32.30 ± 6.72	45.44 ± 8.65	30.87 ± 7.65
2	22.55 ± 6.33	$11.30^{+6.82}_{-5.76}$	$4.72^{+4.24}_{-3.28}$	16.41 ± 5.17	$18.06^{+6.56}_{-5.76}$	24.98 ± 6.32
3	36.52 ± 7.08	$7.99^{+5.07}_{-4.11}$	$0.38^{+4.12}_{-0.00}$	$9.44^{+5.14}_{-4.27}$	$18.22^{+6.66}_{-5.80}$	39.94 ± 7.42
4	47.28 ± 8.09	21.32 ± 5.75	$7.14^{+4.58}_{-3.66}$	$9.31^{+6.37}_{-5.23}$	22.82 ± 6.36	41.54 ± 7.82
5	49.83 ± 9.20	21.42 ± 6.41	18.54 ± 5.53	22.98 ± 6.69	$19.15^{+7.61}_{-6.65}$	45.64 ± 8.82
6	21.84 ± 6.92	23.41 ± 6.49	29.89 ± 6.88	29.67 ± 6.71	48.66 ± 8.94	26.18 ± 7.93

Table 17: Binned signal yields for $K^0_S\pi^+\pi^-\pi^0$ *VS.* $K^0_S\pi^+\pi^-$.

Signal Bin \ Tag Bin	1	2	3	4	5	6	7	8
Uniform binning scheme								
-6	638.57 ± 26.80	294.63 ± 18.50	257.15 ± 16.98	62.31 ± 8.71	90.40 ± 11.27	95.79 ± 10.90	289.86 ± 18.22	359.07 ± 19.98
-5	147.69 ± 13.47	82.10 ± 9.92	106.81 ± 10.89	49.50 ± 7.61	70.87 ± 9.42	54.66 ± 8.35	107.03 ± 11.26	93.46 ± 10.76
-4	51.28 ± 8.65	27.99 ± 5.57	38.56 ± 6.82	19.29 ± 4.64	60.87 ± 8.49	30.35 ± 6.33	42.61 ± 7.16	60.00 ± 7.75
-3	62.25 ± 8.85	27.20 ± 5.85	21.11 ± 5.04	$9.05^{+3.77}_{-3.03}$	39.46 ± 7.03	21.80 ± 5.01	34.48 ± 6.40	45.05 ± 7.54
-2	104.03 ± 11.32	53.99 ± 7.92	20.73 ± 5.63	16.01 ± 4.00	38.85 ± 7.26	17.35 ± 5.02	50.12 ± 7.58	74.77 ± 9.74
-1	503.28 ± 23.92	192.69 ± 15.14	130.13 ± 12.20	32.13 ± 6.19	50.46 ± 9.16	81.86 ± 10.05	204.10 ± 15.57	250.98 ± 17.04
1	405.20 ± 21.68	161.96 ± 13.53	120.22 ± 12.14	29.08 ± 6.19	30.46 ± 7.39	47.73 ± 8.14	106.70 ± 11.23	201.55 ± 15.28
2	51.31 ± 8.31	26.82 ± 5.87	30.35 ± 5.89	17.92 ± 4.94	22.44 ± 6.19	15.25 ± 4.68	$14.31^{+5.25}_{-4.42}$	19.87 ± 5.20
3	30.37 ± 6.55	21.96 ± 4.69	26.95 ± 6.08	17.44 ± 4.53	45.54 ± 7.42	$12.10^{+4.46}_{-3.72}$	$9.05^{+4.33}_{-3.43}$	17.56 ± 5.19
4	40.73 ± 7.43	$8.00^{+4.07}_{-3.26}$	11.47 ± 3.82	$4.90^{+3.33}_{-2.62}$	35.49 ± 6.92	16.90 ± 4.55	33.19 ± 6.30	13.40 ± 4.32
5	102.47 ± 11.26	21.78 ± 5.62	15.71 ± 4.91	12.42 ± 4.01	61.76 ± 8.57	40.97 ± 6.92	52.03 ± 7.94	63.41 ± 8.95
6	567.91 ± 25.53	163.52 ± 13.77	100.04 ± 11.15	29.88 ± 6.39	66.69 ± 9.92	78.51 ± 9.74	189.44 ± 15.03	290.41 ± 18.43
Optimal binning scheme								
-6	451.18 ± 22.48	203.10 ± 15.32	158.52 ± 13.22	42.89 ± 7.18	55.90 ± 8.69	72.24 ± 9.51	197.26 ± 14.70	252.87 ± 16.69
-5	293.71 ± 18.66	153.35 ± 13.43	179.16 ± 14.28	54.11 ± 7.98	82.39 ± 10.51	63.23 ± 8.84	166.87 ± 14.32	170.06 ± 14.22
-4	93.65 ± 11.15	49.40 ± 7.72	65.02 ± 8.73	33.65 ± 6.23	83.09 ± 10.05	45.60 ± 7.80	74.23 ± 9.25	91.71 ± 10.18
-3	89.23 ± 10.48	46.40 ± 7.56	26.24 ± 5.78	17.04 ± 4.65	55.34 ± 8.32	28.91 ± 6.04	54.97 ± 8.07	64.49 ± 9.14
-2	154.40 ± 13.86	63.95 ± 8.96	43.28 ± 7.48	14.97 ± 3.87	35.89 ± 7.28	30.39 ± 6.24	89.33 ± 10.19	104.44 ± 11.18
-1	424.29 ± 21.76	162.39 ± 13.70	104.40 ± 10.95	24.22 ± 5.37	36.94 ± 8.01	61.48 ± 8.71	144.84 ± 13.17	200.99 ± 15.21
1	336.50 ± 19.54	137.46 ± 12.42	101.55 ± 11.12	25.88 ± 5.76	18.83 ± 6.09	43.69 ± 7.63	95.10 ± 10.50	169.13 ± 13.79
2	102.57 ± 11.50	41.81 ± 7.11	41.92 ± 7.14	13.14 ± 4.23	17.17 ± 5.71	$13.11^{+4.89}_{-4.11}$	24.29 ± 5.91	49.22 ± 8.08
3	47.06 ± 8.10	32.95 ± 5.76	34.75 ± 6.61	24.83 ± 5.56	61.56 ± 8.74	17.99 ± 5.07	$9.77^{+4.55}_{-3.70}$	21.56 ± 5.73
4	60.50 ± 8.87	16.19 ± 4.85	15.84 ± 4.49	$10.63^{+4.24}_{-3.52}$	51.77 ± 8.25	30.38 ± 5.95	50.89 ± 7.78	31.13 ± 6.33
5	212.94 ± 16.09	50.66 ± 8.17	26.32 ± 6.08	16.38 ± 4.96	82.66 ± 10.27	54.06 ± 8.12	82.72 ± 9.99	124.36 ± 12.50
6	437.65 ± 22.23	127.15 ± 12.11	83.89 ± 10.14	19.89 ± 5.00	29.34 ± 6.83	54.04 ± 8.11	139.76 ± 12.91	211.76 ± 15.62

Table 18: Binned signal yields for $K^0_S\pi^+\pi^-\pi^0$ *VS.* $K^0_L\pi^+\pi^-$.

Signal Bin \ Tag Bin	1	2	3	4	5	6	7	8
Uniform binning scheme								
-6	624.80 ± 28.24	272.80 ± 19.67	273.66 ± 23.62	211.35 ± 17.33	742.57 ± 33.54	387.30 ± 23.71	610.85 ± 26.98	588.24 ± 26.90
-5	384.71 ± 22.39	138.38 ± 14.74	91.56 ± 12.56	$24.57^{+8.62}_{-7.93}$	201.80 ± 17.67	146.17 ± 14.19	335.88 ± 19.57	311.04 ± 19.29
-4	224.57 ± 17.46	90.43 ± 12.54	66.89 ± 9.28	$15.93^{+6.85}_{-6.17}$	60.78 ± 10.06	57.25 ± 8.80	130.09 ± 12.70	189.16 ± 15.14
-3	199.18 ± 16.19	86.14 ± 10.08	54.42 ± 9.49	22.55 ± 5.74	42.29 ± 8.73	40.08 ± 7.16	95.09 ± 10.26	104.30 ± 11.64
-2	212.53 ± 16.44	94.75 ± 11.11	78.42 ± 11.28	30.11 ± 7.97	93.51 ± 12.56	49.93 ± 8.57	87.09 ± 10.89	128.40 ± 13.09
-1	396.51 ± 23.18	210.64 ± 17.49	238.63 ± 19.30	158.25 ± 16.19	506.82 ± 31.83	253.18 ± 18.81	370.86 ± 21.77	278.47 ± 19.86
1	298.68 ± 19.55	98.81 ± 12.57	161.50 ± 15.64	110.07 ± 13.16	520.55 ± 30.91	228.85 ± 19.27	248.13 ± 18.11	221.74 ± 17.05
2	138.55 ± 13.89	38.32 ± 6.96	$5.50^{+8.02}_{-5.50}$	$6.11^{+4.03}_{-3.38}$	66.32 ± 11.36	20.79 ± 6.59	66.50 ± 9.58	90.85 ± 11.37
3	166.00 ± 15.23	38.19 ± 8.17	28.35 ± 7.43	$5.38^{+4.45}_{-3.73}$	26.75 ± 6.88	$12.04^{+5.59}_{-4.89}$	59.74 ± 9.14	96.81 ± 10.96
4	165.29 ± 15.61	49.81 ± 8.68	56.37 ± 9.70	20.61 ± 6.83	24.51 ± 7.65	$12.44^{+5.19}_{-4.58}$	27.55 ± 6.52	71.68 ± 9.85
5	260.36 ± 18.78	91.93 ± 11.92	120.62 ± 13.58	64.21 ± 10.42	97.39 ± 12.67	$20.45^{+9.65}_{-8.99}$	52.14 ± 8.48	103.43 ± 12.45
6	416.40 ± 23.82	162.63 ± 16.14	255.33 ± 20.10	231.31 ± 18.08	619.73 ± 34.95	220.25 ± 21.51	209.41 ± 16.52	206.30 ± 16.43
Optimal binning scheme								
-6	378.54 ± 21.78	165.40 ± 15.49	185.94 ± 16.33	148.04 ± 14.43	538.09 ± 28.94	267.54 ± 19.30	390.98 ± 21.72	362.15 ± 21.06
-5	498.71 ± 25.29	193.01 ± 17.04	139.54 ± 15.99	84.52 ± 11.87	368.99 ± 23.57	218.67 ± 17.52	447.67 ± 22.76	445.46 ± 23.06
-4	354.76 ± 22.08	146.74 ± 15.22	107.50 ± 12.04	$16.21^{+8.07}_{-7.38}$	105.55 ± 13.25	103.54 ± 11.73	235.10 ± 16.59	279.00 ± 18.72
-3	271.29 ± 18.80	122.76 ± 12.87	88.09 ± 11.73	32.43 ± 7.49	75.67 ± 11.71	61.48 ± 8.89	128.97 ± 12.24	144.06 ± 13.97
-2	267.85 ± 18.61	116.88 ± 12.66	99.01 ± 13.26	64.27 ± 10.11	143.51 ± 17.75	63.48 ± 9.91	135.33 ± 13.62	162.43 ± 14.80
-1	268.99 ± 19.41	150.00 ± 14.69	184.58 ± 16.69	119.88 ± 14.29	430.16 ± 27.47	216.81 ± 17.28	279.66 ± 18.71	206.66 ± 16.94
1	221.31 ± 16.62	81.07 ± 11.19	152.61 ± 14.64	101.32 ± 12.61	439.96 ± 28.00	177.03 ± 17.67	177.72 ± 15.09	174.61 ± 15.04
2	153.12 ± 14.54	46.69 ± 7.59	$16.12^{+9.79}_{-9.17}$	$9.37^{+5.36}_{-4.69}$	136.91 ± 14.80	59.74 ± 9.68	113.49 ± 12.41	105.99 ± 11.51
3	227.75 ± 17.96	48.04 ± 9.04	27.31 ± 7.91	$12.72^{+5.23}_{-4.57}$	38.72 ± 8.69	20.27 ± 6.43	79.20 ± 10.72	128.35 ± 12.71
4	269.26 ± 19.26	78.67 ± 10.98	83.84 ± 11.87	36.57 ± 8.68	41.54 ± 9.58	$18.94^{+7.96}_{-6.14}$	42.01 ± 7.97	104.11 ± 12.05
5	316.94 ± 21.16	132.48 ± 14.17	169.26 ± 16.50	105.69 ± 13.23	217.31 ± 20.06	44.67 ± 11.46	69.40 ± 9.67	121.40 ± 13.12
6	256.02 ± 18.46	92.12 ± 12.68	173.40 ± 16.21	168.93 ± 15.34	483.95 ± 29.98	181.10 ± 19.63	177.05 ± 14.42	158.29 ± 14.10

Strong Phase Measurement

Parameters Measurement

➢ Expected DT yields

flavor

$$N_i^{fg} + N_i^{f\bar{g}} = \frac{S^g + S^{\bar{g}}}{\epsilon^g(1+r_{\bar{g}}^2)} B_f \epsilon_{ij}^{fg} \left[T_j^f + r_{\bar{g}}^2 \bar{T}_j^f - 2r_{\bar{g}} R_{\bar{g}} \sqrt{T_j^f \bar{T}_j^f} (c_j^f \cos\delta_{\bar{g}} - s_j^f \sin\delta_{\bar{g}}) \right]$$

CP

$$N_i^{fg} = \frac{S^g}{\epsilon^g \left[2 - 2y(2F_+^g - 1) \right]} B_f \epsilon_{ij}^{fg} \left[T_j^f + \bar{T}_j^f - (2F_+^g - 1) 2 \sqrt{T_j^f \bar{T}_j^f} c_j^f \right]$$

$K_{S,L}^0 \pi^+ \pi^- (\pi^0)$

$$N_{ij}^{fg} = \frac{S^g}{\epsilon^g \left[2 - 2y(2F_+^g - 1) \right]} B_f \epsilon_{ij,kl}^{fg} \left[T_k^f \bar{T}_l^g + \bar{T}_k^f T_l^g - 2 \sqrt{T_k^f \bar{T}_k^f T_l^g \bar{T}_l^g} (c_k^f c_l^g + s_k^f s_l^g) \right]$$

Input parameters	Reference	Fit Parameters
$N_{D\bar{D}}, B_g$ (for $K_L^0 X$ and Kev_e)	CPC 48, 123001 (2024), PDG	B_f, R_i, c_i, s_i $R_i = \begin{cases} T_i, & i = -6 \\ T_i \Big/ \sum_{j \le i} T_j, & -6 < i < 6 \\ 1, & i = 6 \end{cases}$
ST yields (S^g) and efficiency (ϵ^g)	BESIII Doc-1504 and Doc-1600	
r and δ of Kpi, y	HFLAV	
r, R and δ of Kpipi0 and K3pi	JHEP05(2021)164	
Ki/ci/si of $K_{S,L}^0 \pi^+ \pi^-$	JHEP06(2025)086	
Ki/ci/si of $K_{S,L}^0 \pi^+ \pi^- \pi^0$	BESIII Doc-1540 Model prediction	

Strong Phase Measurement

Likelihood Construction

➢ Likelihood fit: $-2\ln L = -2\sum_i \ln G(N_{obs_i}^{exp}; p_{obs_i}^{fit})$

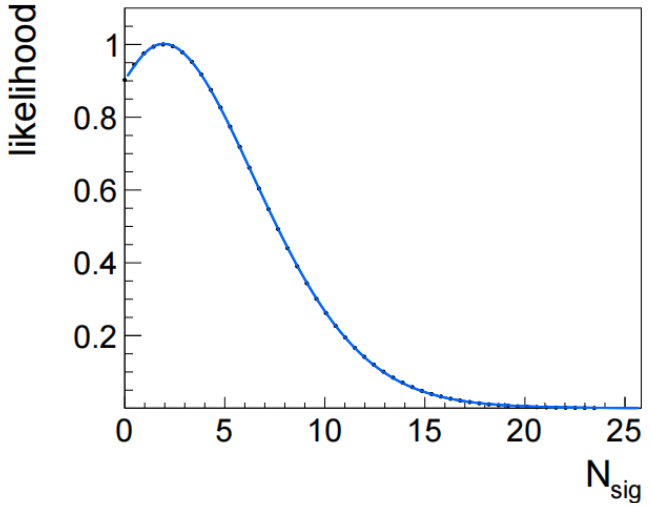
- $N_{obs_i}^{exp}$: The expected event number
- $G(x;p)$: The likelihood function of N_{sig} in DT fit
- $p_{obs_i}^{fit}$: parameters of likelihood distribution

Nominal fit to obtain the N_{sig}^{obs} and σ_{sig}^{obs} $\xrightarrow{N_{sig}^{obs}/\sigma_{sig}^{obs} < 3}$

$N_{sig}^{obs}/\sigma_{sig}^{obs} >= 3$ ↓

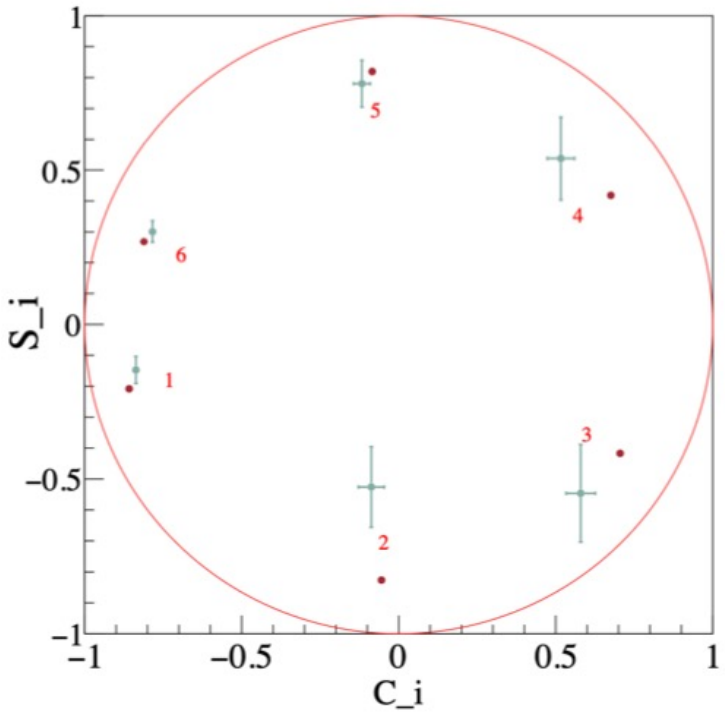
$$G(N;p) = Gaus(N; N_{sig}^{obs}, \sigma_{sig}^{obs})$$

Fit to N_{sig}^{obs} v. s. likelihood

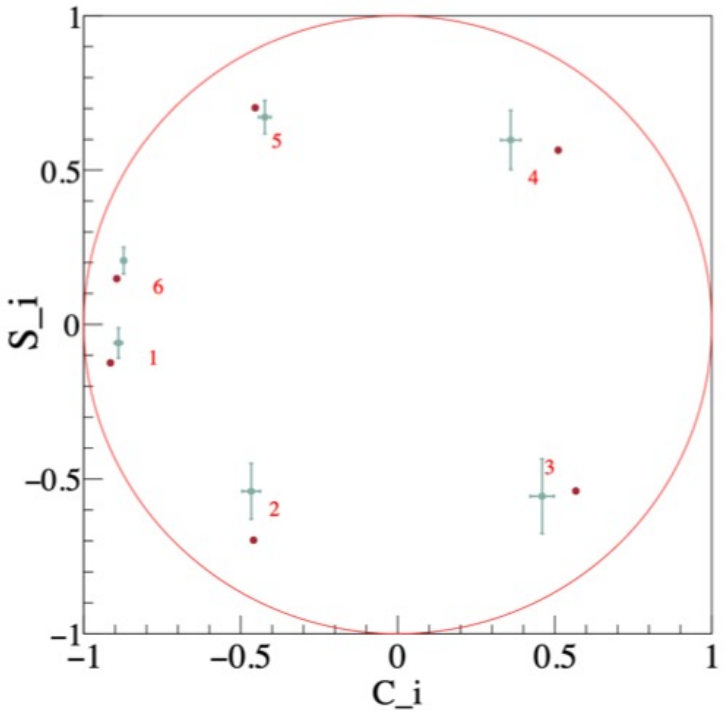


Strong Phase Measurement

Fit Result



Uniform binning scheme



Optimized binning scheme

Parameter	Uniform binning scheme	Optimized binning scheme
R_{-6}	$0.12454 \pm 0.00120 \pm 0.00077$	$0.09935 \pm 0.00111 \pm 0.00056$
R_{-5}	$0.02608 \pm 0.00064 \pm 0.00035$	$0.04627 \pm 0.00079 \pm 0.00051$
R_{-4}	$0.01096 \pm 0.00049 \pm 0.00018$	$0.01835 \pm 0.00059 \pm 0.00026$
R_{-3}	$0.01125 \pm 0.00049 \pm 0.00035$	$0.01606 \pm 0.00057 \pm 0.00029$
R_{-2}	$0.01485 \pm 0.00056 \pm 0.00031$	$0.02654 \pm 0.00070 \pm 0.00032$
R_{-1}	$0.12350 \pm 0.00134 \pm 0.00060$	$0.10880 \pm 0.00130 \pm 0.00056$
R_1	$0.26296 \pm 0.00175 \pm 0.00074$	$0.20158 \pm 0.00168 \pm 0.00084$
R_2	$0.09850 \pm 0.00136 \pm 0.00057$	$0.13635 \pm 0.00146 \pm 0.00063$
R_3	$0.08296 \pm 0.00134 \pm 0.00077$	$0.11605 \pm 0.00147 \pm 0.00091$
R_4	$0.11824 \pm 0.00159 \pm 0.00083$	$0.19288 \pm 0.00186 \pm 0.00078$
R_5	$0.28304 \pm 0.00230 \pm 0.00082$	$0.48064 \pm 0.00276 \pm 0.00114$
c_1	$-0.83688 \pm 0.01189 \pm 0.00523$	$-0.88946 \pm 0.01255 \pm 0.00892$
c_2	$-0.08719 \pm 0.04119 \pm 0.01199$	$-0.46649 \pm 0.02879 \pm 0.00782$
c_3	$0.57957 \pm 0.04638 \pm 0.02500$	$0.45974 \pm 0.03769 \pm 0.01307$
c_4	$0.51644 \pm 0.04350 \pm 0.00863$	$0.35979 \pm 0.03185 \pm 0.00825$
c_5	$-0.11715 \pm 0.02653 \pm 0.00741$	$-0.42312 \pm 0.01930 \pm 0.00846$
c_6	$-0.78397 \pm 0.01067 \pm 0.00582$	$-0.87279 \pm 0.01166 \pm 0.00511$
s_1	$-0.14755 \pm 0.04362 \pm 0.01379$	$-0.06007 \pm 0.04872 \pm 0.01567$
s_2	$-0.52576 \pm 0.13010 \pm 0.03822$	$-0.53956 \pm 0.08993 \pm 0.02912$
s_3	$-0.54616 \pm 0.15770 \pm 0.06980$	$-0.55559 \pm 0.12060 \pm 0.03858$
s_4	$0.53764 \pm 0.13447 \pm 0.03409$	$0.59779 \pm 0.09645 \pm 0.04176$
s_5	$0.78028 \pm 0.07572 \pm 0.03429$	$0.67211 \pm 0.05366 \pm 0.02973$
s_6	$0.30089 \pm 0.03525 \pm 0.01802$	$0.20634 \pm 0.04309 \pm 0.01531$
Br	$0.05413 \pm 0.00015 \pm 0.00161$	$0.05419 \pm 0.00015 \pm 0.00161$
$Br_{K^0_L\pi^+\pi^-}$	$0.05439 \pm 0.00052 \pm 0.00453$	$0.05434 \pm 0.00052 \pm 0.00468$

Red Line: Prediction by Amplitude Mode

Strong Phase Measurement

Systematic Uncertainty

Pseudo-experiments are performed by sampling the relevant quantities according to their uncertainties for 1000 times, and repeating the fit to extract the strong phase parameters. The standard deviations of the parameter distributions are taken as systematic uncertainties.

- **ST yields and efficiency:** The ST yields and efficiencies are varied according to their uncertainties.
- **DT yields:**
  - ✓ **Signal shape:** Replace the Gaussian function of resolution to double-Gaussian.
  - ✓ **Peaking BKG:** Vary the BKG and signal ratio according to the error propagated from BF, ϵ and QC factor.
  - ✓ **Wrong ST/DT BKG:** Vary the background yields according to statistical uncertainties
- **Input Parameter:** Vary the hadronic parameters, charm mixing parameters, c_i, s_i of $K_s/K_L\pi^+\pi^-, F_+^{\pi^+\pi^-\pi^0}$ according to their uncertainties.
- **MC statistics:** Vary the efficiencies matrix within their statistical uncertainties.
- **PID & tracking efficiency:** Vary the data-MC efficiency ratios for tracking and PID from works of Yijia Zeng, the differences in this result between the nominal result is taken as uncertainty
- **Amplitude model:** Vary the amplitude model based on its error matrix, then re-weight the PHSP MC to get the efficiency matrix

Strong Phase Measurement

Systematic Uncertainty

Parameter	ST yields	Signal shape	Peak background	WST background	WDT background	Input parameters	Ks Reconstruction	Pi Reconstruction	Pi0 Reconstruction	MC statistics	MC model	Total
Ri_{-6}	0.57	3.10	0.40	0.01	0.01	3.31	2.44	0.52	0.10	3.16	4.65	7.68
Ri_{-5}	0.28	0.54	0.10	0.00	0.00	2.87	0.44	0.21	0.05	1.58	0.94	3.50
Ri_{-4}	0.03	0.28	0.12	0.01	0.00	1.01	0.18	0.15	0.01	1.12	0.97	1.84
Ri_{-3}	0.07	1.87	0.10	0.00	0.00	0.59	0.20	0.06	0.10	1.14	2.69	3.53
Ri_{-2}	0.12	2.57	0.08	0.00	0.00	0.85	0.32	0.12	0.02	1.28	0.87	3.14
Ri_{-1}	0.21	1.52	0.34	0.01	0.01	2.09	3.31	0.88	0.33	3.40	2.38	5.99
Ri_{1}	0.26	3.32	0.65	0.02	0.02	3.10	2.74	0.24	0.51	4.15	3.01	7.43
Ri_{2}	0.21	1.63	0.42	0.02	0.01	2.80	1.97	1.27	0.30	3.30	2.31	5.70
Ri_{3}	0.41	0.13	0.52	0.02	0.01	2.86	0.97	0.64	0.91	3.16	6.26	7.74
Ri_{4}	0.44	6.65	0.81	0.02	0.01	1.29	0.65	2.29	0.53	3.77	1.31	8.29
Ri_{5}	0.42	2.72	0.85	0.04	0.02	2.27	2.99	2.71	0.19	5.38	2.97	8.22
c_1	31.30	1.23	9.65	0.20	0.11	27.22	3.30	0.91	8.32	8.20	27.83	52.33
c_2	52.94	95.61	9.47	1.13	0.89	17.01	3.63	12.11	29.45	22.42	22.65	119.87
c_3	25.70	184.21	13.16	0.82	0.76	27.76	3.41	7.48	18.01	45.69	156.40	249.96
c_4	28.84	33.99	13.82	0.62	0.34	31.88	1.54	4.25	22.54	49.14	36.10	86.26
c_5	61.33	5.57	8.11	0.42	0.21	22.34	1.66	1.07	23.78	16.05	17.31	74.05
c_6	39.65	15.63	9.22	0.17	0.13	28.62	2.37	1.41	9.60	8.72	22.09	58.18
s_1	0.10	39.04	28.71	0.64	0.21	105.44	5.25	2.93	1.96	32.24	66.78	137.86
s_2	6.97	128.73	51.19	3.13	2.64	315.40	19.60	45.75	19.62	104.68	116.13	382.16
s_3	6.05	602.32	50.10	2.60	2.22	311.88	12.20	9.32	2.28	117.43	102.77	698.00
s_4	4.93	159.15	46.68	4.50	3.17	261.03	2.50	22.79	4.63	103.81	95.71	340.86
s_5	12.25	158.89	28.63	3.50	0.55	290.61	5.91	6.33	29.58	53.22	56.07	342.94
s_6	7.78	120.42	31.53	0.40	0.17	113.29	6.31	2.09	9.55	24.30	57.96	180.21
Br	2.12	1.69	0.04	0.00	0.00	0.58	4.25	7.62	13.29	0.41	0.26	16.14
$Br_{K\pi\pi\pi}$	38.90	7.06	0.50	0.00	0.00	2.32	4.06	17.25	12.95	0.32	1.11	45.30

Parameter	ST yields	Signal shape	Peak background	WST background	WDT background	Input parameters	Ks Reconstruction	Pi Reconstruction	Pi0 Reconstruction	MC statistics	MC model	Total
Ri_{-6}	0.37	2.09	0.33	0.01	0.00	1.93	2.64	0.38	0.15	2.97	2.64	5.59
Ri_{-5}	0.47	0.71	0.13	0.01	0.00	4.07	0.54	0.27	0.12	1.99	1.99	5.05
Ri_{-4}	0.13	0.34	0.14	0.00	0.00	1.74	0.27	0.22	0.01	1.38	1.26	2.61
Ri_{-3}	0.05	1.40	0.12	0.01	0.01	0.90	0.30	0.04	0.13	1.30	1.98	2.92
Ri_{-2}	0.15	1.56	0.09	0.00	0.00	1.59	0.38	0.23	0.01	1.63	1.54	3.20
Ri_{-1}	0.26	0.22	0.31	0.01	0.00	1.62	3.45	1.03	0.32	3.37	1.99	5.58
Ri_{1}	0.40	5.24	0.58	0.01	0.01	1.88	3.70	0.58	0.58	4.13	2.91	8.45
Ri_{2}	0.24	0.43	0.43	0.02	0.01	3.61	2.14	1.73	0.05	3.59	2.36	6.29
Ri_{3}	0.44	2.71	0.60	0.01	0.01	3.83	1.58	0.33	1.08	3.48	6.65	9.09
Ri_{4}	0.58	4.09	0.91	0.01	0.01	1.82	1.09	3.47	0.59	4.46	2.33	7.75
Ri_{5}	0.56	4.33	0.95	0.02	0.01	2.94	5.93	1.09	0.07	6.75	4.41	11.40
c_1	27.04	73.64	9.95	1.11	0.18	26.01	2.88	0.07	8.35	11.42	28.59	89.20
c_2	44.42	46.85	11.43	1.17	0.48	26.74	1.07	5.74	16.34	22.04	17.85	78.23
c_3	36.57	57.18	9.08	0.61	0.38	26.72	3.54	9.04	23.20	39.68	97.29	130.67
c_4	47.98	31.85	10.49	0.39	0.19	26.88	1.31	1.58	24.28	34.35	29.75	82.51
c_5	59.32	45.24	9.55	0.23	0.12	27.34	0.08	0.21	18.77	13.28	15.00	84.60
c_6	29.99	11.20	9.57	0.56	0.20	28.80	1.24	2.11	6.47	12.04	21.74	51.10
s_1	0.62	60.32	29.89	0.77	0.26	114.68	1.31	3.07	1.85	32.98	75.94	156.69
s_2	7.75	143.28	36.74	2.81	1.58	220.26	15.94	43.85	11.66	65.86	87.61	291.18
s_3	4.98	142.27	41.06	4.38	3.32	331.64	13.18	18.94	2.29	89.93	90.81	385.80
s_4	8.49	313.96	36.96	2.60	1.31	245.43	5.11	21.04	22.26	69.09	91.46	417.56
s_5	13.64	113.82	28.50	1.77	0.61	261.24	3.72	2.87	22.51	38.76	64.35	297.28
s_6	4.73	105.48	34.83	1.03	0.33	86.63	4.01	1.16	6.99	30.17	50.90	153.08
Br	2.13	0.64	0.04	0.00	0.00	0.58	4.26	7.62	13.30	0.42	0.26	16.08
$Br_{K\pi\pi\pi}$	38.84	13.97	0.41	0.00	0.00	2.33	4.06	17.24	12.94	0.34	1.08	46.81

Strong Phase Measurement

I/O Check

To validate the likelihood fit of the strong phase parameters:

- The signal yields are calculated with model predicted strong phase parameters, and then are re-sampled in Poisson distribution for each toy bin for 500 times.
- Re-perform the likelihood fit to extract strong phase parameters.

$$N_{f_i g}^{\rm sig} = \frac{N_g^{\rm ST}}{2\varepsilon_g^{ST}\left[1-(2F_+^g-1)y_D\right]}\mathcal{B}^f\sum_j \varepsilon_{ij}^{DT}\cdot\left[\bar{T}_j^f + T_j^f - 2\sqrt{T_j^f\bar{T}_j^f}c_j^f(2F_+^g-1)\right],$$

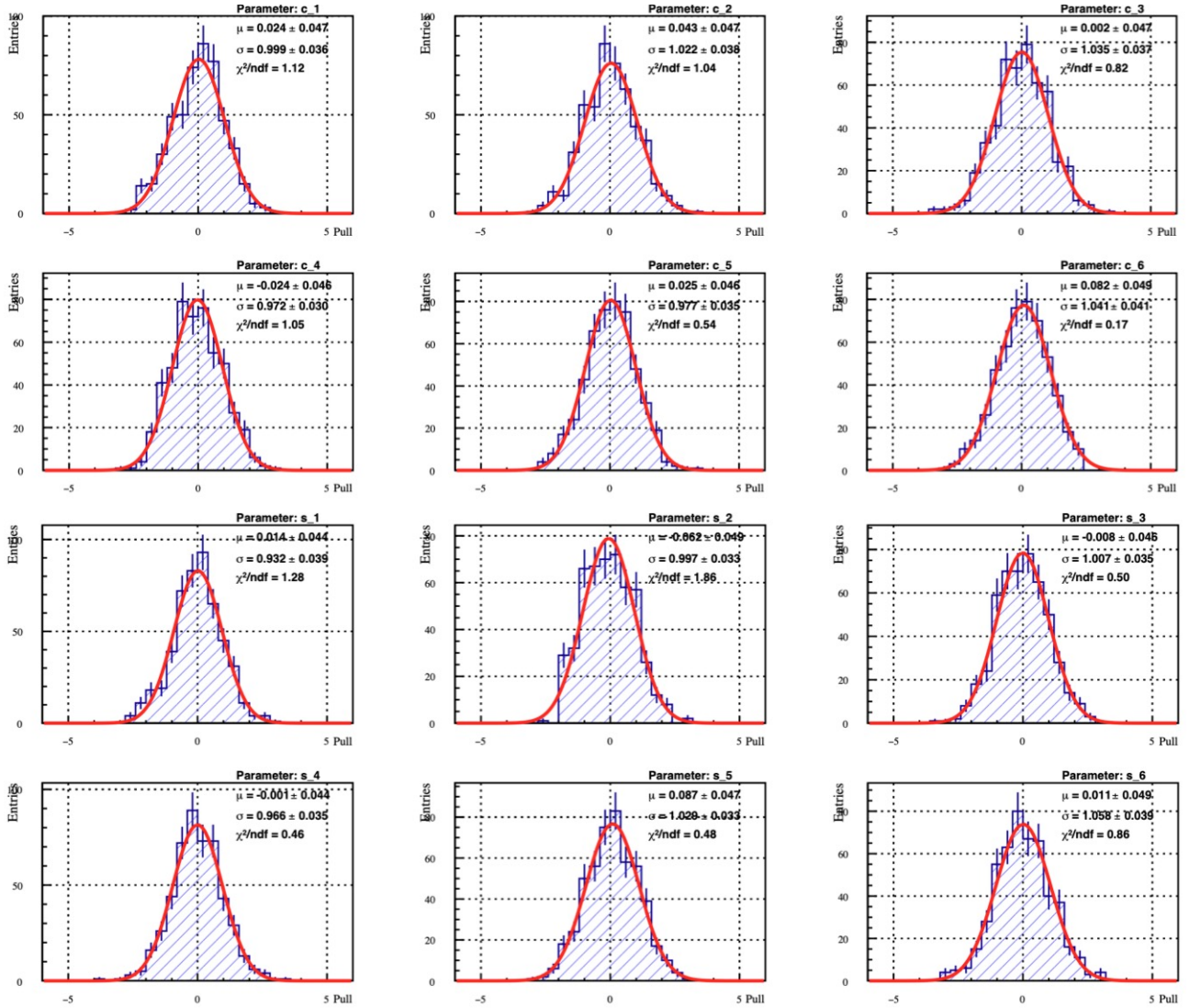
$$N_{f_i g}^{\rm sig} = \frac{N_g^{ST}}{\varepsilon^{ST}}\mathcal{B}^f\sum_j \varepsilon_{ij}^{DT}\cdot\left[\bar{T}_j^f + r_g^2 T_j^f - 2r_g R_g\sqrt{T_j^f\bar{T}_j^f}\left(c_j^f\cos(\Delta\delta^g)+s_j^f\sin(\Delta\delta^g)\right)\right],$$

$$N_{f_i g_j}^{\rm sig} = \frac{N_g^{\rm ST}}{2\varepsilon_g^{ST}\left[1-(2F_+^g-1)y_D\right]}\mathcal{B}^f\sum_{mn} \varepsilon_{im,jn}^{DT}\cdot\left[T_m^f\bar{T}_n^g + \bar{T}_m^f T_n^g \mp 2\sqrt{T_m^f\bar{T}_n^g\bar{T}_m^f T_n^g}\left(c_m^f c_n^g + s_m^f s_n^g\right)\right].$$

$$\chi = \frac{\mu_{fit}-\mu_{exp}}{\sigma_{fit}}$$

Strong Phase Measurement

I/O Check



Strong Phase Measurement

Impact on γ measurement

- Generate 1000 toy parameters according to correlation matrix in this work and calculate expected B decay yields.
- Extract γ by fitting expected B decay yields.
- The contribution to γ:
  - ✓ Uniform binning scheme: 1.234°
  - ✓ Optimal binning scheme: 1.167°

$$N\left[B^- \to DK^-, D \to f_i\right] = h_B\left[\bar{T}_i^f r_B^2 + T_i^f + 2\sqrt{T_i^f \bar{T}_i^f}\left(c_i^f x_- + s_i^f y_-\right)\right]$$

$$N\left[B^+ \to DK^+, D \to f_i\right] = h_B\left[T_i^f r_B^2 + \bar{T}_i^f + 2\sqrt{T_i^f \bar{T}_i^f}\left(c_i^f x_+ + s_i^f y_+\right)\right]$$

Normalization factor

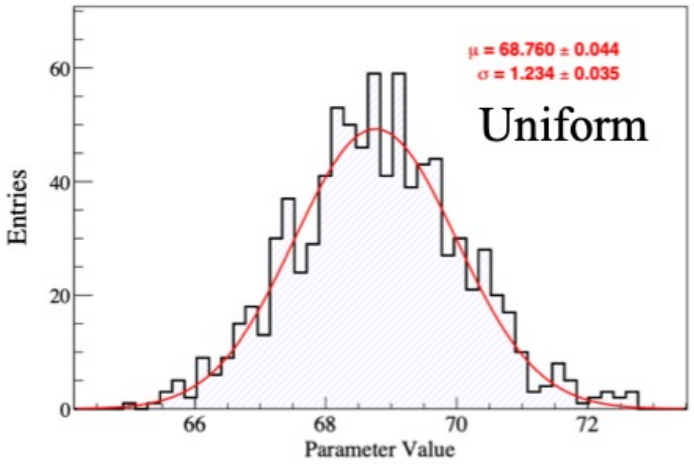
h_B is set to 1M

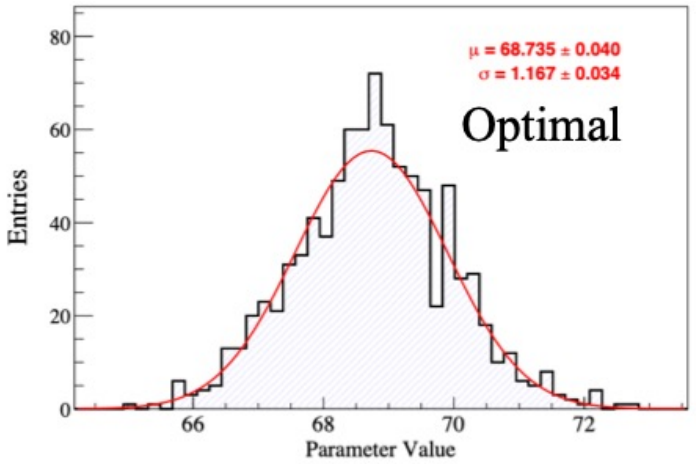
$\gamma = 68.7°$

$r_B = 0.0904$

$\delta_B = 118.3°$

JHEP02(2021)169





Summary

Based on 20.3 fb^{-1} $\psi(3770)$ data collected by BESIII

✓Finish the amplitude analysis of $D^0 \to K_S^0\pi^0\pi^+\pi^-$, and predict the CP-even fraction and longitudinal polarization fraction by model.

✓Obtain the binning strong phase parameters under 2×6 bins under the optimal and uniform schemes by the amplitude model.

☐ Next to do

- Finish the BESIII review of these two work.

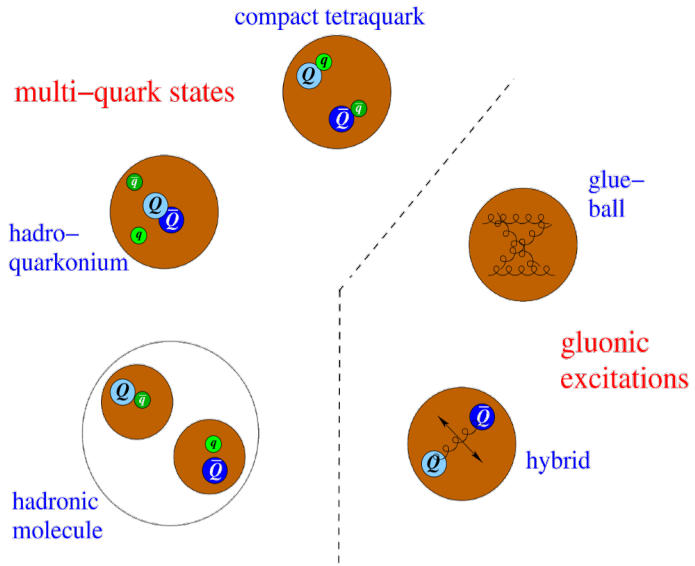
Outline

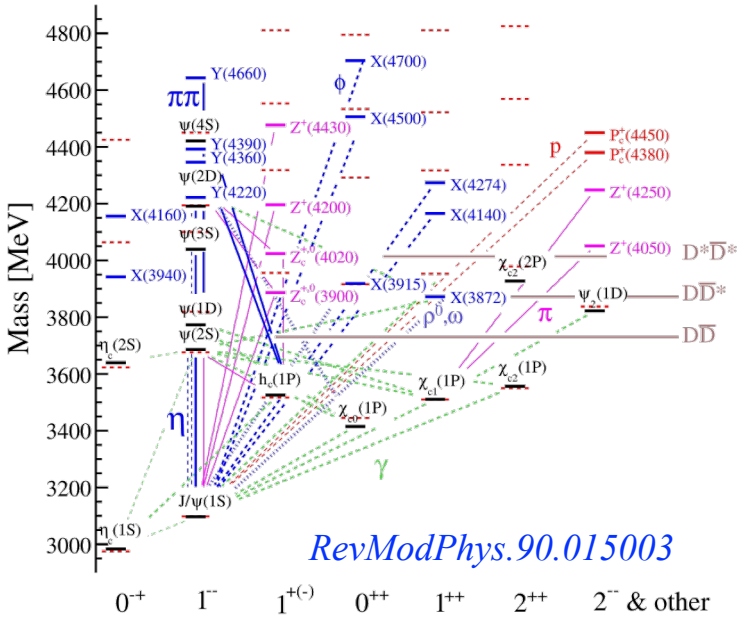
- Works on BESIII
  - Introduction
  - Study of $D^0/\bar{D}^0 \to K_S^0\pi^0\pi^+\pi^-$
  - Measurement of $e^+e^- \to \eta J/\psi$ Cross Section
- Works on STCF
  - Introduction
  - Simulation and Reconstruction of STCF DTOF
- Summary and Prospect

Motivation

- Hadron spectroscopy and the search for exotic hadronic states is crucial for QCD theory.

- Γ, M, σ^B … Important input for the non-perturbative QCD theory model.
- BESIII Advantages: Charmonium produce directly, High product σ, clean BKGs, controllable sys. uncertainties.
- $e^+ e^- \to \eta J/\psi$ process: Rich final state structures → more precise measurement!

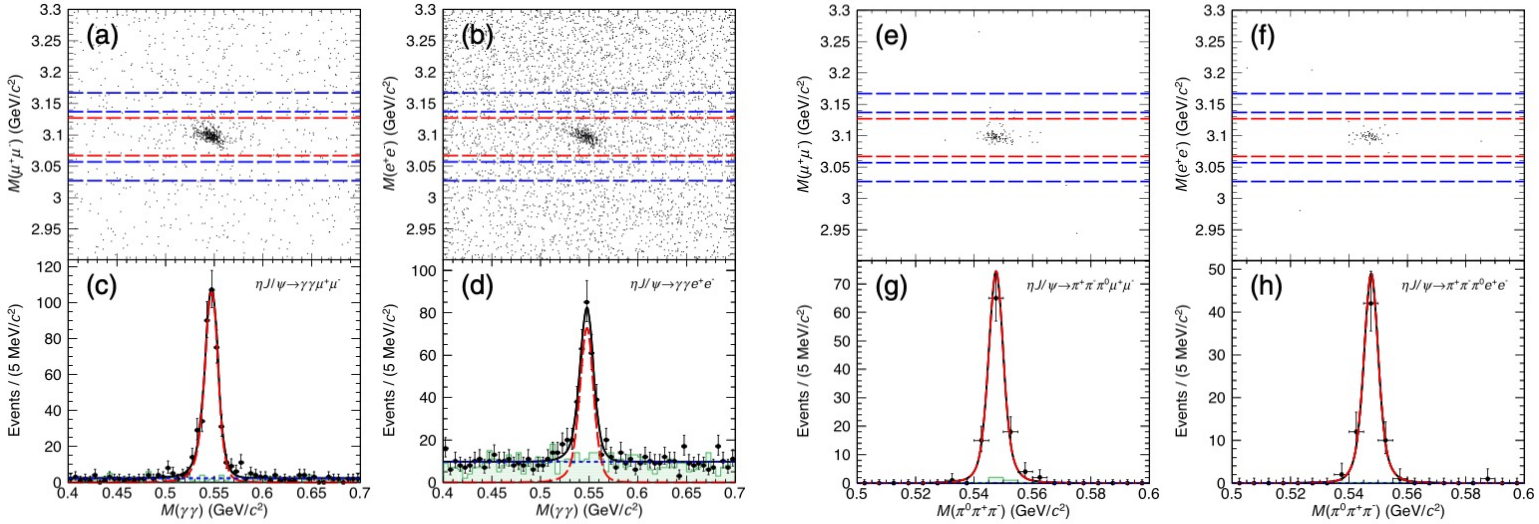


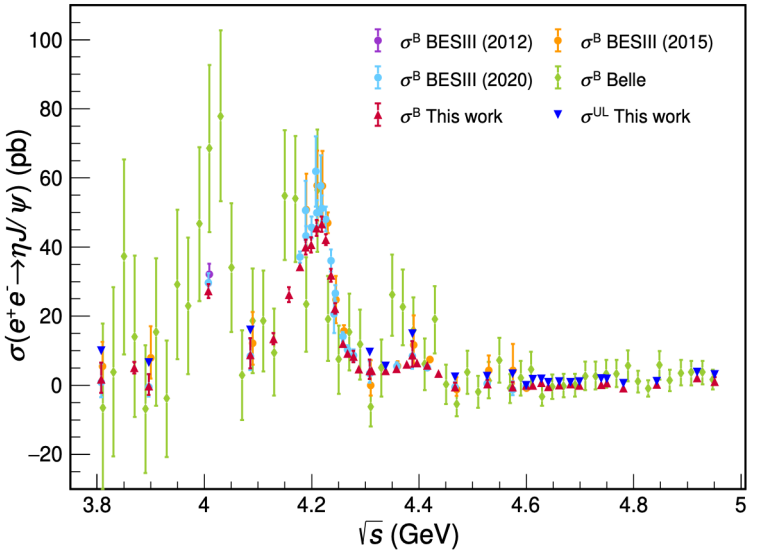


Analysis Strategy

- Data set: 22.42 fb^{-1} (44 energy points @3.808~4.951 GeV)
- Signal process: $\eta \to \gamma\gamma/\pi^0\pi^+\pi^-$, $J/\psi \to e^+e^-/\mu^+\mu^-$
- Signal Extract: Simultaneous fit between 4 decay modes

Shared parameter: $\sigma^B(e^+e^- \to \eta J/\psi) = \dfrac{N_{\rm sig}}{\mathcal{L}_{\rm int} \cdot (1+\delta^{\rm ISR}) \cdot \frac{1}{|1-\Pi|^2} \cdot \mathcal{B} \cdot \epsilon}$,



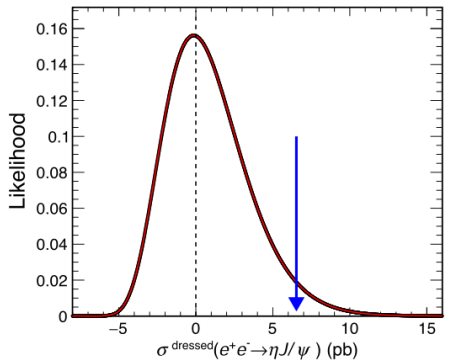


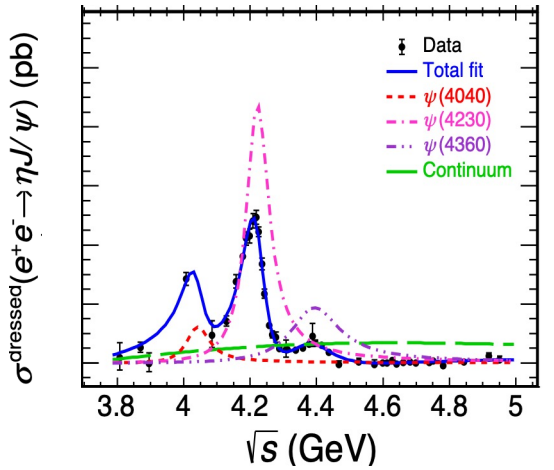
Analysis Strategy

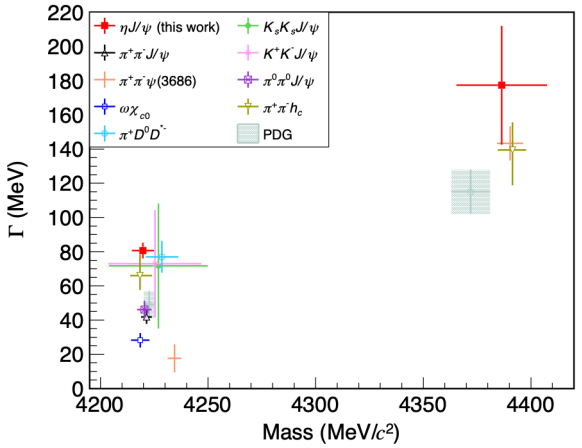
- Fit to cross section spectrum

$$\sigma^{\rm fit}(\sqrt{s}) = |\sqrt{\sigma_{NY}(\sqrt{s})} + \sum_{j=1}^{3} BW_j(\sqrt{s}) e^{i\phi_j}|^2$$

- Maximum-Likelihood Fit:
  - ✓ Large-Statistics: $G_i(\sigma_i^{\rm fit}; \sigma_i, \theta_i) = \frac{1}{\theta_i\sqrt{2\pi}} e^{-\frac{(\sigma_i^{\rm fit}-\sigma_i)^2}{2\theta_i^2}}$,
  - ✓ Low-Statistics: $\mathcal{L}$ shape from $M_{\gamma\gamma/\pi^0\pi^+\pi^-}$
  - ✓ $L = \prod_{i=1}^{N_1=22} G_i(\sigma_i^{\rm fit}) \cdot \prod_{j=1}^{N_2=22} F_j(\sigma_j^{\rm fit})$







Parameter	Solution I	Solution II	Solution III	Solution IV
M_1 (MeV/c^2)		4039 (fixed)		
Γ_1 (MeV)		80 (fixed)		
$\Gamma_1^{e^+e^-}\cdot\mathcal{B}_1$ (eV)	1.0 ± 0.2	7.1 ± 0.6	1.1 ± 0.2	7.8 ± 0.6
M_2 (MeV/c^2)		4219.7 ± 2.5		
Γ_2 (MeV)		80.7 ± 4.4		
$\Gamma_2^{e^+e^-}\cdot\mathcal{B}_2$ (eV)	4.0 ± 0.5	5.5 ± 0.7	8.7 ± 1.0	11.9 ± 1.1
M_3 (MeV/c^2)		4386.4 ± 12.6		
Γ_3 (MeV)		176.9 ± 32.1		
$\Gamma_3^{e^+e^-}\cdot\mathcal{B}_3$ (eV)	1.8 ± 0.6	2.1 ± 0.7	4.3 ± 1.3	5.0 ± 1.5
ϕ_1 (rad)	3.1 ± 0.6	-1.8 ± 0.1	3.3 ± 0.4	-1.6 ± 0.1
ϕ_2 (rad)	-2.8 ± 0.1	2.9 ± 0.2	-2.0 ± 0.1	-2.6 ± 0.2
ϕ_3 (rad)	-2.9 ± 0.1	3.0 ± 0.1	2.8 ± 0.1	2.4 ± 0.7
p_0 (MeV^{-1})	1.5 ± 0.4	1.5 ± 0.4	1.5 ± 0.4	1.6 ± 0.4
p_1 (GeV^{-3})	390.0 ± 155.3	389.3 ± 155.6	389.5 ± 155.1	389.5 ± 154.5

Summary

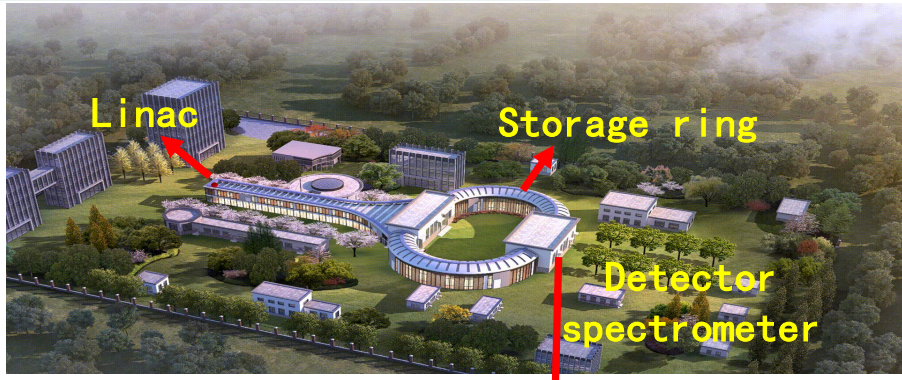
- ✓ Finish the cross sections measurement of $e^+e^- \to \eta J/\psi$ 3.808~4.951 GeV.
- ✓ Obtain 4 solutions of line-shape fit.
- ✓ Provide the M, Γ_{total}, $\Gamma^{e^+e^-} \cdot \mathcal{B}_{R\to\eta J/\psi}$ of $\psi(4040), \psi(4230), \psi(4390)$.
- ✓ Publishes at Phys. Rev. D 109 (2024) 9, 092012.

Outline

- Works on BESIII
  - Introduction
  - Study of $D^0/\bar{D}^0 \to K_S^0\pi^0\pi^+\pi^-$
  - Measurement of $e^+e^- \to \eta J/\psi$ Cross Section
- Works on STCF
  - Introduction
  - Simulation and Reconstruction of STCF DTOF
- Summary and Prospect

STCF Detector

Super Tau-Charm Facility is a natural extension for a post-BEPCII.

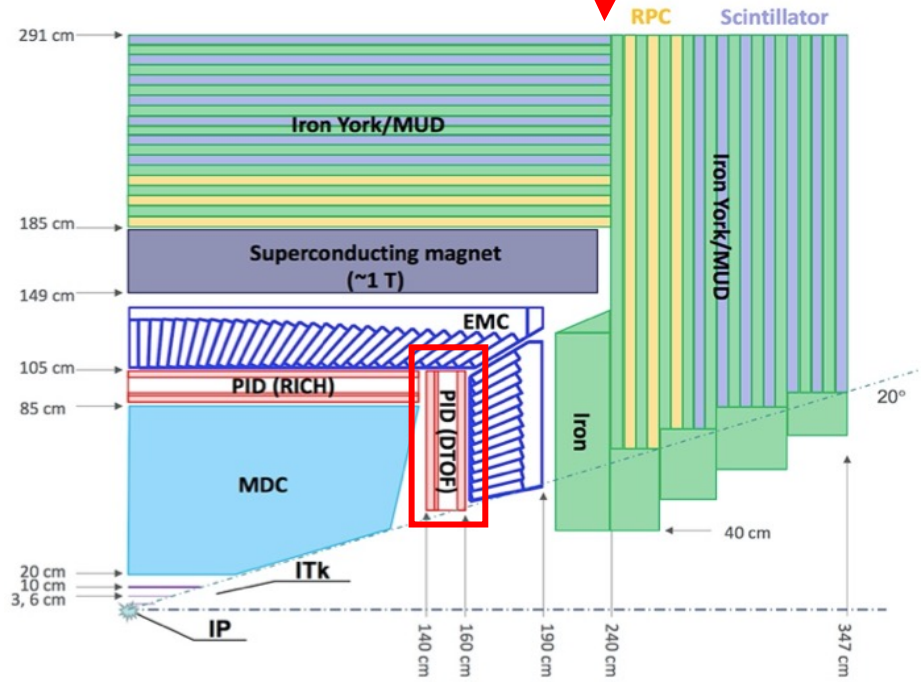


➢ Parameters of STCF:

- $E_{c.m.} = 2 - 7$ GeV Broader energy range
- Peak luminosity: $0.5\sim1\times10^{35}\mathrm{cm}^{-2}\mathrm{s}^{-1}$
  2 orders larger than BEPCII

➢ DTOF Detector

- PID Detect in end-cap
  - ✓ Compact structure
  - ✓ Lower amount of substance
  - ✓ Large momentum working range
  - ✓ High effective photon yields ~ 30
  - ✓ PID requirement: π/K 4σ separation $p \leq 2$ GeV/c

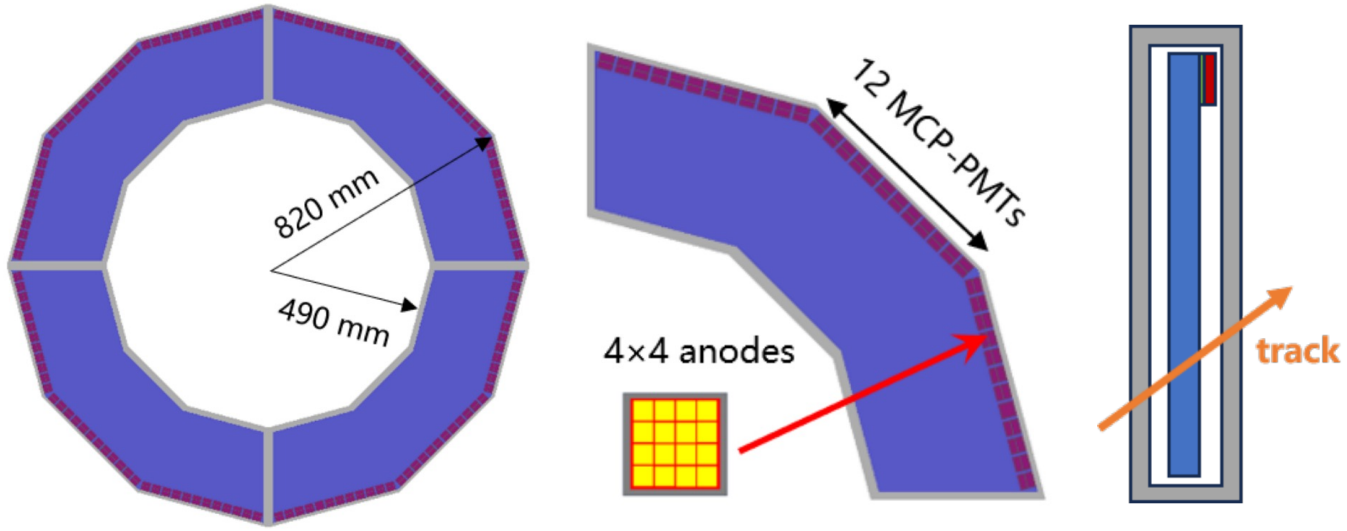


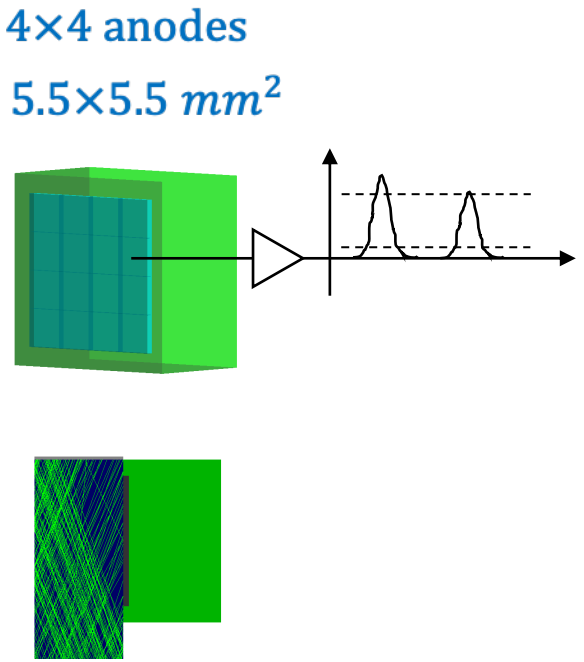
Outline

- Works on BESIII
  - Introduction
  - Study of $D^0/\bar{D}^0 \to K_S^0\pi^0\pi^+\pi^-$
  - Measurement of $e^+e^- \to \eta J/\psi$ Cross Section
- Works on STCF
  - Introduction
  - Simulation and Reconstruction of STCF DTOF
- Summary and Prospect

DTOF Geometry Configuration

- Two identical endcap discs, ~ ±1440 mm away from the collision point along the beam direction.
- Each disc: 4 sectors, $R_{min} = 490$ mm , $R_{max} = 820$ mm.
- Covering polar angles $\theta \in (20° - 28°)$.





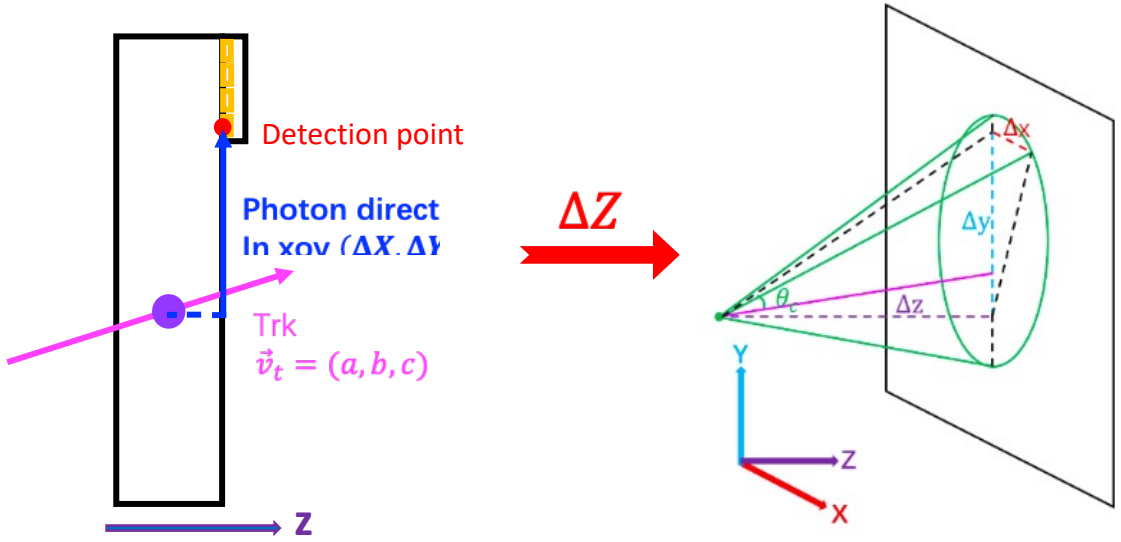
DTOF Reconstruction

Timing Method

- TOF Reconstruction

$$cos\theta_c = \frac{1}{n\beta} = \frac{\vec{v}_t \cdot \vec{v}_p}{|\vec{v}_t| \cdot |\vec{v}_p|} \qquad \begin{cases} \vec{v}_t = (a, b, c) \\ \vec{v}_p = (\Delta X, \Delta Y, \Delta Z) \end{cases}$$

$$LOP = \sqrt{\Delta X^2 + \Delta Y^2 + \Delta Z^2} \implies TOF_{rec} = T - \frac{LOP \cdot \overline{n_g}}{c} - T_0$$

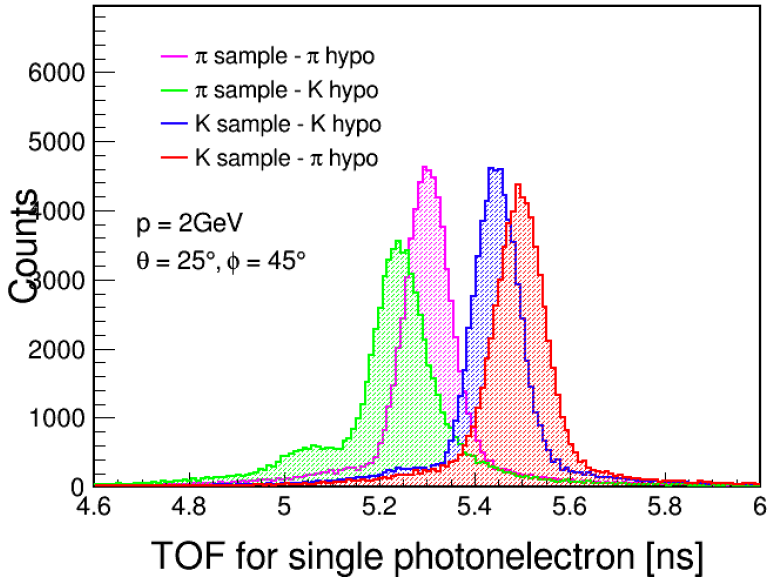


- Likelihood construction

$$\mathcal{L}_h = \prod_{i=1}^{N_{p.e.}} N_h S_h(TOF_{rec} | TOF_{hypo}) + 0.05$$

signal bkg

where $TOF_{hypo} = \frac{LOF}{c\beta_{hypo}}$



DTOF Reconstruction

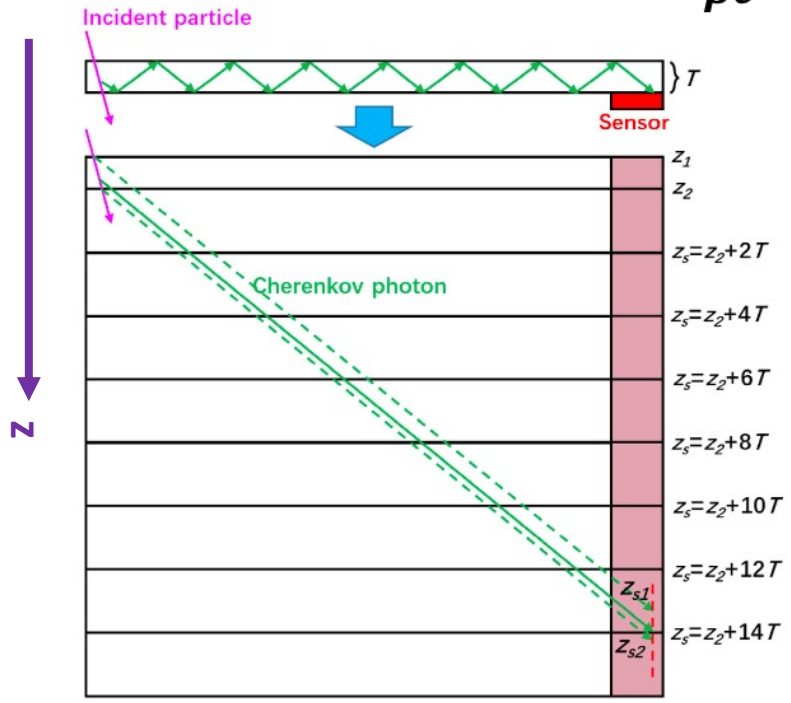
Imaging Method

- Photon TOA v.s. (x_s, y_s) Reconstruction

$$cos\theta_c = \frac{1}{n\beta} = \frac{\vec{v}_t \cdot \vec{v}_p}{|\vec{v}_t| \cdot |\vec{v}_p|} \qquad \begin{cases} \vec{v}_t = (a, b, c) \\ \vec{v}_p = (x_s - x_0, y_s - y_0, z_s - z_0) \end{cases}$$

$$z_s = z_2 + 2mT$$

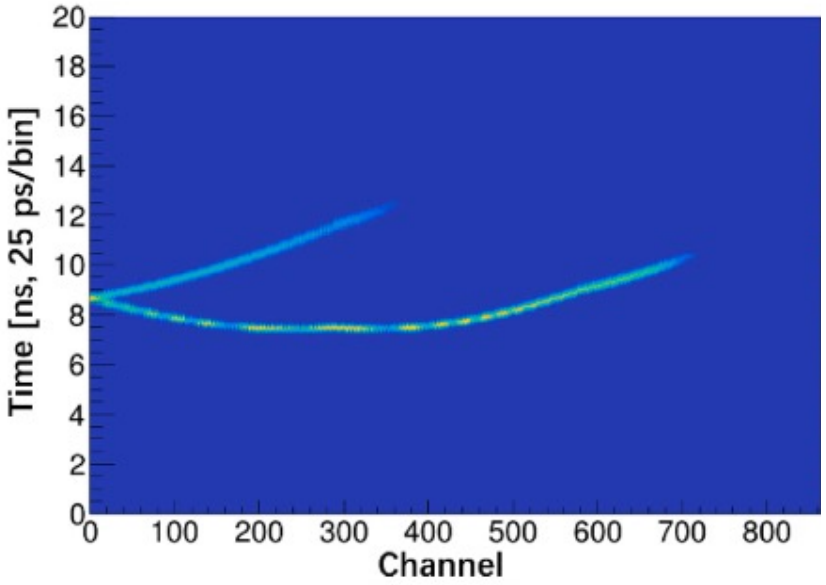
$$(x_s, y_s) \Rightarrow z_e, \phi_c \Rightarrow TOA = TOF + \frac{\Delta LOF_e}{\beta c} + TOP$$



- Likelihood construction

$$\mathcal{L}_h = \prod_{i=1}^{N_{p.e.}} f_h(ch_i, t_i) = \prod_{i=1}^{N_{p.e.}} \bar{N}_h S_h(ch_i, t_i) + B$$

$$\sum_{ch_i, t_i} \bar{N}_h S_h(ch_i, t_i) = N_h$$



DTOF Reconstruction under the OSCAR

➢ Hybrid Reconstruction

- Imaging Method

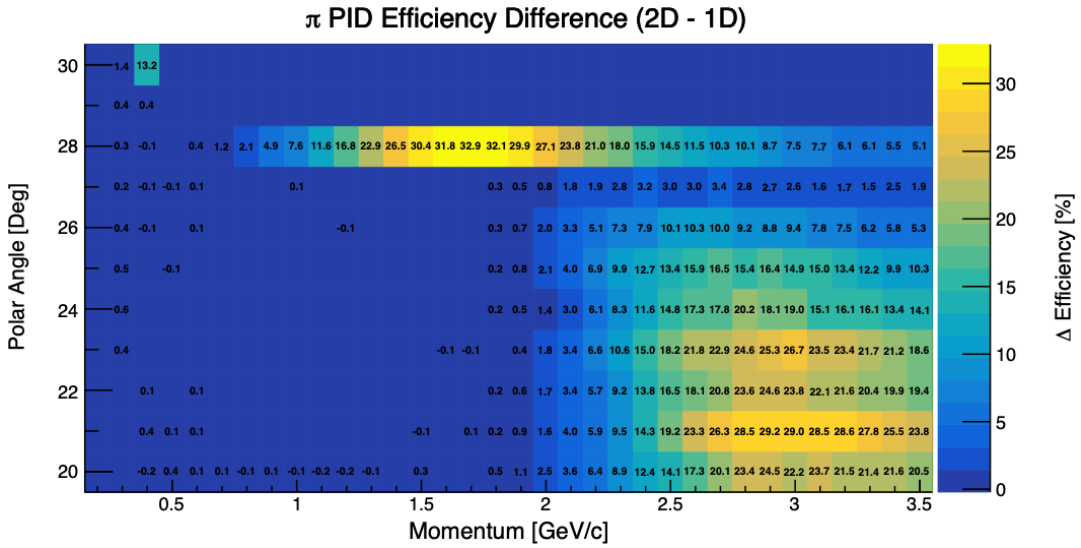
  $\theta_{hit} > 27°$, or $\theta_{hit} \leq 27°$ && $p = 1.8$ GeV/c

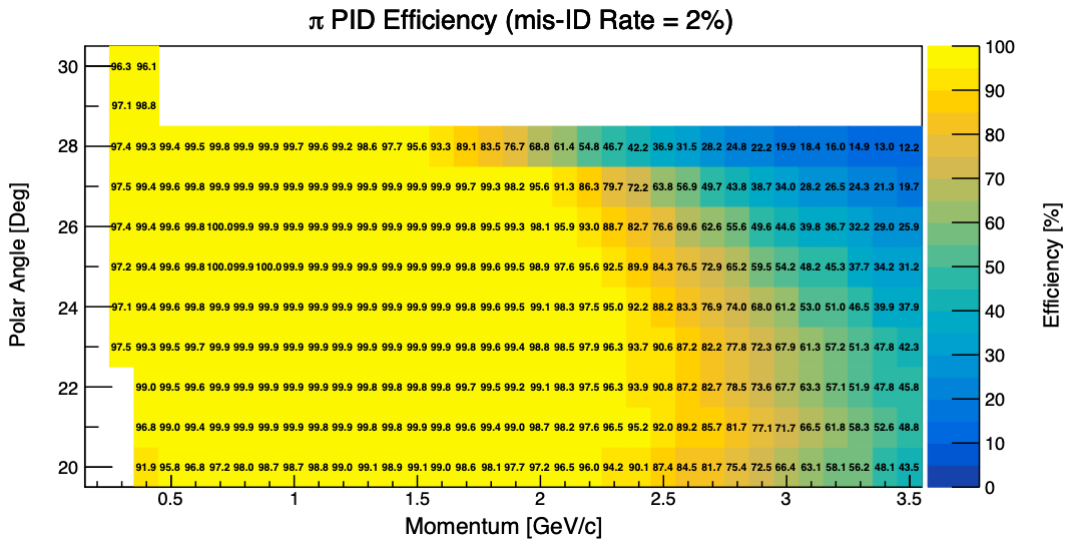
- Timing Method

  Remaining kinematic region

$\sigma_t \sim 69\ ps$ by single photon-electron

π efficiency $\sim 98\%$ at $p = 2.0$ GeV/c





DTOF Reconstruction under the OSCAR

➢ Multi-Track Strategy

Controlled samples ππ, πK and KK : p = 2.0 GeV/c, α = 1°–35° (track opening angle)

- Batch Mode Slightly better α < 5°

  Builds joint hypotheses for all tracks in one sector

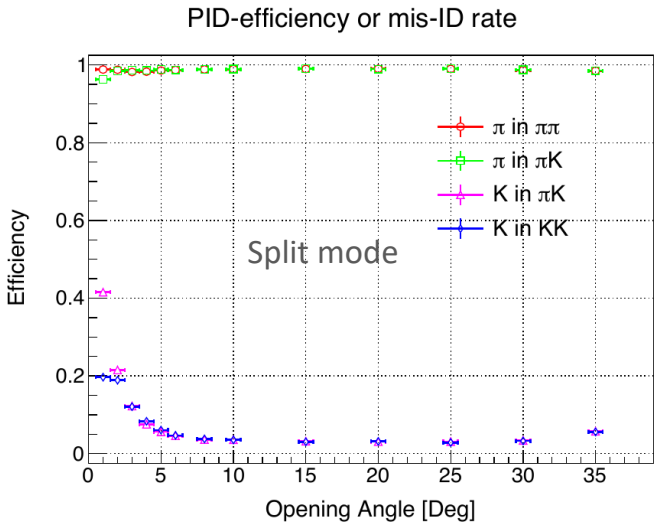
- Split Mode Selected as the baseline for Global PID

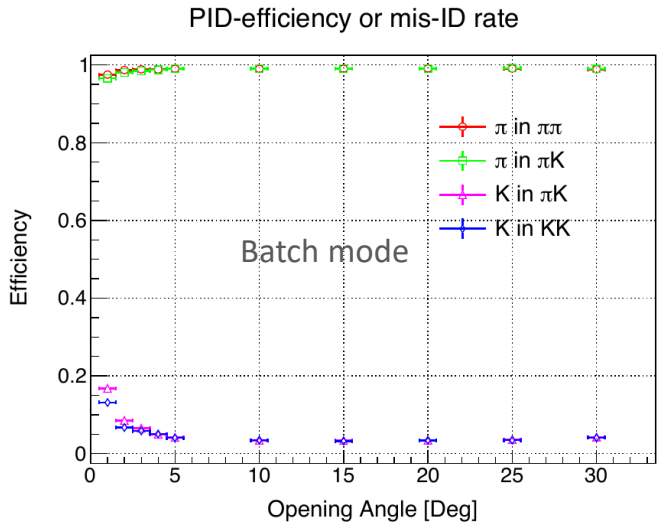
  Reconstructs each track independently

Common criterion: Δlog LπK > 0

For α > 5°: π efficiency > 97%

· K mis-ID < 2%



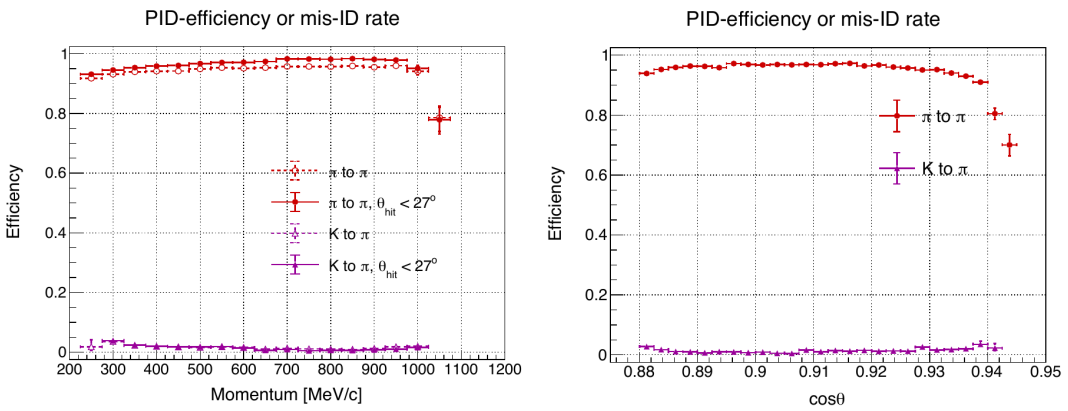


DTOF Reconstruction under the OSCAR

➢ Physics Process Validation

Inclusive $D^0\bar{D}^0$ decays

$\sqrt{s} = 3.773$ GeV, low-to-intermediate momentum

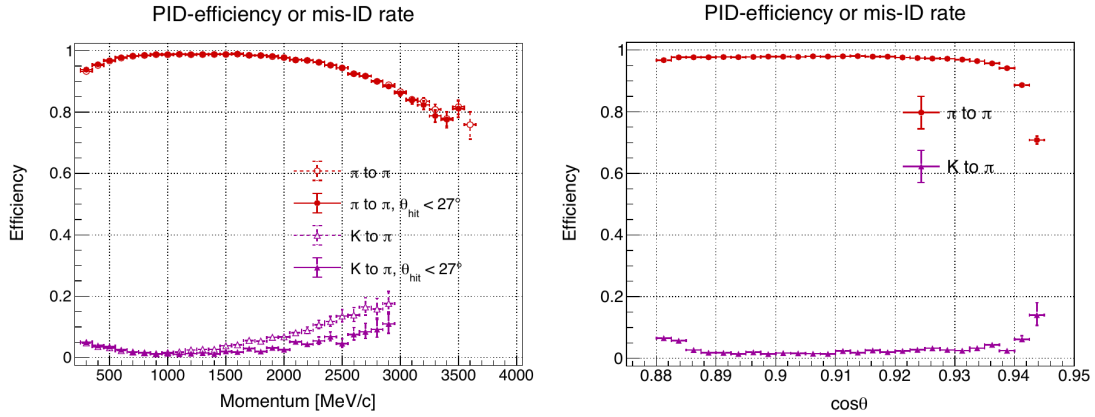


(a) Dependence on momentum.

(b) Dependence on $\cos\theta$.

Inclusive hadronic events

$\sqrt{s} = 7$ GeV, including high-momentum tracks



0.3–1.0 GeV/c: π efficiency 93–96%

K mis-ID typically < 3%

0.4–2.0 GeV/c: π efficiency 95–99%

K mis-ID generally < 5%

θhit < 27° improves efficiency in both samples. Physics analyses require working-point calibration.

Summary

- ✓ Finish the simulation software of DTOF under the OSCAR.
- ✓ Establish the reconstruction algorithm of DTOF under the OSCAR

  Timing Method
  - π efficiency $\sim 98\%$, at p $= 2.0$ GeV/c.
  - Overall reconstructed TOF time resolution ~ 50 ps.

  Imaging Method
  - π efficiency $\sim 99\%$, at $p = 2.0$ GeV/c.
- ✓ Finish the multi-track PID: π efficiency $> 97\%$ (K mis-ID $< 2\%$) at $p = 2$ GeV, $\alpha > 5°$
- ✓ Finish the physics process PID check.
- ☐ Next to do
  - Writing the DTOF performance paper.

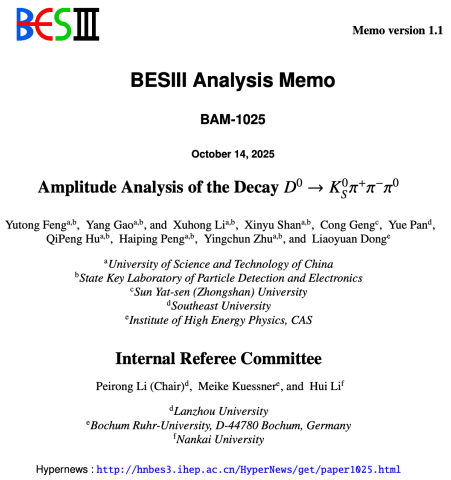
Outline

- Works on BESIII
  - Introduction
  - Study of $D^0/\bar{D}^0 \to K_S^0\pi^0\pi^+\pi^-$
  - Measurement of $e^+e^- \to \eta J/\psi$ Cross Section
- Works on STCF
  - Introduction
  - Simulation and Reconstruction of STCF DTOF
- Summary and Prospect

Summary and Prospect

- Study of $D^0/\bar{D}^0 \to K_S^0\pi^0\pi^+\pi^-$
  - ✓ Amplitude analysis and branching fraction Daft is reviewed.
  - ✓ Strong phase difference Memo is reviewed in BESIII.
  - ☐ Finish the review of these two work.
- Measurement of $e^+e^- \to \eta J/\psi$ Cross Section
  - ✓ Publishes in Phys. Rev. D 109 (2024) 9, 092012.
- Simulation and Reconstruction of STCF DTOF
  - ✓ Simulation and reconstruction established under OSCAR.
  - ☐ Prepare the paper.
- Others Work

I. Update of the strong phase difference in $D^0 \to \pi^+\pi^-\pi^+\pi^-$.
Memo is reviewed in the BESIII.


BESIII Memo version 1.1

BESIII Analysis Memo

BAM-1025

October 14, 2025

Amplitude Analysis of the Decay $D^0 \to K_S^0\pi^+\pi^-\pi^0$

Yutong Feng[a,b], Yang Gao[a,b], and Xuhong Li[a,b], Xinyu Shan[a,b], Cong Geng[c], Yue Pan[d], QiPeng Hu[a,b], Haiping Peng[a,b], Yingchun Zhu[a,b], and Liaoyuan Dong[e]

[a]*University of Science and Technology of China*
[b]*State Key Laboratory of Particle Detection and Electronics*
[c]*Sun Yat-sen (Zhongshan) University*
[d]*Southeast University*
[e]*Institute of High Energy Physics, CAS*

Internal Referee Committee

Peirong Li (Chair)[d], Meike Kuessner[e], and Hui Li[f]

[d]*Lanzhou University*
[e]*Bochum Ruhr-University, D-44780 Bochum, Germany*
[f]*Nankai University*

Hypernews : http://hnbes3.ihep.ac.cn/HyperNews/get/paper1025.html

The 2024 International Workshop on Future Tau Charm Facilities， 2024.1.14-1.18





Backup

Motivation

$$\gamma = \arg\left(-\frac{V_{ud}V_{ub}^*}{V_{cd}V_{cb}^*}\right) = \arg\left(\frac{c_{12}c_{13}s_{13}e^{i\delta}}{(s_{12}c_{23} + c_{12}s_{23}s_{13}e^{i\delta})(s_{23}c_{13})}\right)$$

$s_{13} \ll s_{23} \ll s_{12} \ll 1$, remain leading order

$$\gamma \approx \arg\left(\frac{c_{12}c_{13}s_{13}}{s_{12}c_{23}s_{23}c_{13}}e^{i\delta}\right) \approx \delta$$

$$\alpha = \arg\left(-\frac{V_{td}V_{tb}^*}{V_{ud}V_{ub}^*}\right) = 91.58^\circ \approx \frac{\pi}{2}$$

$$\therefore \beta = \pi - \alpha - \gamma \approx \frac{\pi}{2} - \delta$$

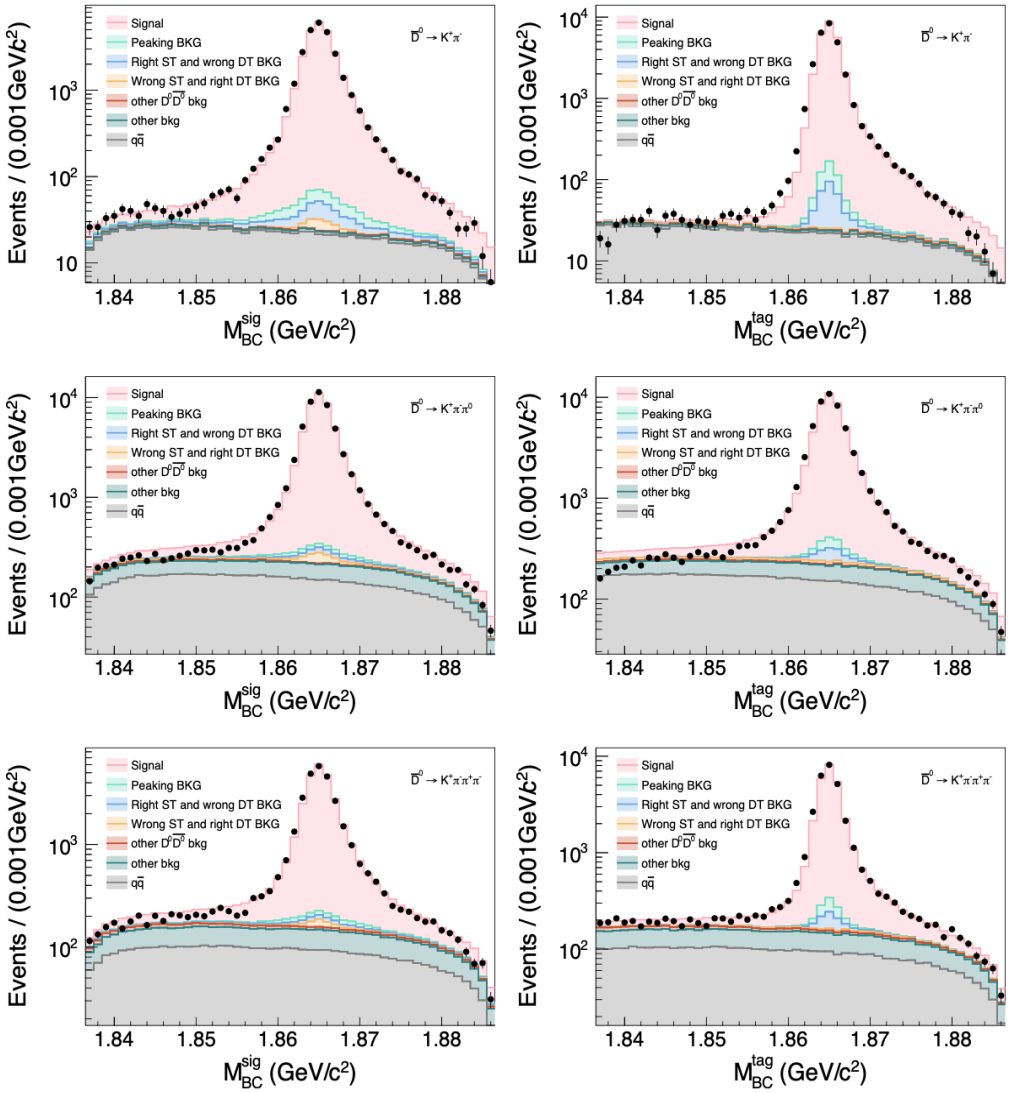
Background Analysis

Main Peaking BKG in DT:

- ✓ $D^0 \to K_S^0\eta',\ \eta' \to \gamma\pi^+\pi^-$
- ✓ $D^0 \to K^-\pi^+\pi^-\pi^+$
- ✓ $D^0 \to \pi^0 K_S^0\eta,\ \ \eta \to \gamma\pi^+\pi^-$

Peaking BKG have the corresponding Model, can be described well.

- BKG I:
  From $\psi(3770) \to D^0\,\bar{D}^0$ with wrong ST D^0 and right signal D^0.
- BKG II:
  From $\psi(3770) \to D^0\,\bar{D}^0$ with right ST D^0 and wrong signal D^0.
- BKG III:
  From $e^+e^- \to q\bar{q}$, distributed along the diagonal in the M_{sig}^{BC} v.s. M_{tag}^{BC} distribution.
- Peaking BKG:
  BKG with Peaking in both ST and signal M^{BC} spectrum.



Isospin Amplitude

Isospin states for hadrons: $|u\rangle : |\frac{1}{2}, \frac{1}{2}\rangle,\ |\bar{u}\rangle : -|\frac{1}{2}, -\frac{1}{2}\rangle,\ |d\rangle : |\frac{1}{2}, -\frac{1}{2}\rangle,\ |\bar{d}\rangle : |\frac{1}{2}, \frac{1}{2}\rangle$

	π^+, ρ^+	π^0, ρ^0, a^0	π^-, ρ^-
I=1	$\lvert u\bar{d}\rangle : \lvert 1, 1\rangle$	$\lvert \frac{u\bar{u}-d\bar{d}}{\sqrt{2}}\rangle : -\lvert 1, 0\rangle$	$\lvert d\bar{u}\rangle : -\lvert 1, -1\rangle$
	η, h, ω, ϕ, f		
I=0	$\lvert (u\bar{u} + d\bar{d}) + g(s\bar{s})\rangle : -\lvert 0, 0\rangle$		

	K^+	K^0	$\bar{K}^0$	K^-
I=$\frac{1}{2}$	$\lvert u\bar{s}\rangle : \lvert \frac{1}{2}, +\frac{1}{2}\rangle$	$\lvert d\bar{s}\rangle : \lvert \frac{1}{2}, -\frac{1}{2}\rangle$	$\lvert \bar{d}s\rangle : \lvert \frac{1}{2}, +\frac{1}{2}\rangle$	$\lvert \bar{u}s\rangle : -\lvert \frac{1}{2}, -\frac{1}{2}\rangle$

Isospin symmetry in strong decay (CG Coefficients):

- $D^0 \to K\pi$:

$$A(D^0 \to K^-\pi^+) = A\left(\rho^-_{\pi^0\pi^-} K^0_S, \pi^+\right) + c\left[A\left(K^-_{K^0_S\pi^-}\pi^0, \pi^+\right) - A\left(\bar{K}^0_{K^0_S\pi^0}\pi^-, \pi^+\right)\right]$$

$$A(D^0 \to K^+\pi^-) = A\left(\rho^+_{\pi^0\pi^+} K^0_S, \pi^-\right) + c\left[A\left(K^+_{K^0_S\pi^+}\pi^0, \pi^-\right) - A\left(K^0_{K^0_S\pi^0}\pi^+, \pi^-\right)\right]$$

$$A(D^0 \to \bar{K}^0\pi^0) = A\left(\rho^0_{\pi^+\pi^-} K^0_S, \pi^0\right) + c2A\left(K^-_{K^0_S\pi^-}\pi^+, \pi^0\right)$$

$$A(D^0 \to K^0\pi^0) = A\left(\rho^0_{\pi^+\pi^-} K^0_S, \pi^0\right) - c2A\left(K^+_{K^0_S\pi^+}\pi^-, \pi^0\right)$$

- $D^0 \to a_1\pi$:

$$A(D^0 \to a_1^0\pi^0) = -A\left(\rho^+_{\pi^+\pi^0}\pi^-, K^0_S\right) + A\left(\rho^-_{\pi^0\pi^-}\pi^+, K^0_S\right) - 2cA(f_{\pi^+\pi^-}\pi^0, K^0_S)$$

- $D^0 \to h_1\pi$:

$$A(D^0 \to h_1\pi^0) = -A\left(\rho^+_{\pi^+\pi^0}\pi^-, K^0_S\right) - A\left(\rho^-_{\pi^0\pi^-}\pi^+, K^0_S\right) + A\left(\rho^0_{\pi^+\pi^-}\pi^0, K^0_S\right)$$

Spin Factor

Decay Chain	Spin Factor
$D[S] \to P\ P_1,\ P[S] \to S\ P_2,\ S[S] \to P_3\ P_4$	1
$D[S] \to P\ P_1,\ P[P] \to V\ P_2,\ V[P] \to P_3\ P_4$	$\tilde{t}_\mu(P)\tilde{t}^\mu(V)$
$D[S] \to P\ P_1,\ P[D] \to T\ P_2,\ T[D] \to P_3\ P_4$	$\tilde{t}_{\mu\nu}(P)\tilde{t}^{\mu\nu}(T)$
$D[P] \to A\ P_1,\ A[S] \to V\ P_2,\ V[P] \to P_3\ P_4$	$\tilde{t}_\mu(D)P^{\mu\nu}(A)\tilde{t}_\nu(V)$
$D[P] \to A\ P_1,\ A[D] \to V\ P_2,\ V[P] \to P_3\ P_4$	$\tilde{t}_\mu(D)\tilde{t}^{\mu\nu}(A)\tilde{t}_\nu(V)$
$D[P] \to A\ P_1,\ A[P] \to S\ P_2,\ S[S] \to P_3\ P_4$	$\tilde{t}_\mu(D)\tilde{t}^{\mu}(A)$
$D[P] \to A\ P_1,\ A[P] \to T\ P_2,\ T[D] \to P_3\ P_4$	$\tilde{t}_\mu(D)\tilde{t}_\nu(A)P^{\mu\nu\rho\sigma}(A)\tilde{t}_{\rho\sigma}(T)$
$D[P] \to A\ P_1,\ A[F] \to T\ P_2,\ T[D] \to P_3\ P_4$	$\tilde{t}_\mu(D)\tilde{t}^{\mu\nu\rho}(A)\tilde{t}_{\nu\sigma}(T)$
$D[P] \to V_1\ P_1,\ V_1[P] \to V_2\ P_2,\ V_2[P] \to P_3\ P_4$	$\tilde{t}^\mu(D)\epsilon_{\mu\nu\rho\sigma}p^\sigma_{V_1}\tilde{t}^\rho(V_1)\tilde{t}^\nu(V_2)$
$D[D] \to PT\ P_1,\ PT[S] \to T\ P_2,\ T[D] \to P_3\ P_4$	$\tilde{t}_{\mu\nu}(D)P^{\mu\nu\alpha\beta}(PT)\tilde{t}_{\alpha\beta}(T)$
$D[D] \to PT\ P_1,\ PT[D] \to T\ P_2,\ T[D] \to P_3\ P_4$	$\tilde{t}_{\mu\nu}(D)P^{\mu\nu\rho\sigma}(PT)\tilde{t}^{\alpha}_{\rho}(PT)P_{\alpha\sigma\beta\gamma}(PT)\tilde{t}^{\beta\gamma}(T)$
$D[D] \to PT\ P_1,\ PT[P] \to V\ P_2,\ V[P] \to P_3\ P_4$	$\tilde{t}_{\mu\nu}(D)P^{\mu\nu\alpha\beta}(PT)\tilde{t}_{\alpha}(PT)\tilde{t}_{\beta}(V)$
$D[D] \to PT\ P_1,\ PT[F] \to V\ P_2,\ V[P] \to P_3\ P_4$	$\tilde{t}_{\mu\nu}(D)\tilde{t}^{\mu\nu\rho}(PT)\tilde{t}_{\rho}(V)$
$D[D] \to PT\ P_1,\ PT[D] \to S\ P_2,\ S[S] \to P_3\ P_4$	$\tilde{t}_{\mu\nu}(D)\tilde{t}^{\mu\nu}(PT)$
$D[D] \to T\ P_1,\ T[D] \to V\ P_2,\ V[P] \to P_3\ P_4$	$\tilde{t}^{\mu\alpha}(D)\epsilon_{\mu\nu\rho\sigma}p^\sigma_T\tilde{t}^\nu_\alpha(T)\tilde{t}^\rho(V)$
$D[D] \to T_1\ P_1,\ T_1[P] \to T_2\ P_2,\ T_2[D] \to P_3\ P_4$	$\tilde{t}_{\mu\nu}(D)P^{\mu\nu\alpha\beta}(T_1)\epsilon_{\alpha\lambda\sigma\rho}p^\rho_{T_1}\tilde{t}^\lambda(T_1)\tilde{t}^\sigma_\beta(T_2)$
$D[S] \to S_1\ S_2,\ S_1[S] \to P_1\ P_2,\ S_2[S] \to P_3\ P_4$	1
$D[P] \to V\ S,\ V[P] \to P_1\ P_2,\ S[S] \to P_3\ P_4$	$\tilde{t}_\mu(D)\tilde{t}^\mu(V)$
$D[S] \to V_1\ V_2,\ V_1[P] \to P_1\ P_2,\ V_2[P] \to P_3\ P_4$	$P^{\mu\nu}(D)\tilde{t}_\mu(V_1)\tilde{t}^\nu(V_2)$
$D[P] \to V_1\ V_2,\ V_1[P] \to P_1\ P_2,\ V_2[P] \to P_3\ P_4$	$\epsilon_{\mu\nu\alpha\beta}p^\beta_D\tilde{t}^\mu(D)\tilde{t}^\nu(V_1)\tilde{t}^\alpha(V_2)$
$D[D] \to V_1\ V_2,\ V_1[P] \to P_1\ P_2,\ V_2[P] \to P_3\ P_4$	$\tilde{t}_{\mu\nu}(D)\tilde{t}^\mu(V_1)\tilde{t}^\nu(V_2)$
$D[D] \to T\ S,\ T[D] \to P_1\ P_2,\ S[S] \to P_3\ P_4$	$\tilde{t}_{\mu\nu}(D)\tilde{t}^{\mu\nu}(T)$
$D[P] \to T\ V,\ T[D] \to P_1\ P_2,\ V[P] \to P_3\ P_4$	$\tilde{t}_\mu(D)P^{\mu\nu\rho\sigma}(D)\tilde{t}_{\rho\sigma}(T)\tilde{t}_\nu(V)$
$D[D] \to T\ V,\ T[D] \to P_1\ P_2,\ V[P] \to P_3\ P_4$	$\epsilon_{\mu\nu\alpha\beta}p^\beta_D\tilde{t}^{\mu\rho}(D)\tilde{t}^\nu_\rho(T)\tilde{t}^\alpha(V)$
$D[S] \to T_1\ T_2,\ T_1[D] \to P_1\ P_2,\ T_2[D] \to P_3\ P_4$	$\tilde{t}_{\mu\nu}(T_1)P^{\mu\nu\rho\sigma}(D)\tilde{t}_{\rho\sigma}(T_2)$
$D[P] \to T_1\ T_2,\ T_1[D] \to P_1\ P_2,\ T_2[D] \to P_3\ P_4$	$\epsilon_{\mu\nu\rho\sigma}p^\sigma_D\tilde{t}^\rho(D)P_{\alpha\beta}(D)\tilde{t}^{\mu\alpha}(T_1)\tilde{t}^{\nu\beta}(T_2)$
$D[D] \to T_1\ T_2,\ T_1[D] \to P_1\ P_2,\ T_2[D] \to P_3\ P_4$	$\tilde{t}^\nu_\mu(D)P^{\mu\alpha\beta\gamma}(D)\tilde{t}_{\beta\gamma}(T_1)P_{\nu\alpha\rho\sigma}(D)\tilde{t}^{\rho\sigma}(T_2)$

- **Blatt-Weisskopf barrier factor**

$$B_0(q) = 1$$

$$B_1(q) = \sqrt{\frac{2}{q^2 + q_0^2}}$$

$$B_2(q) = \sqrt{\frac{13}{q^4 + 3q^2q_0^2 + 9q_0^4}}$$

q: breakup momentum

$q_0 = 0.197321/R\ GeV/c$

$R = 5 * 0.197321 \approx 1\ fm$ for D0

$R = 3 * 0.197321 \approx 0.6\ fm$ for other resonance

- **Spin projection operator:**

$$P^{(0)}(p_a) = 1$$

$$P^{(1)}_{\mu\mu'}(p_a) = -g_{\mu\mu'} + \frac{p_{a\mu}p_{a\mu'}}{p_a^2}$$

$$P^{(2)}_{\mu\nu\mu'\nu'}(p_a) = \frac{1}{2}[P^{(1)}_{\mu\mu'}(p_a)P^{(1)}_{\nu\nu'}(p_a) + P^{(1)}_{\mu\nu'}(p_a)P^{(1)}_{\nu\mu'}(p_a)] - \frac{1}{3}P^{(1)}_{\mu\nu}(p_a)P^{(1)}_{\mu'\nu'}(p_a)$$

- **Pure orbital angular momentum**

$$\tilde{t}^{(L)}_{\mu_1\cdots\mu_l} = (-1)^L P^{(L)}_{\mu_1\cdots\mu_L\mu'_1\cdots\mu'_L}(p_a)r^{\mu'_1}\cdots r^{\mu'_L}$$

Amplitude Analysis

Fit Result

Amplitude	Magitude	Phase (rad)	Fit Fraction(%)	Significance (σ)	Decay Chain
ωK_S^0	2.000 (fixed)	0.000 (fixed)	21.10 ± 0.15	> 10.0σ	
ϕK_S^0	0.103 ± 0.002	1.009 ± 0.024	1.04 ± 0.04	> 10.0σ	
$\omega(1420)$	2.852 ± 0.098	2.946 ± 0.033	2.84 ± 0.19	6.0σ	
$\omega(1650)$	9.355 ± 0.231	0.747 ± 0.025	6.73 ± 0.35	8.5σ	
$K(1410)^-\pi^+$ [$K(1410) \to K_S^0\rho(770)$]	0.584 ± 0.057	0.365 ± 0.102	0.10 ± 0.02	6.7σ	VP
$\bar{K}^*(1680)^0\pi^0$	1.518 ± 0.064	−1.426 ± 0.042	0.91 ± 0.06	> 10.0σ	
$K^*(1680)^-\pi^+$	1.592 ± 0.077	1.442 ± 0.052	0.70 ± 0.06	> 10.0σ	
$K^*(1680)^+\pi^-$	0.889 ± 0.059	−0.434 ± 0.064	0.22 ± 0.03	> 10.0σ	
$\pi(1300)K_S^0$	6.036 ± 0.171	3.700 ± 0.030	2.03 ± 0.11	> 10.0σ	
$\bar{K}(1460)^0\pi^0$	1.927 ± 0.057	2.159 ± 0.029	2.03 ± 0.16	> 10.0σ	PP
$K(1460)^-\pi^+$	3.602 ± 0.098	0.174 ± 0.027	1.61 ± 0.09	> 10.0σ	
$h_1(1170)K_S^0$	2.446 ± 0.090	−1.427 ± 0.037	0.69 ± 0.05	> 10.0σ	
$a_1(1260)K_S^0$	12.484 ± 0.185	1.464 ± 0.016	10.49 ± 0.30	> 10.0σ	
$a_1(1640)K_S^0$	10.964 ± 0.509	−0.146 ± 0.043	1.55 ± 0.15	9.2σ	
$K_1(1270)^-\pi^+$	6.498 ± 0.097	4.183 ± 0.019	6.78 ± 0.15	> 10.0σ	
$\bar{K}_1(1270)^0\pi^0$	2.760 ± 0.062	1.281 ± 0.027	1.47 ± 0.06	> 10.0σ	AP
$\bar{K}_1(1400)^0\pi^0$	2.201 ± 0.036	0.616 ± 0.018	4.04 ± 0.12	> 10.0σ	
$K_1(1400)^-\pi^+$	0.756 ± 0.052	3.444 ± 0.068	0.23 ± 0.03	> 10.0σ	
$\bar{K}_1(1650)^0\pi^0$	1.974 ± 0.102	0.104 ± 0.052	0.52 ± 0.04	> 10.0σ	
$K_1(1650)^-\pi^+$	1.966 ± 0.118	3.376 ± 0.060	0.26 ± 0.03	> 10.0σ	
$a_2(1320)K_S^0$	0.103 ± 0.008	−1.300 ± 0.080	0.09 ± 0.01	> 10.0σ	
$K_2^*(1430)^-\pi^+$	0.058 ± 0.002	1.766 ± 0.046	0.35 ± 0.03	> 10.0σ	TP
$\bar{K}_2^*(1430)^0\pi^0$	0.036 ± 0.002	4.457 ± 0.050	0.20 ± 0.02	> 10.0σ	
$K^*(892)^-\rho(770)^+$	-	-	38.49 ± 0.39	-	
$K^*(892)^-\rho(770)^+[S]$	3.320 ± 0.039	0.895 ± 0.014	7.63 ± 0.17	> 10.0σ	
$K^*(892)^-\rho(770)^+[P]$	1.415 ± 0.012	4.706 ± 0.011	16.38 ± 0.25	> 10.0σ	
$K^*(892)^-\rho(770)^+[D]$	0.772 ± 0.008	0.022 ± 0.013	11.22 ± 0.22	> 10.0σ	
$\bar{K}^*(892)^0\rho(770)^0$	-	-	4.09 ± 0.10	-	
$\bar{K}^*(892)^0\rho(770)^0[S]$	1.370 ± 0.029	2.601 ± 0.024	1.33 ± 0.05	> 10.0σ	
$\bar{K}^*(892)^0\rho(770)^0[P]$	0.440 ± 0.009	−1.526 ± 0.023	1.62 ± 0.07	> 10.0σ	
$\bar{K}^*(892)^0\rho(770)^0[D]$	0.319 ± 0.007	−0.094 ± 0.024	1.93 ± 0.08	> 10.0σ	VV
$K^*(892)^-\rho(1450)^+[S]$	17.424 ± 0.482	3.932 ± 0.030	2.45 ± 0.14	> 10.0σ	
$K^*(892)^-\rho(1450)^+[P]$	3.189 ± 0.151	2.127 ± 0.045	0.89 ± 0.08	> 10.0σ	
$K^*(892)^-\rho(1450)^+[D]$	1.478 ± 0.080	0.456 ± 0.060	0.49 ± 0.05	> 10.0σ	
$\bar{K}^*(892)^0\rho(1450)^0$ [D]	1.157 ± 0.064	0.806 ± 0.059	0.30 ± 0.03	> 10.0σ	
$K^*(1680)^-\rho(770)^+$ [S]	19.533 ± 0.990	−0.272 ± 0.049	0.57 ± 0.06	> 10.0σ	
$(K_S^0\pi^0)^{L=1}\rho(1450)^0$ [P]	36.597 ± 1.242	1.418 ± 0.033	1.24 ± 0.08	> 10.0σ	

Amplitude	Magitude	Phase (rad)	Fit Fraction(%)	Significance (σ)
$(K_S^0\pi^-)^{L=0}\rho(770)^+$	197.265 ± 0.582	4.051 ± 1.611	1.48 ± 0.11	> 10.0σ
R	−0.005 ± 0.100		-	-
ϕ_R	−0.178 ± 0.395		-	-
ϕ_F	−0.066 ± −0.003		-	-
$(K_S^0\pi^0)^{L=0}\rho(770)^0$	579.148 ± 2.074	−0.906 ± 1.626	0.45 ± 0.04	> 10.0σ
R	−0.063 ± 1.336		-	-
ϕ_R	2.719 ± 0.013		-	-
ϕ_F	−3.167 ± −0.001		-	-
$\bar{K}^*(892)^0(\pi^+\pi^-)^{L=0}$	-	-	1.31 ± 0.07	> 10.0σ
β_5	260.436 ± 8.910	1.332 ± 0.033	-	-
$f_{\pi\pi}^{\text{prod}}$	6.534 ± 0.193	3.751 ± 0.031	-	-
$\bar{K}^*(1680)^0(\pi^+\pi^-)^{L=0}$	-	-	0.89 ± 0.06	> 10.0σ
β_1	207.487 ± 4.158	3.876 ± 0.018	-	-
β_3	2355.190 ± 47.293	0.426 ± 0.017	-	-
$f_{\eta\eta}^{\text{prod}}$	94.244 ± 10.926	0.229 ± 0.108	-	-
$(K_S^0\pi^0)^{L=0}(\pi^+\pi^-)^{L=0}$	-	-	6.87 ± 0.18	> 10.0σ

Amplitude	Magitude	Phase (rad)	Relative Fit Fraction(%)	Significance (σ)
$K_1(1270) \to \rho(770)K_S^0$ [S]	1 (fixed)	0 (fixed)	76.84 ± 1.84	> 10.0σ
$K_1(1270) \to \rho(1450)K_S^0$ [D]	0.650 ± 0.052	2.659 ± 0.086	1.89 ± 0.31	8.8σ
$K_1(1270) \to K^*(892)\pi$ [S]	0.134 ± 0.005	0.628 ± 0.034	11.93 ± 0.68	> 10.0σ
$K_1(1270) \to K^*(892)\pi$ [D]	0.036 ± 0.002	0.184 ± 0.058	2.59 ± 0.28	> 10.0σ
$K_1(1270) \to (K_S^0\pi)^{L=0}\pi$ [P]	123.600 ± 0.550	2.743 ± 1.623	10.29 ± 0.95	> 10.0σ
R	−0.002 ± 0.028		-	-
ϕ_R	0.731 ± 0.262		-	-
ϕ_F	−0.007 ± 0.000		-	-
$K_1(1400) \to K^*(892)\pi$ [S]	1 (fixed)	0 (fixed)	102.28 ± 0.22	> 10.0σ
$K_1(1400) \to \rho(770)K_S^0$ [D]	0.184 ± 0.016	−0.420 ± 0.088	1.83 ± 0.32	8.4σ
$K_2^*(1430) \to K^*(892)\pi$	1 (fixed)	0 (fixed)	65.45 ± 3.10	> 10.0σ
$K_2^*(1430) \to \rho(770)K_S^0$	1.382 ± 0.118	0.112 ± 0.089	19.25 ± 2.49	> 10.0σ
$K(1460) \to K^*(892)\pi$	1 (fixed)	0 (fixed)	45.61 ± 3.16	> 10.0σ
$K(1460) \to (K_S^0\pi)^{L=0}\pi$	108.928 ± 2.564	−1.077 ± 1.696	54.56 ± 3.18	> 10.0σ
R	0.249 ± 0.477		-	-
ϕ_R	0.962 ± 0.039		-	-
ϕ_F	3.073 ± −0.032		-	-
$K_1(1650) \to \rho(770)K_S^0$ [S]	1 (fixed)	0 (fixed)	32.77 ± 2.79	> 10.0σ
$K_1(1650) \to K^*(892)\pi$ [S]	0.371 ± 0.029	0.335 ± 0.074	32.47 ± 3.64	8.2σ
$K_1(1650) \to K_S^0(\pi^+\pi^-)^{L=0}$	-	-	44.85 ± 4.45	8.7σ
β_1	2.995 ± 0.896	0.622 ± 0.299	-	-
β_2	15.620 ± 2.046	−1.201 ± 0.139	-	-
$f_{\eta\eta}^{\text{prod}}$	34.540 ± 2.983	3.962 ± 0.086	-	-
$K^*(1680) \to \rho(770)K_S^0$ [P]	1 (fixed)	0 (fixed)	20.07 ± 1.21	> 10.0σ
$K^*(1680) \to K^*(892)\pi$ [P]	0.613 ± 0.025	2.684 ± 0.042	63.74 ± 1.51	> 10.0σ

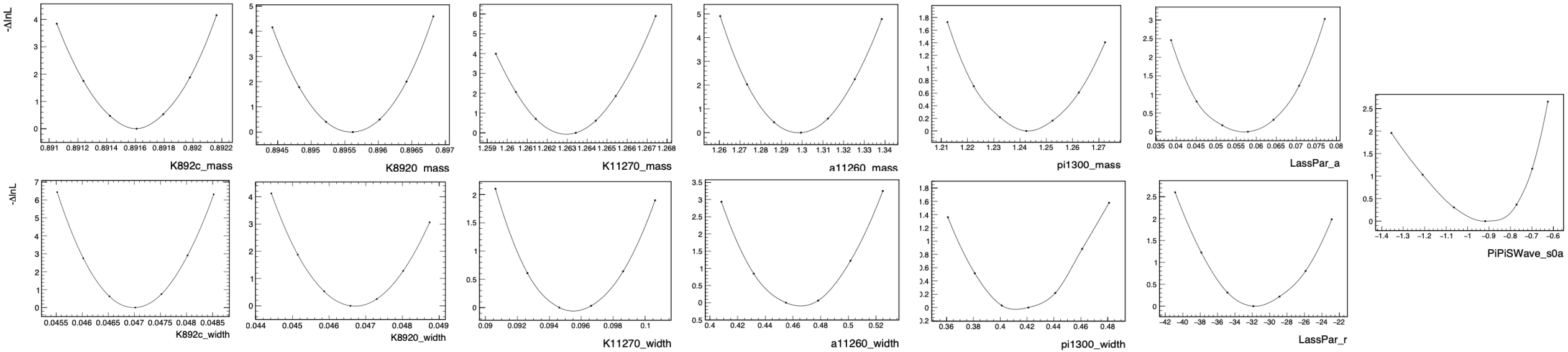
Amplitude Analysis

Fit Result

- The parameters of $a_1(1260), \pi(1300), K_1(1270)$ and $K\pi$ S-wave will be determined in our fit due to their dominant contribution in the channel and inaccurate results from PDG.

	This Work		PDG [49]	
Resonance	Mass(GeV/c^2)	Width(GeV)	Mass(GeV/c^2)	Width(GeV)
$a_1(1260)$	1.298 ± 0.013	0.465 ± 0.024	1.230 ± 0.040	$0.250 \sim 0.600$
$\pi(1300)$	1.243 ± 0.017	0.412 ± 0.034	1.300 ± 0.100	$0.200 \sim 0.600$
$K_1(1270)$	1.263 ± 0.001	0.096 ± 0.003	1.253 ± 0.007	0.090 ± 0.020
$K^*(892)^-$	0.8916 ± 0.0002	0.0470 ± 0.0004	0.8917 ± 0.0003	0.0514 ± 0.0008
$\bar{K}^*(892)^0$	0.8956 ± 0.0004	0.0467 ± 0.0008	0.8956 ± 0.0002	0.0473 ± 0.0005

Parameter	Value
$K\pi$ S-wave LASS model	
a	0.058 ± 0.009
r	-31.795 ± 4.254
$\pi\pi$ S-wave K-matrix model	
s_0^{Prod}	$-0.8956^{+0.1399}_{-0.8956}$



Amplitude Analysis
Longitudinal Polarization fraction

Covariant Helicity Amplitude for $D \to V_1V_2 \to (P_1P_2)(P_3P_4)$

$$H_{\lambda_{V_1},\lambda_{V_2}} = F^{J_D}_{\lambda_{V_1},\lambda_{V_2}} D^{J_D}_{\lambda_D,\lambda_{V_1}-\lambda_{V_2}}(\Omega_D) \cdot T_{V_1}(m_{V_1})\, F^{J_{V_1}}_{\lambda_{P_1},\lambda_{P_2}}\, D^{J_{V_1}}_{\lambda_{V_1},\lambda_{P_1}-\lambda_{P_2}}(\Omega^{\{D\}}_{V_1}) \cdot T_{V_2}(m_{V_2})\, F^{J_{V_2}}_{\lambda_{P_3},\lambda_{P_4}}\, D^{J_{V_2}}_{\lambda_{V_2},\lambda_{P_3}-\lambda_{P_4}}(\Omega^{\{D\}}_{V_2})$$

$$J_D = 0 \implies \lambda_{V_1} = \lambda_{V_2} \quad \therefore |A|^2 = \left|\sum_{\lambda_{V_1}\lambda_{V_2}} H_{\lambda_{V_1}\lambda_{V_2}}\right|^2 = |H_{11} + H_{-1-1} + H_{00}|^2$$

$$F^{J_D}_{\pm1\pm1} = \sqrt{\frac{1}{3}}g_{00} \pm \sqrt{\frac{1}{2}}Wrg_{11} + \sqrt{\frac{1}{6}}r^2 g_{22} \quad , \quad F^{J_D}_{00} = \gamma_1\gamma_2(-\sqrt{\frac{1}{3}}g_{00} + \sqrt{\frac{2}{3}}r^2 g_{22}) \qquad r = 2|q|$$

$|q|$: momentum of V in D rest frame γ: Lorentz factor of V in D rest frame W: mass of D (m)

- $D \to V_1V_2$, fix at mass of V_1V_2
  - Fix mass of V_1V_2 at PDG value, their momentum can be calculated.
  - V_1V_2 is considered as final stat

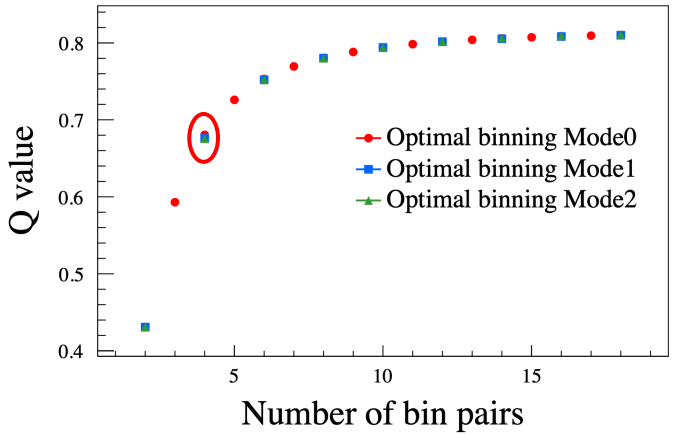
$$f_L = \frac{|H_{00}|^2}{|H_{11} + H_{-1-1} + H_{00}|^2}$$

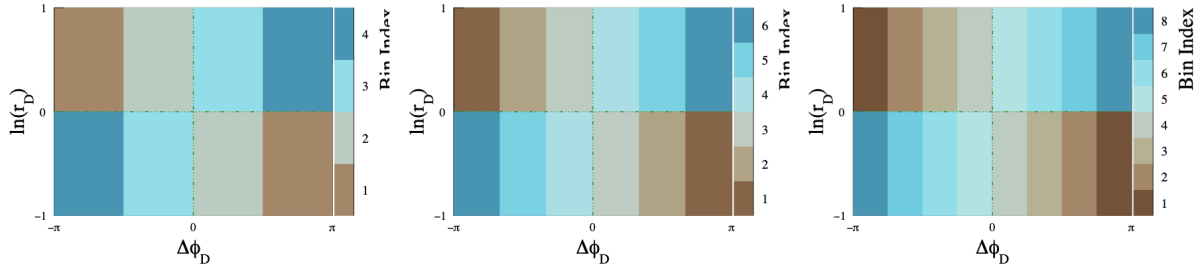
Process	$D^0 \to K^{*-}(892)\,\rho(770)^+$	$D^0 \to \bar{K}^{*0}(892)\,\rho(770)^0$
$D \to V_1V_2 \to (P_1P_2)(P_3P_4)$	$0.509 \pm 0.005 \pm 0.012$	$0.108 \pm 0.008 \pm 0.013$
$D \to V_1V_2$	$0.468 \pm 0.005 \pm 0.011$	$0.077 \pm 0.007 \pm 0.010$

Strong Phase Measurement

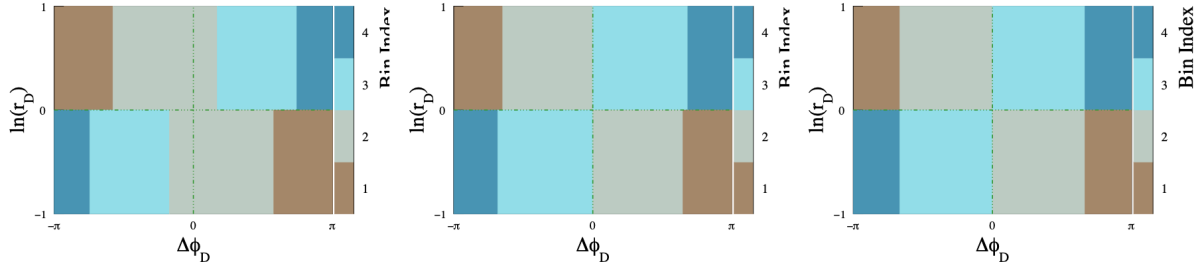
Binning Scheme

- **Mode I**: The bin boundaries are allowed to vary independently, as shown in Figure 2d. The number of bin pairs of this mode could be odd.
- **Mode II**: The middle bin boundaries 0 is fixed, and the left and right bin boundaries are allowed to vary independently, as shown in Figure 2e.
- **Mode III**: The middle bin boundaries 0 is fixed, and the left and right bin boundaries are allowed to vary symmerrically, as shown in Figure 2f.





(a) Uniform 2 × 4 bins (b) Uniform 2 × 6 bins (c) Uniform 2 × 8 bins



(d) Mode I optimized 2 × 4 bins (e) Mode II optimized 2 × 4 bins (f) Mode III optimized 2 × 4 bins

Table 2: c_i, s_i, and T_i for the optimized 2 × 4 binning scheme.

Bin	c_i	s_i	T_i	$\bar{T}_i$
1	-0.8579	-0.2089	0.1951	0.1028
2	0.2738	-0.6499	0.0919	0.0216
3	0.1596	0.6920	0.1594	0.0295
4	-0.8105	0.2691	0.2823	0.1172

Strong Phase Measurement

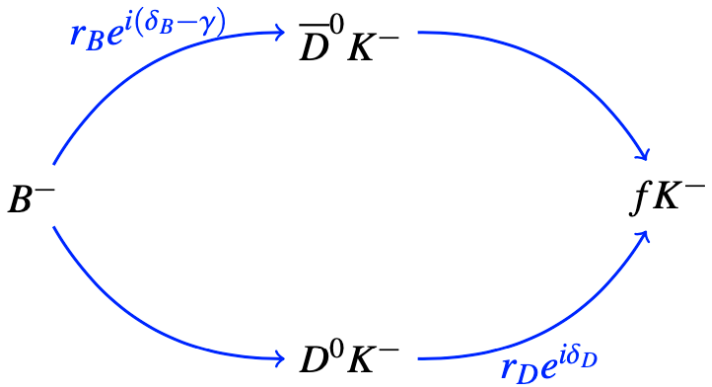
$$A_f = \langle f| H |D^0\rangle = a_f e^{i\phi_f}, \quad \bar{A}_f = \langle f| H |\bar{D}^0\rangle = \bar{a}_f e^{i\bar{\phi}_f}, \qquad A_{f\bar{g}} = A_f \bar{A}_g - \bar{A}_f A_g,$$

$$A_g = \langle g| H |D^0\rangle = a_g e^{i\phi_g}, \quad \bar{A}_g = \langle g| H |\bar{D}^0\rangle = \bar{a}_g e^{i\bar{\phi}_g}. \qquad A_{fg} = \frac{p}{q} A_f A_g - \frac{q}{p} \bar{A}_f \bar{A}_g.$$

$$A_\pm = \frac{(A_g \pm \bar{A}_g)}{\sqrt{2}}. \quad F_+^g = \frac{\int |A_+|^2 \, d\Phi_g}{\int |A_+|^2 + |A_-|^2 \, d\Phi_g} = \frac{\int |A_g|^2 + |\bar{A}_g|^2 + 2|A_g||\bar{A}_g| \cos\Delta\phi_f \, d\Phi_f}{\int 2\left(|A_g|^2 + |\bar{A}_g|^2\right) d\Phi_g}.$$

According to this definition, it is easy to know that $F_+^g = 1$ for CP even mode, and $F_+^g = 0$ for CP odd mode. And the CP parity can be expressed as $\eta_{CP} = (2F_+^g - 1)$.

Strong Phase Measurement



$$\mathcal{A}\left(B^- \to (f)_D K^-\right) = A_B\left(A_f + r_B e^{i(\delta_B-\gamma)}\bar{A}_f\right)$$
$$= A_B\left(a_f e^{i\phi_f} + r_B e^{i(\delta_B-\gamma)}\bar{a}_f e^{i\bar{\phi}_f}\right)$$

$$A(B^- \to \bar{D}^0 K^-)/A(B^- \to D^0 K^-) = r_B e^{i(\delta_B-\gamma)}$$

where r_B is the magnitude, and δ_B is the strong phase difference.

With the decay amplitudes, the decay rates are then written as

$$\Gamma\left[B^- \to DK^-, D \to f_{\mathbf{p}}\right] \propto \left|\bar{A}^f_{\mathbf{p}}\right|^2 r_B^2 + \left|A^f_{\mathbf{p}}\right|^2 + 2\left|A^f_{\mathbf{p}}\right|\left|\bar{A}^f_{\mathbf{p}}\right|\left[x_- \cos\left(\Delta\phi^f_{\mathbf{p}}\right) + y_- \sin\left(\Delta\phi^f_{\mathbf{p}}\right)\right]$$

where the index word $\mathbf{p}$ represents the point in the PHSP of $D \to f$, $x_\pm = r_B\cos(\delta_B \pm \gamma)$ and $y_\pm = r_B\cos(\delta_B \pm \gamma)$. For the B^+ decay, the decay rate is similar as follows:

$$\Gamma\left[B^+ \to DK^+, D \to f_{\mathbf{p}}\right] \propto \left|\bar{A}^f_{\mathbf{p}}\right|^2 r_B^2 + \left|A^f_{\mathbf{p}}\right|^2 + 2\left|A^f_{\mathbf{p}}\right|\left|\bar{A}^f_{\mathbf{p}}\right|\left[x_+ \cos\left(\Delta\phi^f_{\mathbf{p}}\right) - y_+ \sin\left(\Delta\phi^f_{\mathbf{p}}\right)\right]$$

If the event number N^f of $D \to f$ has been measured, then the event number in each bin is given by $K_i^f = N^f T_i^f, \bar{K}_i^f = N^f \bar{T}_i^f$. Therefore, T_i^f and $\bar{T}_i^f$ can also be defined as $T_i^f = \frac{K_i^f}{\sum_i K_i^f}$ and $\bar{T}_i^f = \frac{\bar{K}_i^f}{\sum_i \bar{K}_i^f}$.

After binning the PHSP, the decay rates of $B^- \to DK^-$ is re-written as

$$\Gamma\left[B^- \to DK^-, D \to f_i\right] \propto \bar{K}_i^f r_B^2 + K_i^f + 2\sqrt{K_i^f \bar{K}_i^f}\left(c_i^f x_- + s_i^f y_-\right)$$

$$T_i^f \equiv \int_i \left|A^f_{\mathbf{p}}\right|^2 \mathrm{d}\Phi(\mathbf{p}),$$
$$\bar{T}_i^f \equiv \int_i \left|\bar{A}^f_{\mathbf{p}}\right|^2 \mathrm{d}\Phi(\mathbf{p}),$$
$$c_i^f \equiv \frac{1}{\sqrt{T_i^f \bar{T}_i^f}} \int_i \left|A^f_{\mathbf{p}}\right|\left|\bar{A}^f_{\mathbf{p}}\right| \cos\left(\Delta\phi^f_{\mathbf{p}}\right) \mathrm{d}\Phi(\mathbf{p}),$$
$$s_i^f \equiv \frac{1}{\sqrt{T_i^f \bar{T}_i^f}} \int_i \left|A^f_{\mathbf{p}}\right|\left|\bar{A}^f_{\mathbf{p}}\right| \sin\left(\Delta\phi^f_{\mathbf{p}}\right) \mathrm{d}\Phi(\mathbf{p}).$$

with our measured $c_i^f, s_i^f, T_i^f, x_\pm$ and $y_\pm$ can be obtained from fit to B meson decay, and γ can be extracted !

U-spin

- The U-spin symmetry forms a SU(2) doublet under the exchange of d and s quarks.

In addition to the pure CF and DCS sub-transitions, a mixture of these, where the two pions are produced in a CP eigenstate resonance, is also a viable transition process to the $K^0_S\pi^+\pi^-$ final state. Using the phase convention $CP\left|K^0\right\rangle = -\left|\bar{K}^0\right\rangle$, the partial amplitude of intermediate processes involving only neutral CP eigenstate resonances i.e. $D^0 \to K^0_S(\pi^+\pi^-)_r$ can be written as a superposition of $D^0 \to \bar{K}^0\pi^+\pi^-$and $D^0 \to K^0\pi^+\pi^-$as follows:

$$A\left(D^0 \to K^0_S(\pi\pi)_{k_{CP}}\right) = \frac{1}{\sqrt{2}}\left(A\left(D^0 \to \bar{K}^0(\pi^+\pi^-)\right) - A\left(D^0 \to K^0(\pi^+\pi^-)\right)\right)$$
$$= \frac{1}{\sqrt{2}}A\left(D^0 \to \bar{K}^0(\pi^+\pi^-)\right)\left(1 - \frac{A\left(D^0 \to K^0(\pi^+\pi^-)\right)}{A\left(D^0 \to \bar{K}^0(\pi^+\pi^-)\right)}\right),$$

with $\left|\frac{A(D^0\to K^0(\pi^-\pi^+))}{A(D^0\to \bar{K}^0(\pi^-\pi^+))} = -\tan^2\theta_C\hat{\rho}\right|$, where θ_C was defined as the Cabibbo angle and $\hat{\rho}$ was defined as "normalized ratio of transition amplitudes" by Bigi and Yamamoto and may also be understood as "U-spin breaking " parameter, the $K^0_S\pi^-\pi^+$ CP transition amplitude can be written as,

$$A\left(D^0 \to K^0_S(\pi\pi)_{k_{CP}}\right) = \frac{1}{\sqrt{2}}A\left(D^0 \to \bar{K}^0(\pi^+\pi^-)\right)\left(1 + \hat{\rho}_{k_{CP}}\tan^2\theta_C\right).$$

The U-spin breaking parameter, $\hat{\rho}(= re^{i\delta})$ is a complex and purely empirical quantity. For a three-body decay with multiple exclusive CP eigenstate resonant contributions (k_{CP}), $\hat{\rho}$ factors for each are denoted by $\hat{\rho}_{k_{CP}}$. The $\hat{\rho}$ parameters primarily carry the phase-shifts generated as a result of DCS interference, and naively, the magnitudes ($|\hat{\rho}|$) are expected to be $\sim O(1)$. However, the magnitudes are to be empirically measured for the possibility of deviation from the nominal $\tan^2\theta_C$ Cabibbo factor. A similar treatment to the decay process $D^0 \to K^0_L\pi^-\pi^+$ yields,

$$A\left(D^0 \to K^0_L(\pi\pi)_{k_{CP}}\right) = \frac{1}{\sqrt{2}}A\left(D^0 \to \bar{K}^0(\pi^+\pi^-)\right)\left(1 - \hat{\rho}_{k_{CP}}\tan^2\theta_C\right).$$

$$\frac{A\left(D^0 \to K^0_L(\pi\pi)_{k_{CP}}\right)}{A\left(D^0 \to K^0_S(\pi\pi)_{k_{CP}}\right)} = \frac{1 - \tan^2\theta_C\hat{\rho}_{k_{CP}}}{1 + \tan^2\theta_C\hat{\rho}_{k_{CP}}} \approx 1 - 2\tan^2\theta_C\hat{\rho}_{k_{CP}} + O\left(\tan^4\theta_C\right),$$

$$A\left(D^0 \to K^0_L(\pi\pi)_{k_{CP}}\right) = \left(1 - 2\tan^2\theta_C\hat{\rho}_{k_{CP}}\right) \times A\left(D^0 \to K^0_S(\pi\pi)_{k_{CP}}\right).$$

$$A\left(D^0 \to K^0_S\pi^+\pi^-\right) = \sum_r A^{CF}_{\bar{K}^0\pi\pi} + \sum_{r'} A^{DCS}_{K^0\pi\pi} + \sum_{k_{CP}} A^{CP}_{K^0_S(\pi^+\pi^-)_{k_{CP}}},$$
$$A\left(D^0 \to K^0_L\pi^+\pi^-\right) = \sum_r A^{CF}_{\bar{K}^0\pi\pi} - \sum_{r'} A^{DCS}_{K^0\pi\pi} + \sum_{k_{CP}} \left(1 - 2\tan^2\theta_C\hat{\rho}_{k_{CP}}\right) A^{CP}_{K^0_S(\pi^+\pi^-)_{k_{CP}}}.$$

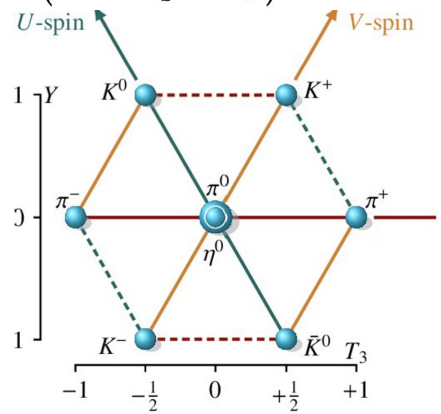


Figure 1: The octet of 0^- mesons. Unitarity of hadrons, U-spin and V-spin.

CP-even fraction & Strong Phase Difference

- What is F_+? ➡ The fraction of CP + to f.

$$F_+ = \frac{\Gamma_+}{\Gamma_+ + \Gamma_-} = \frac{\int |A_+|^2 d\phi_f}{\int |A_+|^2 d\phi_f + \int |A_-|^2 d\phi_f}$$

- Define CP eigenstates and ignore CPV:

$$|D_+^0> = |D^0> + |\bar{D}^0>$$
$$|D_-^0> = |D^0> - |\bar{D}^0>$$

- We have before:

$$A(D^0 \to f) = A_f = a_f e^{i\delta_f}$$
$$A(\bar{D}^0 \to f) = A_{-f} = a_{-f} e^{i\delta_{-f}}$$

- So we have:

$$F_+ = \frac{\int |a_f|^2 + |a_{-f}|^2 + 2|a_f||a_{-f}|\cos(\Delta\delta_f) d\phi_f}{2\int |a_f|^2 + |a_{-f}|^2 d\phi_f}$$

$$2F_+ - 1 = \frac{2}{\int |a_f|^2 + |a_{-f}|^2 d\phi_f} \int |a_f||a_{-f}|\cos(\Delta\delta_f) d\phi_f$$

Strong Phase Measurement

- Used in LHCb-PUB-2016-025

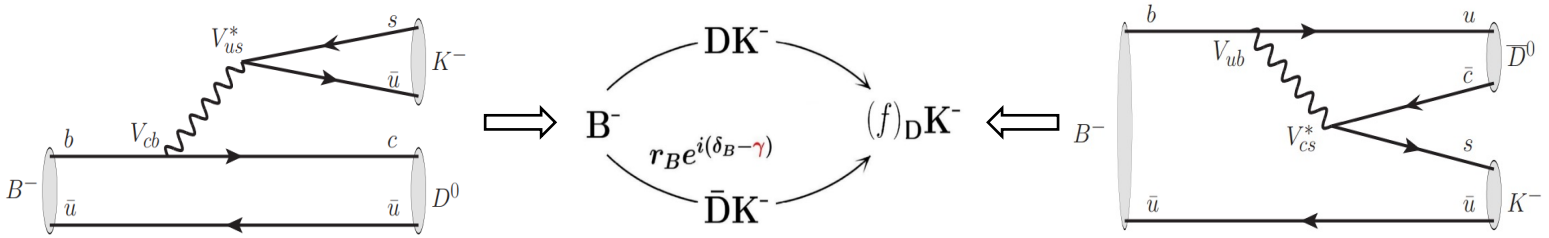
Decay Mode	Parameters	Status@BESIII (2.93 fb^{-1})
$K_S^0\pi^+\pi^-$	c_i, s_i	Finished
$K_S^0K^+K^-$	c_i, s_i	Finished
$K^-\pi^+\pi^+\pi^-$	R, δ	Finished
$K^+K^-\pi^+\pi^-$	F_+ or c_i, s_i	On Going
$\pi^+\pi^-\pi^+\pi^-$	F_+ or c_i, s_i	On Going
$K^-\pi^+\pi^0$	R, δ	Finished
$K_S^0K^\pm\pi^\mp$	R, δ	……
$\pi^+\pi^-\pi^0$	F_+	On Going
$K_S^0\pi^+\pi^-\pi^0$	F_+ or c_i, s_i	On Going
$K^+K^-\pi^0$	F_+	On Going
$K^-\pi^+$	δ	Finished (Update)

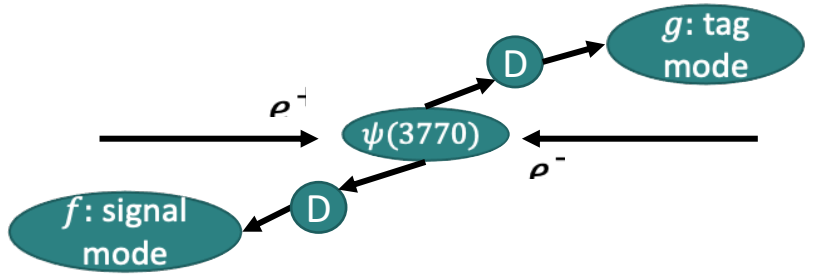
学术能力｜北京谱仪 BESIII 物理分析

$D^0 \to K^0_S\pi^0\pi^+\pi^-$ 过程的分波分析与分支比测量

- CKM 矩阵的幺正性是检验标准模型的重要方法之一。测量 γ 角需要中性粲介子的衰变信息作为输入参数，其实验精度是高精度检验三角形幺正性的重大挑战。
- 中性粲介子量子关联性的研究是深入探索非微扰 QCD 本质的重要途径，也是精密测量粲介子衰变的强相位差、CP 本征态成分比例等参数最理想的场所。
- 味物理的研究是寻找新物理重要途径；对于 $B \to VV$ 过程的预测与测量均表明其纵向极化率 $f_L = 1$，但 $D \to VV$ 过程具有明显不同的衰变性质，有助于寻找 $D^0 - \bar{D}^0$ 混合中的新物理。

$$\gamma \equiv \varphi_3 \equiv \arg\left(-\frac{V_{ud}V_{ub}^*}{V_{cd}V_{cb}^*}\right)$$





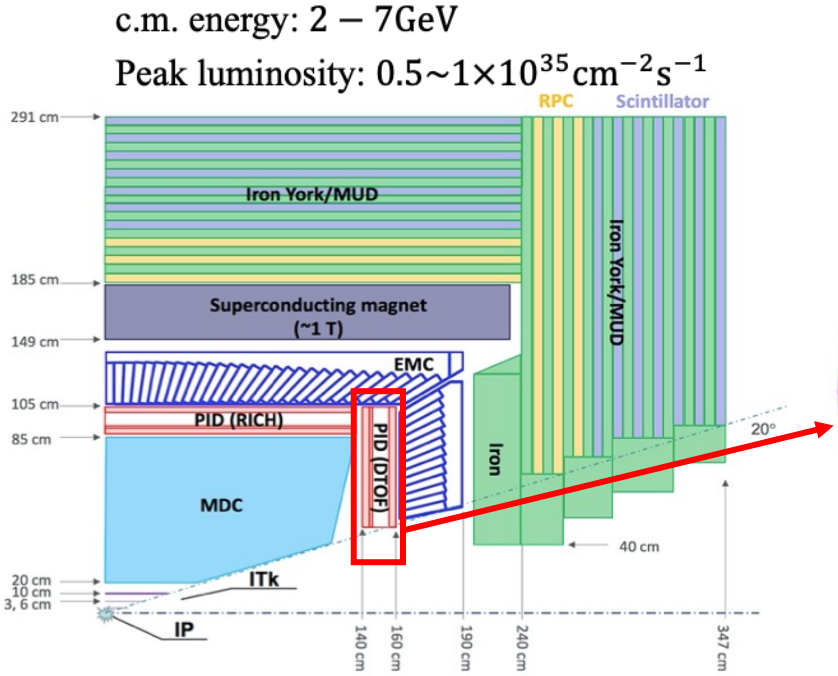
- CKM 矩阵的幺正性是检验标准模型的重要方法之一。测量 γ 角需要中性粲介子的衰变信息作为输入参数，其实验精度是高精度检验三角形幺正性的重大挑战。
- 中性粲介子量子关联性的研究是深入探索非微扰 QCD 本质的重要途径，也是精密测量粲介子衰变的强相位差、CP 本征态成分比例等参数最理想的场所。
- 味物理的研究是寻找新物理重要途径；对于 $B \to VV$ 过程的预测与测量均表明其纵向极化率 $f_L = 1$，但 $D \to VV$ 过程具有明显不同的衰变性质，有助于寻找 $D^0 - \bar{D}^0$ 混合中的新物理。

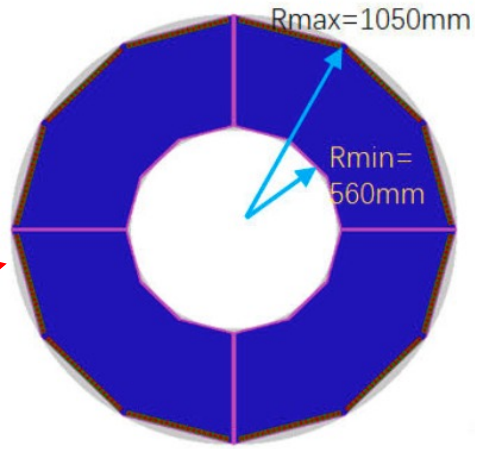
- BESIII 实验具有 20/fb 的 $\psi(3770)$ 数据，具有较高的重建效率，可提供大量且干净的量子关联 $D^0/\bar{D}^0$样本。
- 本过程具有较大的衰变分支比，可获得大量的信号样本，给出目前最精确的分波分析结果，进而可得到相关衰变参数及 $D^0 \to VV, VP$ 和 AP 等过程分支比。

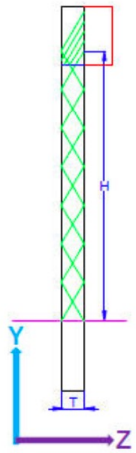
学术能力 | STCF 粒子模拟软件开发

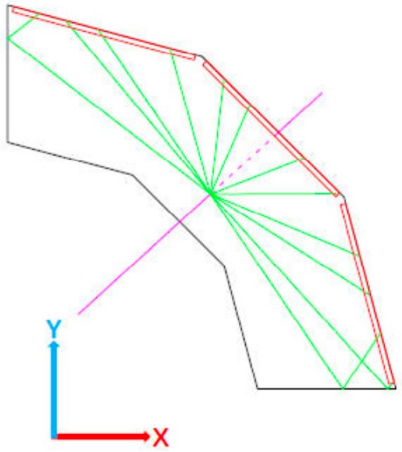
STCF 端盖粒子鉴别探测器 DTOF(DIRC-like TOF) 在全模拟框架下的软件开发

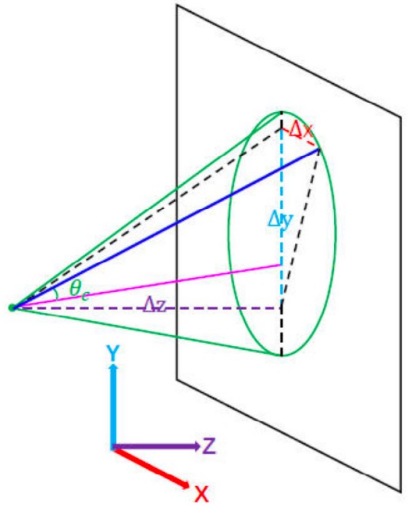
- STCF 是我国预研的工作在 τ-c 能区具有更高亮度的新一代正负电子对撞机，强大的粒子鉴别能力是支撑丰富的物理分析工作的基础
- DIRC 已被广泛应用至国际其他高能物理实验中，其紧致的结构、较低的物质量、优秀的位置和时间分辨在保证了较高的粒子分辨能力







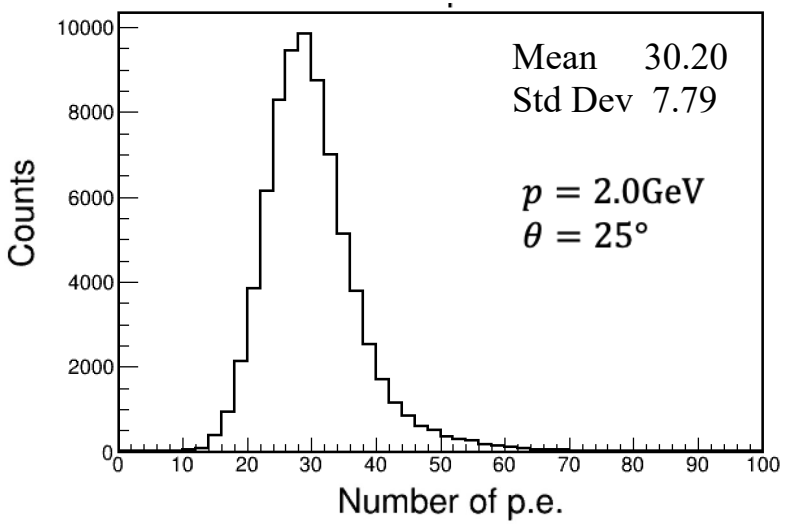


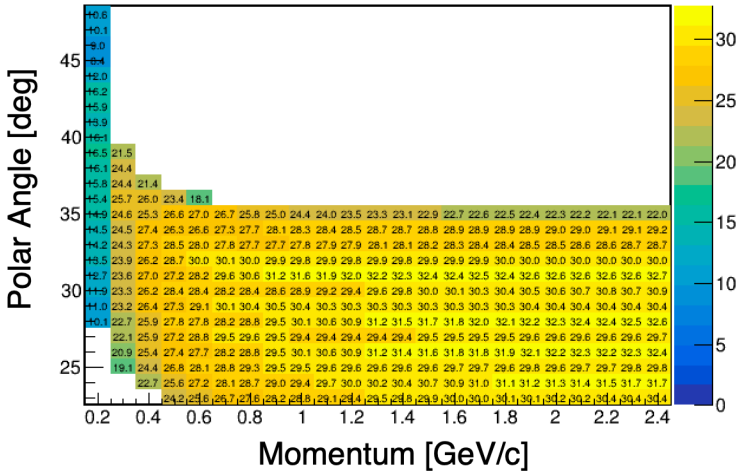


DTOF Simulation

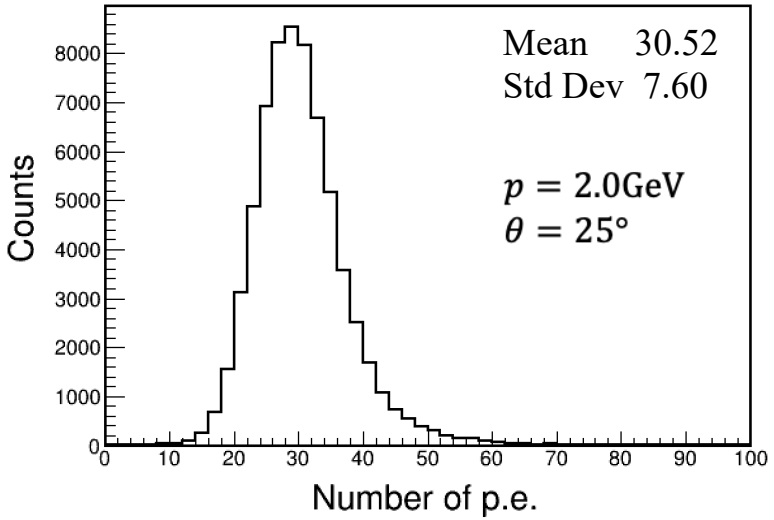
Photon Yield

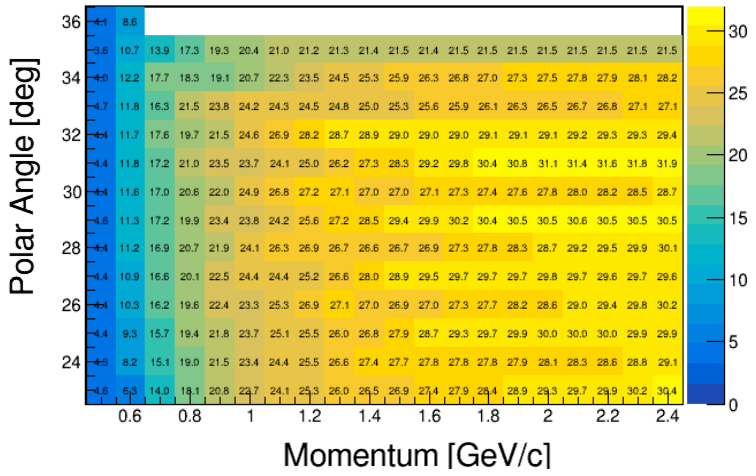
π Sample





K Sample

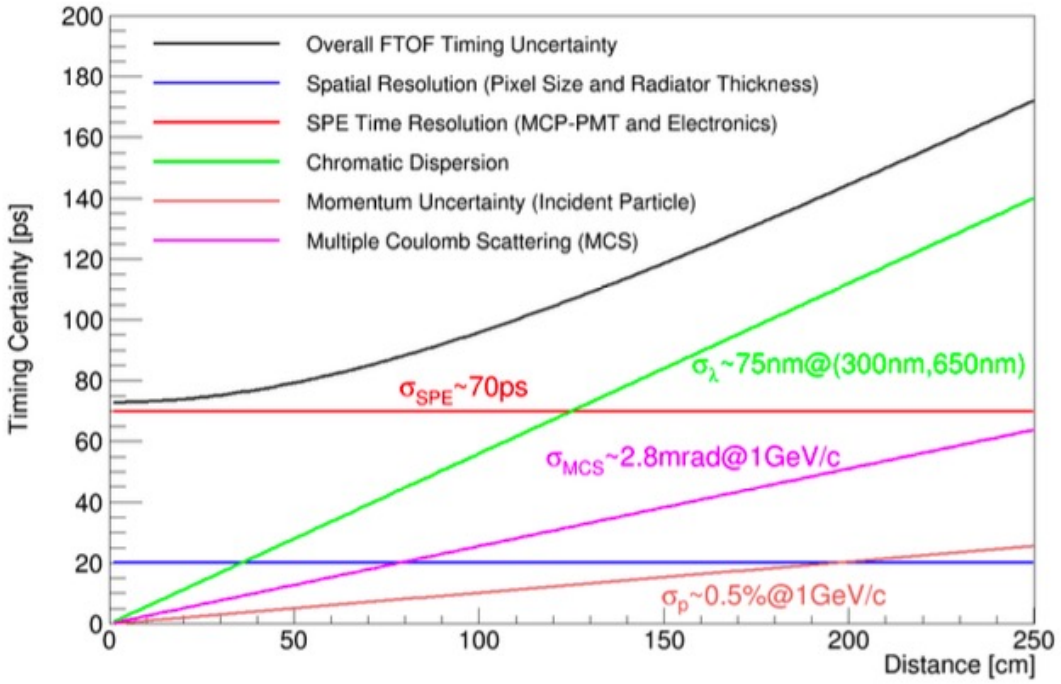




DTOF Reconstruction

Single Timing Uncertainties

$$\sigma_t = \sigma_{T_0} \oplus \sigma_{t_{MCS}} \oplus \sigma_{t_{ext(\vec{r},\vec{p})}} \oplus \frac{\sigma_{t_\lambda}}{\sqrt{N_{p.e.}}} \oplus \frac{\sigma_{t_D}}{\sqrt{N_{p.e.}}} \oplus \frac{\sigma_{TTS}}{\sqrt{N_{p.e.}}}$$



B. Qi *et al* 2021 *JINST* **16** P08021

- Single photon timing uncertainty:

@2GeV

Overall σ_t ~50 ps

π	σ_{T_0}	$\sigma_{t_{MCS}}$	$\sigma_{t_{ext}}$	σ_{t_λ}	σ_{t_D}	σ_{TTS}	Total
/ps	40	9.8	16.5	40.7	14.4	30	68.8

